KTH Industrial Engineering and Management

Aalto University
School of Engineering

Towards Flexible Cogeneration

Techno-economic Optimization of Advanced Combined Cycle Combined Heat and Power Plants Integrated with Heat Pumps and Thermal Energy Storage

Supervisors

Mika Järvinen

Rafael Guédez

MSc Students

Antti Nuutinen

Giovanni Graziano

Master of Science

KTH: Royal Institute of Technology, Stockholm - Sweden SE-100 44

Aalto University, Helsinki - Finland FI-000 76

Aalto University
School of Engineering

Aalto University, P.O. BOX 11000, 00076
AALTO
www.aalto.fi

Abstract of master's thesis

Author(s) Antti Nuutinen, Giovanni Graziano

Title of thesis Towards Flexible Cogeneration - Techno-economic Optimization of Advanced Combined Cycle Combined Heat and Power Plants Integrated with Heat Pumps and Thermal Energy Storage

Master programme Innovative Sustainable Energy Engineering **Code** ENG215

Thesis supervisor Mika Järvinen, Rafael Guédez

Thesis advisor(s) -

Date 20.09.2018 **Number of pages** 106 **Language** English

Abstract

The liberalization of electricity markets and a growing penetration of renewables is changing operation of electrical grids. The boundary conditions for the operation of conventional power plants are changing and, as such, an improved understanding of the varying loads and prices on the electricity grid is required to assess the performance of emerging combined cycle gas turbine (CCGT) concepts and to further optimize their design for these new markets in the pursuit of increasing their profitability, especially when considering combined heat and power (CHP).

To increase the flexibility of CCGT-CHP plants, three new plant layouts have been investigated by integrating different storage concepts and heat pumps in key sections of the traditional plant layout. The present study analyses the influence that market has on determining the optimum CCGT-CHP plant layout that maximizes profits (in terms of plant configuration, sizing and operation strategies) for a given location nearby Turin, Italy, for which hourly electricity and heat prices, as well as meteorological data, have been gathered. A multi-parameter approach for design and operation was followed using KTH's and EPS' techno-economic modeling tool DYESOPT. Results are shown by means of a comparative analysis between optimal plants found for each layout and the state-of-the art CCGT-CHP. It is shown that a plant configuration in which a cold storage unit is integrated together with a heat pump at the inlet of the gas turbine unit increases the net present value of the plant by approximately 0.3% when compared against conventional plant layouts. Using the same concept with a heat pump alone can improve lifetime profitability by 1.6%. A layout where district heating supply water is preheated with a combination of a heat pump with hot thermal tank increases plant profitability by up to 0.5%.

This work has been performed as part of the PUMP-HEAT project, an EU Horizon 2020 research project in which KTH collaborates with other 13 stakeholders including industry and research institutions. The results will directly influence future work of the project.

Keywords co-generation, power plant flexibility, combined cycles, combined heat and power, thermal storage, heat pump

Acknowledgments

We would like to express our gratitude towards our main supervisor *Rafael Guédez* who was always very supportive despite challenging times and who found time for us in his busy schedule. Our colleague for most of the work, *Jose Angel Garcia Frediani*, deserves a big thank you for working through difficult modeling-related issues with us.

A word of gratitude is also expressed for our supervisor from Aalto, *Mika Järvinen*, as well as the partners from the Pump-Heat consortium who brought valuable information used in this work.

Finally, we would like to conclude that it has been a great opportunity to work on this project together as friends.

Contribution of the Authors

To execute this study, the project was conducted by two students, Antti Nuutinen and Giovanni Graziano, from the Joint Nordic master's degree in Innovative Sustainable Energy Engineering (ISEE) between KTH - Royal Institute of Technology in Stockholm, Sweden, and Aalto University in Helsinki, Finland.

For the first phase of the project, Antti focused on the Introduction and laid down the literature review, while Giovanni worked on the theoretical framework and the description of the study case. Moreover, both equally contributed in laying down the abstract and the thesis methodology and structure.

For the second phase of the project, Antti focused on the modelling and the description of the Power-Oriented Combined Cycle (POCC), mainly based on a quasi-dynamic model created in MATLAB. Meanwhile, Giovanni focused on the modelling and description of the cogenerative CHP layouts, carried out by the means of DYESOPT (Dynamic Energy System OPTimizer). Both together established the KPIs involved in this project in order to set up the post-processing system and determining the progress of this project in achieving the predefined goals. Both, throughout their respective results, have drawn their own conclusions and together set the stages for the future work. However, this project has been conducted as a team work in order to support each other in the respective parts; in turn, this facilitated to develop a well-thought-out study and double check the analyses, with Antti keener on the thermodynamic optimization and Giovanni on the techno-economic performance.

For the post processing of the thesis work, Antti focused on the visual attractiveness and layout of the figures and tables, while Giovanni dedicated the time on formatting the final report layout and compiling all the analyses in a consistent single report.

Nomenclature

Abbreviation	Significate	Unit
A	Surface Area	[m^2]
B	Benefits	[€]
C	Cost	[€]
Cp	Isobaric Specific Heat Capacity	[J/kgK]
Cr	Heat Capacity Ratio	[-]
d	Diameter	[m]
E	Electrical/Thermal Power	[MW]
fload	Load Factor	[-]
h	Enthalpy	[J/kg]
H	Height	[m]
HTM	Heat Transfer Medium	[-]
HTF	Heat Transfer Fluid	[-]
i	Real Debt Interest Rate	[%]
IRR	Internal Rate of Return	[%]
kins	Annual Insurance Rate	[%]
LCoE	Levelized Cost of Electricity	[€/MWh_{el}]
LHV	Lower Heating Value	[J/kg]
m	Mass Flow	[kg/s]
n	Average service life	[yr]
NPV	Net Present Value	[€]
NTU	Number of Transfer Units	[-]
P	Total produced el./th. power	[MW]
Pa	Ambient Pressure	[bar]
PBT	Payback Time	[yr]
PCM	Phase Change Material	[-]
sp	Electricity/Heat selling price	[€/MWh]
Ta	Ambient Temperature	[°C]
TIT	Turbine Inlet Temperature	[K]
U	Overall Heat Transfer Coefficient	[W/m2K]
x	fraction	[-]

Symbol	Significate	Unit
μ	Capital charge factor	[-]
ε	Heat Exchanger Effectiveness	[-]
Δ	Delta	[-]
ΔTmin	Minimum Approach Temperature	[K]
η	Efficiency	[-]
ηel	Electrical Efficiency	[-]
ηcc	Combined Cycle Efficiency	[-]
ηth	Thermal Efficiency	[-]
Π	Pressure Ratio	[-]
ρ	Material/fluid Density	[kg/m^3]

Subscript	Significate
amb	Ambient
aux	Auxiliaries
CC	Combined cycle
comb	Combustor
compr	Compressor
cond	Condenser
cons	Construction time
dec	Decommissioning
DH	District Heating
el	Electricity
equip	Equipment
evap	Evaporator
fuel	Fuel
gener	Generator
GT	Gas turbine
HRSG	Heat recovery steam generator
HP	Heat pump
HX	Heat exchanger
inv	Investment
ISO	At Standard Conditions
mec	Mechanical
MF	Mass Flow
o	At Nominal Conditions
O&M	Operation and Maintenance
oper	Operational
para	Parasitic
ref	At Reference Conditions
ST	Steam turbine
TES	Thermal Energy Storage
th	Thermal
tot	Total
turb	Turbine
WG	Water-Glycol

Table of Contents

Abstract 2

Acknowledgments 3

Contribution of the Authors 4

Nomenclature 5

1 Introduction 13

1.1 Literature review 15

1.2 Scope and Objectives 16

1.3 Thesis methodology 16

1.4 Thesis structure 16

2 Background information 18

2.1 Gas Turbine Combined Cycle 18

2.2 Combined Heat and Power Cycle 19

2.2.1 District heating network 20

2.3 Combined Cycle start-up and fast cycling 20

2.4 Heat Pump 22

2.5 Thermal Energy Storage 22

3 Study case 23

3.1 Moncalieri Power Plant 23

3.1.1 Operating range 26

4 Key Performance Indicators – KPI 27

4.1 Technical KPIs 27

4.2 Economic KPIs 28

4.3 Environmental KPIs 29

5 Layout 1: Power-Oriented Combined Cycle 30

5.1 Inlet Conditioning with TES 31

5.2 Continuous cooling 34

5.3 Component description 35

5.3.1 Thermal energy storage 35

5.3.2 Latent Thermal Energy Storage 35

5.3.3 Heat Pump 39

5.4 Modeling 40

5.4.1 Combined Cycle load and efficiency 40

5.4.2 Pressure drop 41
5.4.3 Heat pump 41
5.4.4 Gas Turbine Heat Exchanger 42
5.4.5 Ambient Heat Exchanger 42
5.4.6 Pumping power 43
5.4.7 TES transient function 43
5.5 Operation Modes 46
5.5.1 Continuous cooling 46
5.5.2 Charging 46
5.5.3 Discharging 46
5.5.4 Anti-ice system 47
5.6 Economic considerations 48
5.6.1 Capital Expenditure (CAPEX) 48
5.6.2 Operation and Maintenance Expenditure (OPEX) 50
5.7 Thermo-economic analysis 51
5.7.1 Technical performance 53
5.7.2 Technical KPIs 56
5.7.3 Economic KPIs 57
5.8 Sensitivity analysis 58
5.8.1 Electricity price 58
5.8.2 Continuous Cooling performance 60
6 Layouts 2 and 3: Cogenerative combined cycle 62
6.1 Introduction 62
6.1.1 Heat recovery from Heat Recovery Steam Generator feed water 63
6.1.2 Bottoming Cycle Constraints 64
6.2 Steady-state design 66
6.2.1 Topping cycle 66
6.2.2 Bottoming cycle 68
6.3 Transient Model 72
6.3.1 Methodology - Modelling 72
6.3.2 TRNSYS model input 73
6.3.3 Load control 73
6.3.4 Turbomachinery performance 76

6.3.5 Heat pump 78
6.3.6 Thermal energy storage 78
6.3.7 District heating condensers 79
6.4 Economic considerations 81
6.4.1 Capital Expenditure (CAPEX) 81
6.4.2 Operation and Maintenance Expenditure (OPEX) 83
6.5 Thermo-economic analysis 85
6.5.1 Control logic and modes definition 85
6.5.2 Technical performance 87
6.5.3 Economic performance 91
6.6 Sensitivity analysis 92
6.6.1 Unit cost variation 92
6.6.2 Power plant load variation 92
7 Conclusion 94
8 Future work 96
Bibliography 98
Appendix 101

Index of Figures

Figure 1 Moncalieri iron diagram with expected effects from Pump-Heat (PHCC) project. . 13

Figure 2 Nitrogen oxide production vs gas turbine load [3]. 14

Figure 3 CCGT thermodynamic cycle. 18

Figure 4 CCGT three-pressure level plant configuration. 19

Figure 5 CHP plant configuration. 20

Figure 6 CCGT start-up time. 21

Figure 7 CCGT fast cycling and rapid start-up [8] 21

Figure 8 Heat pump T-s, vapor compression cycle (left), Heat pump, ideal reversed Carnot cycle (right). 22

Figure 9 Thermal Energy Storage layout. 22

Figure 10 Moncalieri Power Plant with GTCC units' location. 23

Figure 11 Moncalieri Power Plant - RPW2GT unit. 24

Figure 12 Location of the units. 25

Figure 13 Moncalieri CCGT, design operating range at ambient temperature of 15 °C. 26

Figure 14 Power oriented combined cycle 30

Figure 15 Charging flow diagram (left), discharging flow diagram (right). 31

Figure 16 . Combined cycle performance vs Inlet temperature. (a) Efficiency, (b) Power output. [21] 32

Figure 17 Continuous cooling flow diagram 34

Figure 18 T-Q diagram for sensible and latent TES [24] 36

Figure 19 . Heat storage processes of phase change materials. (a) Freezing process, (b) Melting process 36

Figure 20 Thermal energy storage with encapsulated material. 37

Figure 21 TES Model Geometry: Discretized Column (left), Capsule Geometry (right) 38

Figure 22 Power and energy capacity of TES with encapsulated PCMTF4.8. 39

Figure 23 Combined Cycle power output curve. 40

Figure 24 Water-glycol mixture specific heat. 42

Figure 25 Charging polynomial functions at 265.68 K inlet temperature. 44

Figure 26 Charging polynomial functions at 266.15 K inlet temperatures. 44

Figure 27 . Polynomial functions for discharging at 281.15 K. 45

Figure 28 Polynomial functions for discharging at 293.15 K. 45

Figure 29 Thermal energy storage cost curve. 49

Figure 30 Heat Pump cost curve. *49*
Figure 31 Reference plant capital cost breakdown. *51*
Figure 32 Operation mode effect on power generation. *53*
Figure 33 State of charge for all cases. *54*
Figure 34 POCC technical performance. *54*
Figure 35 Power difference between Case 3 and Reference plant. *55*
Figure 36 Power difference (Case 3), varying GT inlet temperature. *55*
Figure 37 Heat pump transient operation during continuous cooling (Case 5). *56*
Figure 38 Case 3 (left) and Case 5 (right) equipment cost breakdown. *60*
Figure 39 Continuous cooling power output. *60*
Figure 40 PHCC concept solution for CHP CC. *62*
Figure 41 Cogenerative PHCC layout with series configuration (Layout 2). *63*
Figure 42 Cogenerative PHCC layout with parallel configuration (Layout 3). *64*
Figure 43 GT sub-components configuration and mass flows. *67*
Figure 44 Pinch-point diagram for three-pressure level HRSG. *69*
Figure 45 DYESOPT programming logic. *72*
Figure 46 Meteorological Data for Turin, Italy *73*
Figure 47 District heating demand (RPW2GT) *74*
Figure 48 Electricity price vs heat price ratio. *74*
Figure 49 Heat demand vs electricity price ratio. *75*
Figure 50 Power plant load (Layout 2 and 3). *75*
Figure 51 Generator off-design efficiency values [31] *77*
Figure 52 COP catalogue for Ammonia Heat Pump. *78*
Figure 53 Series configuration *79*
Figure 54 Parallel configuration *79*
Figure 55 Investment Cost function water tank *82*
Figure 56 CAPEX breakdown of the CHP reference plant model *83*
Figure 57 OPEX breakdown of CHP Reference plant model *84*
Figure 58 Monthly and weekly thermodynamic behaviour, January *88*
Figure 59 Monthly and weekly thermodynamic behaviour, May *88*
Figure 60 Monthly and weekly thermodynamic behaviour, November *89*
Figure 61 Annual thermal production. *90*
Figure 62 Annual electricity generation. *90*

Figure 63 CAPEX breakdown best configuration, Mode 4. ..... *91*
Figure 64 Annual income difference between Mode 4 and CHP Reference plant model. *91*

Index of Tables

Table 1 Comparison between TES and Continuous Cooling Solution [20] *34*
Table 2 TES modeling parameters *38*
Table 3. Gas turbine heat exchanger design parameters. *42*
Table 4. Ambient heat exchanger design parameters. *42*
Table 5. Operation mode conditions. *47*
Table 6. Reference plant KPIs. *51*
Table 7. Common simulation parameters. *52*
Table 8. Simulated cases. *52*
Table 9. Technical KPIs. *57*
Table 10. Ramp-up KPIs. *57*
Table 11. Economic KPIs. *57*
Table 12. Sensitivity analysis with electricity price. *58*
Table 13. Sensitivity analysis with fuel price. *59*
Table 14. CAPEX breakdown. (M€) *59*
Table 15. Continuous Cooling KPIs. *61*
Table 16 GT nominal operating conditions *66*
Table 17 ST Nominal operating conditions. *70*
Table 18 DH nominal operating conditions. *71*
Table 19 Reference load operating hours. *76*
Table 20 ST Isentropic efficiency *77*
Table 21 TES parameters. *78*
Table 22 Investment parameters. *81*
Table 23 Control logic. *85*
Table 24 Modes (configurations). *85*
Table 25 KPIs for Reference CHP plant model. *85*
Table 26 KPIs for CHP plant model, Mode 1 and 4. ..... *86*
Table 27 KPIs CHP plant for Mode 4 (unit cost variation). *92*
Table 28 Load operating hours (load variation). *92*
Table 29 KPIs CHP plant (load variation). *93*

1 Introduction

This thesis has been conducted as a part of the Pump-Heat (Performance Untapped Modulation for Power and Heat via Energy Accumulation Technologies) project which is funded by the EU Horizon 2020 scheme. The project belongs to the European Union research topic "LCE-28-2017 - Highly flexible and efficient fossil fuel power plants".

Climate change is one of the major challenges nations around the world currently face. The response has been to increase photovoltaic and wind energy capacity as carbon dioxide emissions may be effectively nullified by using carbon neutral energy technologies. The inherent intermittency that comes with the varying generation of solar and wind must be matched with stabilizing efforts such as demand-side response (DSR), batteries and other electrical energy storage methods. Current fossil fuel fired capacity may not be all eliminated, however, as all demand cannot be met with the two forms of renewable electricity generation. Therefore, it is necessary to have generation capacity which can reliably and quickly provide electricity to the grid when solar or wind production falls behind the demand.

According to the framework set by Pump-Heat, combined cycle gas turbine (CCGT) power plants will be a large player in providing the backup that renewable energies require. They are highly efficient thermal power plants, which run on natural gas. In the future, integrated gasification combined cycle (IGCC) may be implemented, which could further increase the fuel flexibility of these power plants. Often combined cycle is used in context of combined heat and power (CHP), whenever district heating or process steam demand calls for it. In the EU, an estimated 50% of energy consumption in buildings and industry is heating or cooling demand meaning that some thermal plants have to be kept in operation at all times [1]. As CHP plants are constrained by thermal demand, they can only provide limited grid services i.e. ancillary services whose purpose is to ensure the grid stability so that supply continually meets demand. Combined cycle power plants, which have a certain operational range, can be optimized for heat or electricity production with relatively high efficiency. The range where a combined heat and power plant can operate is often presented with an iron diagram. The iron diagram shows the relation between power and heat production. The purpose of the project is to increase this operational range by addition of heat pumps and thermal energy storage to cover the heat demand when power and heat demands don't match.

The operational range for Moncalieri CCGT, with the expected effect from the goal of the project is depicted in Figure 1.

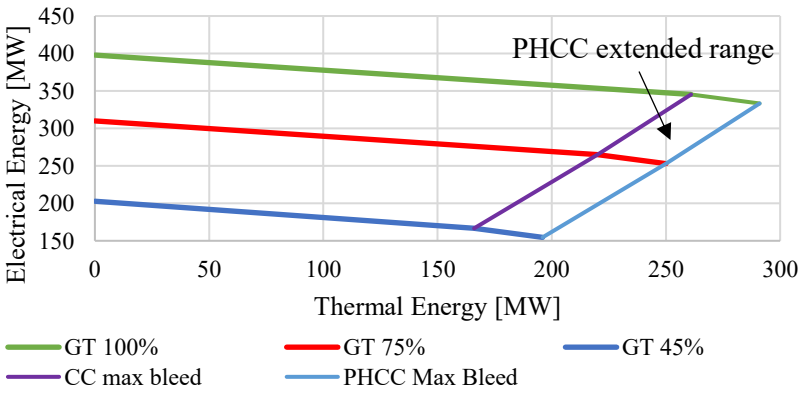

Figure 1 Moncalieri iron diagram with expected effects from Pump-Heat (PHCC) project.

On top left, the plant is running in full electric mode where most of the heat is released via the condenser at a low temperature which cannot be used for heating purposes. Shifting towards the right side of the diagram, cogenerative operating mode is applied. Now, electric output is decreased but for each MW_{el} lost, approximately 5 MW_{th} of heat output is gained. For reference, the gas turbine may be run at as low as 45% of its nominal power. At the minimum power, around 166 MW_{th} of district heating is produced, with 166 MW_{el} of electric output.

If heat pumps are integrated into power plant operation, the range can be extended. The newest technology can reach a coefficient of performance (COP) of 4, meaning that for each 1 MW of electricity used, 4 MW of thermal output is received. In the case of Figure 1, a modest COP of 2.5 was used accounting for a varying temperature level of waste heat. Heat pumps help decrease the power when ancillary services call for it, while larger heat demand can be fulfilled. As thermal power plants are expected to mainly meet the heat requirement, this plays well into the goals of the project; reducing the environmental impact of fossil fuel power plants and increase their flexibility and global efficiency. With heat pumps, the combined cycle could even be turned off and it could still provide a balancing effect to the grid – an equivalent of electrical storage or a smart load on the electrical market. This should be achieved while at the same time ensuring the minimum environmental load (MEL). MEL refers to the state of running a gas turbine at the minimum load in which emissions, particularly nitrogen oxide and carbon monoxide, are still within legislative limits [2]. The NOx emissions tend to increase as load is increased, as high temperatures lead to thermal NOx formation. Figure 2 demonstrates the effect of increasing gas turbine load on nitrogen oxide formation. For reference, General Electric data on gas turbine emissions was used [3].

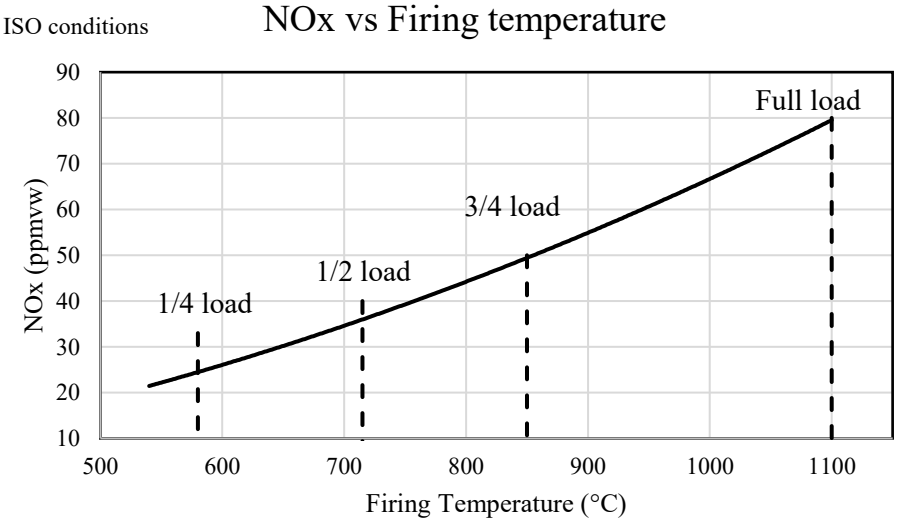

Figure 2 Nitrogen oxide production vs gas turbine load [3].

The Pump-Heat project proposes various layouts to increase the operational flexibility of combined cycle power plants while minimizing the environmental impact. These layouts include heat pump integrated with thermal energy storage. Out of the layouts proposed, one focuses on the compressor inlet air conditioning as air feed temperature influences greatly the compressor power used and consequently the power and heat output of the plant. The other layouts implement changes within the heat recovery steam generator (HRSG), with heat pump cold side installed to either the feed water stream into the HRSG or flue gas condenser.

However, for the sake of limiting the scope of the thesis, the flue gas condenser was not studied here. In addition to heat pumps, a latent heat thermal energy storage (LHTES) is placed into the system as a demand-balancing measure. The evaporator of the heat pump can therefore be heated with either waste heat from the combined cycle or by utilizing the phase change of a phase-change material (PCM) contained in the tanks of the LHTES system. In addition, smart scheduling for control concept is implemented to cope with the primary reserve market constraints, decrease water consumption, reduce MEL and increase power ramp rates. Savings in operating costs are expected as fuel consumption and number of start-ups are decreased considerably.

1.1 Literature review

As legislation towards a carbon-neutral economy is being pushed in the European Union and other parts of the world, renewable energy sources (RES) are brought into the energy system. These sources include mainly solar and wind power, both of which are intermittent and thus, by default not dispatchable. In other words, power from these sources is not derived at the same time as energy demand occurs. Although RES power plants are the most capital-intensive, they are the cheapest to operate. This leads to a situation where, in the absence of reliable energy storage measures, renewable power plants are operated whenever possible causing traditional fossil power plants to have to vary their load significantly [4].

A large amount of research has been conducted under the topic of increasing demand with an increase in variable renewable energy penetration in the grid. More flexibility is required from power plants, and often this means operating at off-design conditions. Whenever power plant equipment is operated at varying conditions, it leads to losses in capacity and/or efficiency of the plant. When a thermal power plant is ramped up or down to meet the electricity and heat market demands, thermo-mechanical fatigue, creep and corrosion must also be considered as factors affecting operation feasibility [5][6][7]. Increasing the ramp-up/down capabilities of combined cycle power plants have been recently studied vigorously. Original equipment manufacturers such as General Electric and Siemens have developed their own methods of decreasing the start-up and ramping times of their equipment [8].

Some measures of increasing the flexibility of conventional power plants are improving and redesigning components, defining new operational strategies and identifying new market mechanisms [5]. Generation flexibility is seen as the best solution in short to medium-term when it comes to delivering flexibility, since energy storage and demand response are currently limited in capacity. However, both solutions will have to be implemented in the future to achieve low-carbon energy systems. Gas turbine combined cycle power plants (CCGT) have to be ran at a minimum load of 20% of full load, and they have a long start-up time along with a low ramping rate. This means that in order to operate them profitably, CCGTs must be designed to operate as mid-merit plants which are able to change their generation level to cope with demand variations and start at a short notice [4].

1.2 Scope and Objectives

Performance Untapped Modulation for Power and Heat via Energy Accumulation Technologies:

- Increase power flexibility of natural gas fired power-oriented CCGT power plants
- Improve turn-down ratio and power ramping capabilities
- Propose a heat pump integrated with thermal storage and advanced control techniques with smart scheduling

Thesis objectives:

- Develop techno-economic models of the proposed layouts in the Pump-Heat project with the Moncalieri plant as reference
- Perform techno-economic optimizations of the layouts
- Determine under which conditions are these layouts more profitable when compared to state of the art

1.3 Thesis methodology

In this thesis, three different layouts are defined and then optimized with Dynamic Energy System OPTimizer (DYESOPT), a MATLAB-based program in which the thermodynamically optimal power plant configuration is designed. After the design, plant parameters are taken into TRNSYS where the plant's annual performance is evaluated with respect to varying electricity and heat prices, ambient air temperature and several critical parameters. Afterwards, the techno-economic calculations are used to find the optimal solution for the study case of Moncalieri. Here layouts for already existing power plants are referred to as retrofit options.

Hence, the methodology used to complete this master thesis project can be summarized as follows:

1. Literature review on previous work on this topic and on general background of the technology presented in this study, namely combined cycle, CHP, district heating network, thermal energy storage and heat pump. This is mainly presented in Chapter 2 and in the description of each layout.
2. Acquaintance with the existing techno-economic modeling tool developed in KTH, namely DYESOPT, and understanding the code structure and the DYESOPT functions involved in a "single run" for the adopted model. A detailed explanation of the modeling approach is provided in the methodology paragraph of each layout.
3. Development and implementation of a suitable model for both the steady-state analysis performed in MATLAB and the dynamic simulation in TRNSYS. The modeling approach followed to design the layouts is presented in the respective chapters.
4. Techno-economic performance evaluation using multi-parameter approach under different market circumstances, units' size and working conditions related to the case study power plant.

1.4 Thesis structure

This thesis consists of several chapters, with the main research findings being presented in *Chapter 5* and *Chapter 6*. This first chapter began with an introduction about the Pump-Heat EU founded research project and its main scope as well as the objectives and methodology followed to complete the thesis.

Chapter 2 discusses further the basic principles of CC-CHP plants to give background to what is the state-of-the-art technology.

In *Chapter 3*, the reference case of Moncalieri power plant in Turin, Italy, is established.

In *Chapter 4*, the key performance indicators used to analyze the power plant performance are presented and briefly described.

In *Chapter 5*, the Power Oriented Combined Cycle (POCC) is described and the modeling aspects are explained after which the respective results are presented.

In *Chapter 6*, the cogenerative CHP plant configurations are described and the modeling aspects are explained after which the respective results are presented.

Chapter 7 gives conclusions for both the layouts.

Finally, *Chapter 8* concludes the work of this thesis and sets the stage for future studies.

2 Background information

In this chapter a general description of the theoretical framework regarding this project is presented.

2.1 Gas Turbine Combined Cycle

A Gas Turbine Combined Cycle (CCGT) power plant converts the energy of the fuel into electrical energy through the combination of a gas *topping* cycle, which operates at high temperatures, and a steam *bottoming* cycle, which operates at lower temperature level, into a single power plant. Either natural gas or syngas (from coal or equivalent sources) is commonly used in the gas turbine (GT) as a fuel and the produced exhaust gas are then converted via a Heat Recovery Heat Generator (HRSG) into steam which subsequently run the steam turbine (ST). Such a configuration can reach electrical efficiencies up to 60% with respect to the poorer efficiency of 35-40% of a traditional open gas turbine cycle [9].

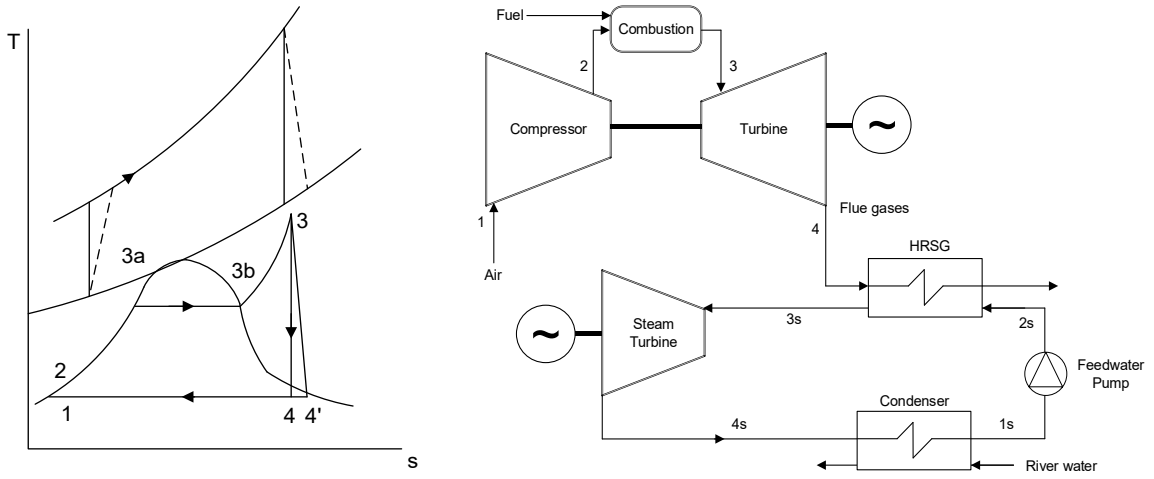

Figure 3 CCGT thermodynamic cycle.

The Heat Recovery Steam Generator is one of the main components in a combined cycle since it is the unit where the heat exchange between the exhaust gas from the gas turbine and the working fluid of the bottoming cycle occurs. The HRSG basically consists of three main sections: the economizer, the evaporator and the superheater, where the feed water heating, water vaporization and steam superheating occur, respectively. It generates steam at one or more pressure levels. The steam is fed into the steam turbine which drives either the same generator of the GT (single-shaft arrangement) or a separate generator (multi-shaft arrangement).

Nowadays, the most widely used HRSG configuration is the three pressure levels (high, intermediate and low pressure) with reheat (RH) system, as it is shown in Figure 4. In this type of HRSG, the pressure at which the reheating occurs is equal to the one of the intermediate (IP) vaporization. The vapour comes from the high pressure (HPT) turbine, is then mixed with the vapour generated in the IP section and finally re-superheated until the maximum allowed temperature for the exhaust gas before entering the turbine is reached [10].

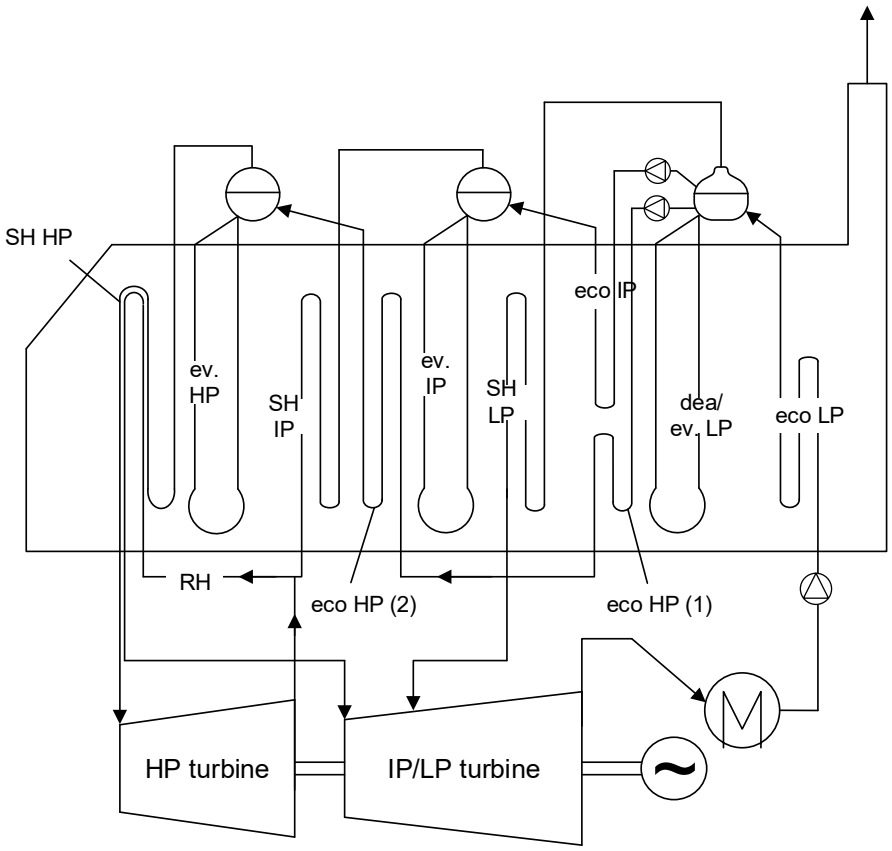

Figure 4 CCGT three-pressure level plant configuration.

2.2 Combined Heat and Power Cycle

Essentially, the combined heat and power plant (CHP) is a gas turbine combined cycle capable to produce both steam and hot water as a thermal energy output. It recovers the heat that would otherwise be wasted in conventional condensing generation of electric power. This operating concept is the cogeneration mode.

There are many advantages associated with the CHP: a significant reduction of fuel consumption, lower GHG emissions and the possibility to increase the independency from fossil fuel. Usually, a CHP has a total efficiency between 80% up to 90%, depending on the type of technology, unit capacity and operating conditions (units' workload). However, a high global efficiency is also dependent on how the thermal energy is utilized, thus achieving high-performant operational schemes. Therefore, a plant operating in cogeneration mode adds another layer of cycle configuration flexibility.

In turn, a combined heat and power plant can play a significant role in the energy production systems and district (or community) heating networks, matching efficiently both heat and power demands both at constant and time-varying rate.

Figure 5 depicts a cogeneration CHP plant with three pressure levels and a reheat system.

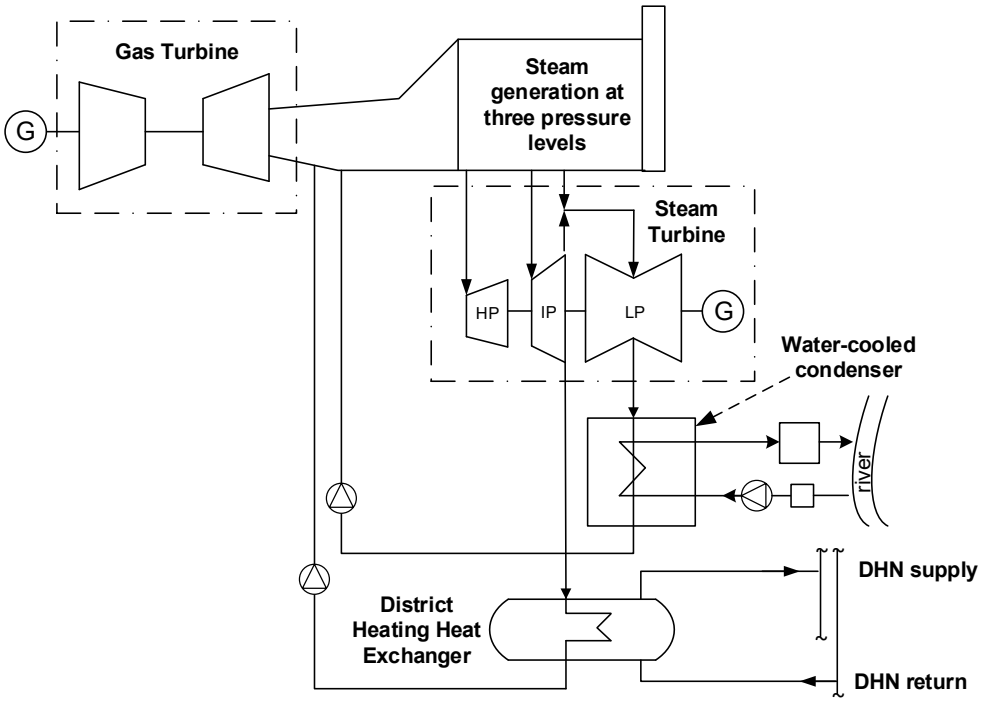

Figure 5 CHP plant configuration.

2.2.1 District heating network

District heating network (DHN) is mainly used for the residential heating and the domestic hot water (DHW). It also fits in a network where both households and manufacturing industries are integrated due to the capability to provide constant thermal energy.

DHN is often associated with cold climate countries such as the Nordics, where the heat demand can be predicted to follow the seasons. However, the north of Italy, and Turin especially uses district heating to cover a large portion of the demand as it is a reliable way of distributing heat via a piping system. The water in the DHN is distributed with an underground double-piped system, where the supply water flows in a pipe and the return water in another. The supply and return temperatures vary depending on the season and the weather, with the lowest temperatures occurring during the summer when primarily DHW is needed. DHW only requires temperatures in the range of 50-55°C as lower temperatures might allow legionella bacteria to thrive in the piping and lead to health risks. Residential heating water is generally supplied at 70-120°C to account for the heat losses occurring in the pipe system.

2.3 Combined Cycle start-up and fast cycling

The start-up of a combined cycle that provides both electric power and district heating essentially consists in switching on the power plant from an off mode to an on-operating mode when 100% of its nominal capacity is reached. The cooler is the power plant, i.e. the longer it is kept shut down, the longer is the time required to start up the unit. In this regard, the maximum temperature gradient, which varies depending on both the thermo-mechanical fatigue capability of the material and the design configuration of the steam turbine (ST) and heat recovery steam generator (HRSG) is the most affecting factor [11].

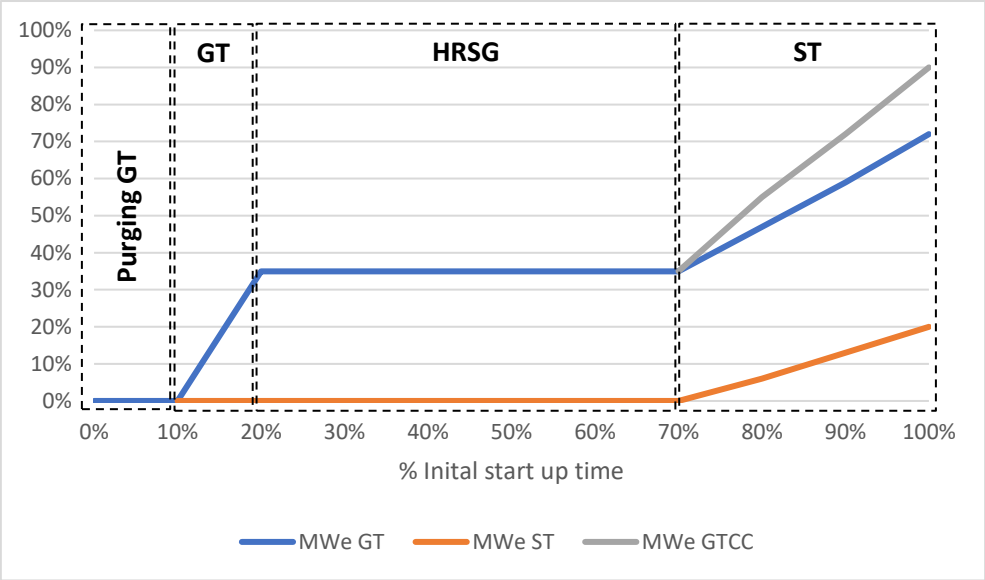

Figure 6 CCGT start-up time.

As can be noted from Figure 6, the HRSG is the unit that requires more time to be run at nominal operating conditions, followed by the steam turbine; however, this behaviour does not depend only on the temperature gradient previously mentioned but also on other relevant factors which are related to all the operating and thermodynamic requirements to be considered when coupling the ST with the HRSG.

To reduce the start-up time and thus increase the flexibility of the power plant several adjustments can be put in place. The procedure to shut down the plant can be modified, integrating several systems capable to limit the thermal dissipation, thus keeping the units as close as possible to the thermal conditions of a plant that is already warm. Moreover, the gas and steam turbines can be switched on in parallel instead of starting them up in series, optimizing the start-up procedure. Finally, the automation of the operations will further increase both the reliability and lifetime of the machines [8]. All these adjustments lead to an improved start-up sequence as it is shown in Figure 7.

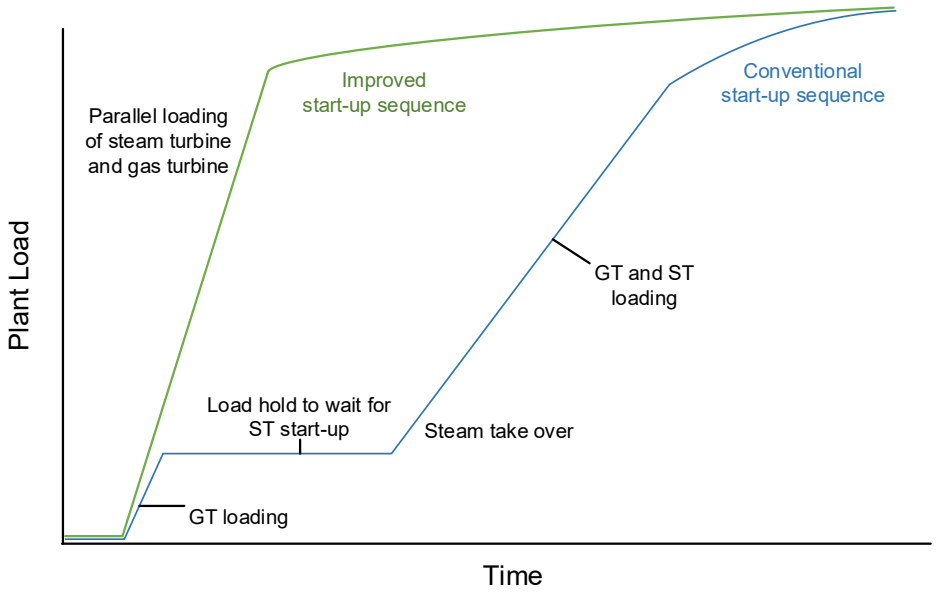

Figure 7 CCGT fast cycling and rapid start-up [8].

2.4 Heat Pump

Heat pump (HP) is a device that takes low-grade heat and increases it to a higher grade via compression or absorption cycle. The principle of refrigeration is here applied in a reverse manner. A refrigerant, which is commonly ammonia or butane, is circulated in a closed loop. It takes heat from a heat source, such as the ambient, in the evaporator where it evaporates in low pressure conditions. The refrigerant is then compressed to a high pressure, high temperature state with a compressor in vapor compression cycle (VCC) or by using absorber/desorber in an absorption/adsorption cycle. The heat is released in the condenser which acts as a heat sink. The refrigerant flows through the expansion valve where its pressure and temperature are decreased. To prevent the compressor from damage, it is important that the working fluid is slightly overheated after evaporation at the compressor input, since the liquid refrigerant particles can damage the compressor blades [12].

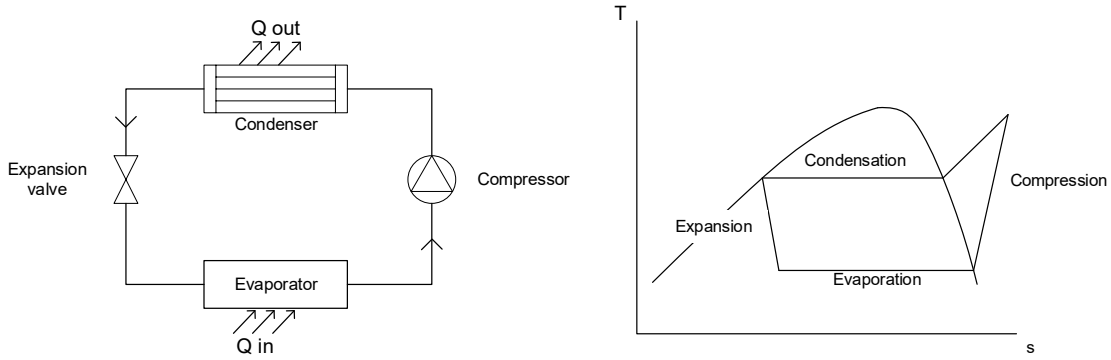

Figure 8 Heat pump T-s, vapor compression cycle (left), Heat pump, ideal reversed Carnot cycle (right).

The usual process used in refrigeration and heat pumps is the simple vapor compression cycle. It makes use of latent heat, as opposed to gas cycles. As the refrigerant boils in the evaporator, it gains the latent heat of evaporation while in the condenser this latent heat is released.

2.5 Thermal Energy Storage

The thermal energy storage (TES) is an integrated plant´s unit, which is used to store the excess thermal energy that can be used when necessary and to meet the peaks in heat demand. Therefore, implementation of storage in the combined cycle power plant allows higher flexibility of plant operation. Among the TES systems, latent heat-based phase change material (PCM) has shown promising thermal storage density in the recent decades. However, the sensible heat storage is still the most widely used technology for power plant since it is a mature and relatively cheap technology and due to its operational range.

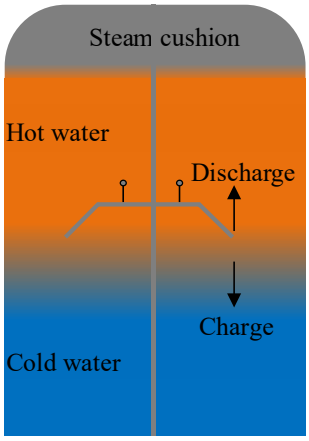

Figure 9 Thermal Energy Storage layout.

3 Study case

IREN S.p.A is a multi-utility company operating in the north of Italy. Its services include generation and distribution of electricity with mainly hydropower and thermal power plants, as well as district heating which it distributes in district heating network. IREN is the owner of the combined cycle gas turbine power plant used as a reference case in this thesis.

Moncalieri power plant consists of two cogeneration Gas Turbine Combined Cycle (CCGT) units, RPW2GT unit and 3GT unit, with an overall electrical power of about 800 MW, in full electric mode, and a thermal power of about 520 MW, in full cogeneration mode.

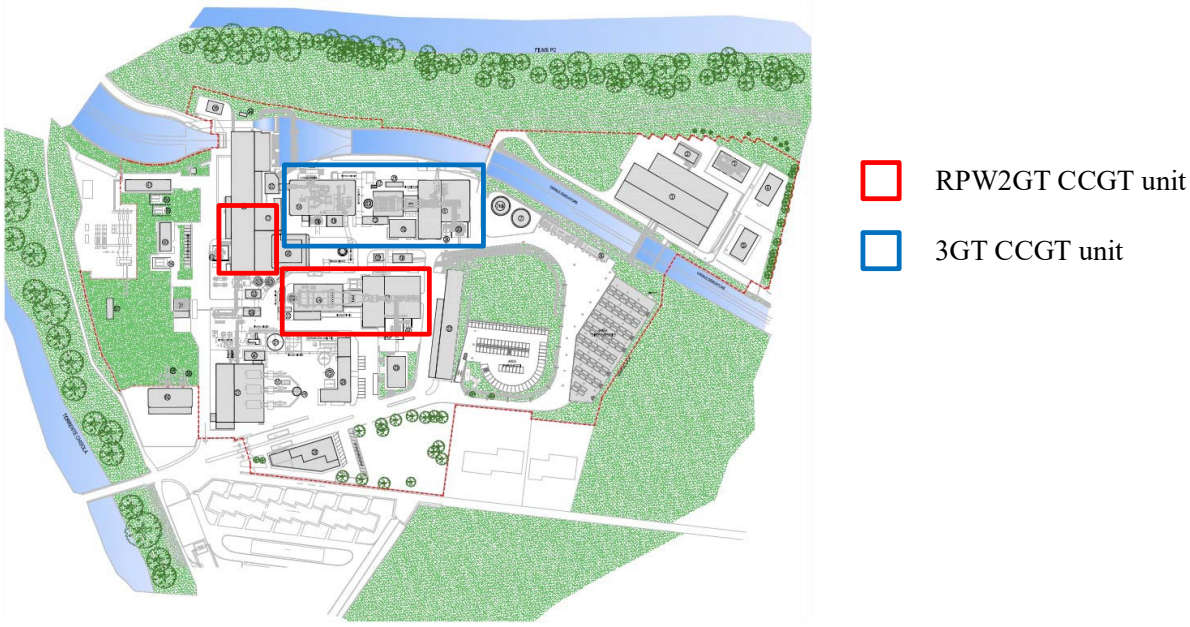

Figure 10 Moncalieri Power Plant with GTCC units' location.

For this study, the RPW2GT CCGT unit was taken as test subject and the related data provided by the operator as the setpoints to compare the model outputs and validate the model itself.

3.1 Moncalieri Power Plant

The main components of the Moncalieri Power Plant – RPW2GT unit are:

- Natural GT generator
- Heat recovery steam generator (HRSG)
- ST generator
- Distributed Control System
- Natural gas system
- Water boiler system
- Condensate system
- District heating system (DHS)
- Electrical substations and transformers

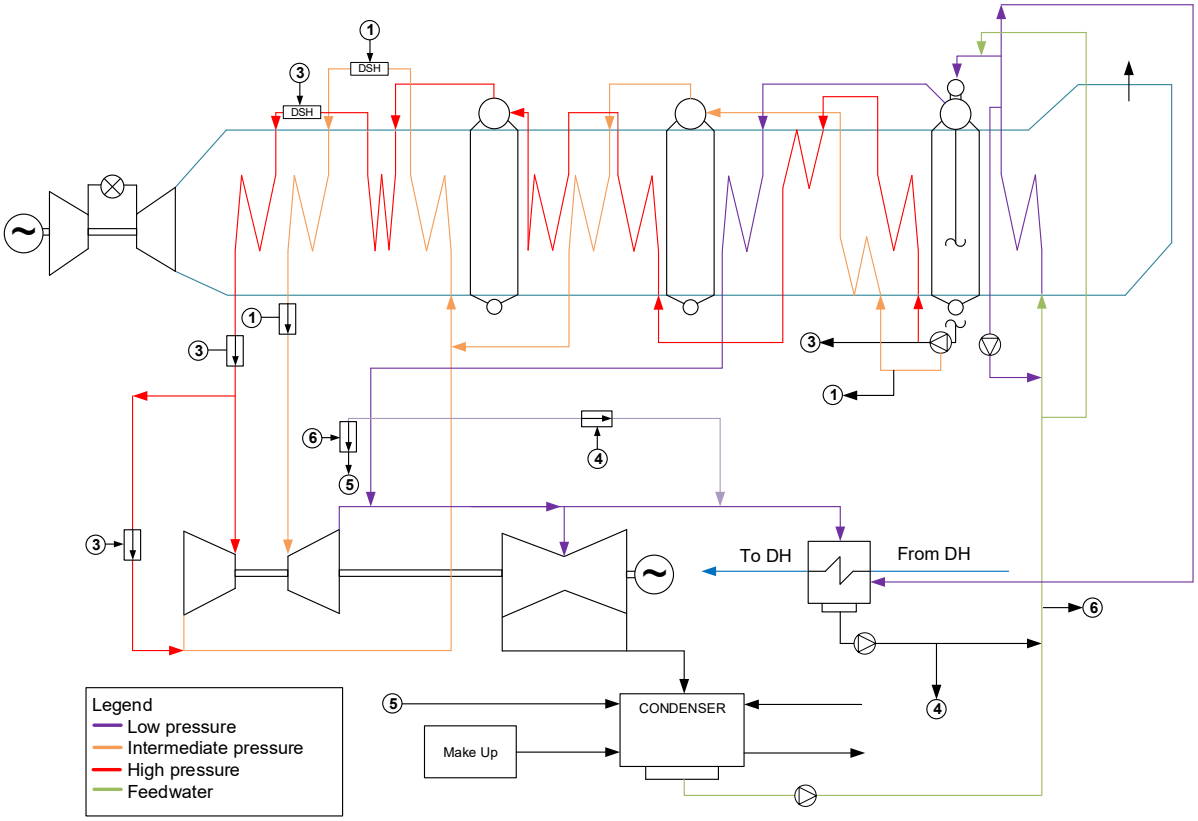

Figure 11 Moncalieri Power Plant - RPW2GT unit.

The thermodynamic cycle consists of one V94.3A4 gas turbine (GT), a heat recovery steam generator (HRSG) featuring a horizontal drum and three pressure levels with a re-superheater and a steam turbine (ST) that discharges into a water-cooled condenser. The condenser is cooled with water drawn from a branch of the Po river. The rated electrical power is approximately 400 MW_e. A bleed on the discharge of the average pressure section of the steam turbine and a withdrawal of water from the LP economizer of the HRSG feed a heat exchanger for district heating. The maximum thermal power of the district heating system is approximately 260 MW_{th}.

The deaerator device, which is built into the low-pressure drum, is fed by the two condensate pumps via the low-pressure economizer. The temperature of the condensed water, output by the economizer, is controlled by the economizer bypass regulation. The inlet temperature of the economizer is kept no lower than 55°C by the recirculation system (pumps with valve), in order to prevent corrosion caused by the formation of acid condensation from the HRSG exhaust gas.

Steam produced by the low-pressure drum that is more than the required degassing amount is delivered to the LP superheater and then to the low-pressure section of the steam turbine. The feeding pumps draw water from the low-pressure drum. Two variable speed multi-stage pumps are provided for the boiler, which fuel the medium and high-pressure drums. The medium-pressure drum is fed by an intermediate bleed from the pumps. The steam produced by the high-pressure drum is sent to the superheater. The temperature of the superheated steam is kept at a temperature below 542°C via a desuperheater positioned between the two superheated sections. The tempering water is withdrawn at the feeding pump outlet. The steam flow is sent to the high-pressure section of the steam turbine. After the HP section of the steam turbine, the steam is sent to the re-superheater of the heat recovery boiler.

The reheated steam entering the boiler is mixed with the superheated steam from the medium pressure section. Just as with the high-pressure steam, the re-superheated hot steam is tempered to a temperature below 542°C via a desuperheater located between the two re-superheated sections. The tempering water is withdrawn at the intermediate bleed of the feeding pump outlet. The re-superheated steam output by the re-superheater is sent to the medium-pressure steam turbine. When it leaves this section, via the crossover, the steam feeds the low-pressure section of the steam turbine, where it expands to the condensation pressure. The steam produced by the low-pressure drum of the heat recovery boiler is fed into the outlet of the medium-pressure section. When heat is required for district heating (cogeneration mode), part of the outlet steam from the medium-pressure exhaust and the LP section of the boiler is sent to the hot condenser. On system start-up/shut-down, or in the event of steam turbine unavailability, the steam is sent to the condenser via the MP bypass system.

The system is designed for a base load operation at ambient temperatures of 15°C. It can be operated continuously at only above 60% of the rated power of the gas turbine as in this range the burners operate in dry low NOx premix mode. The gas turbine is designed to burn natural gas. Alternative fuels are not suitable. The start-up of the steam generator is controlled by regulating the gas turbine load.

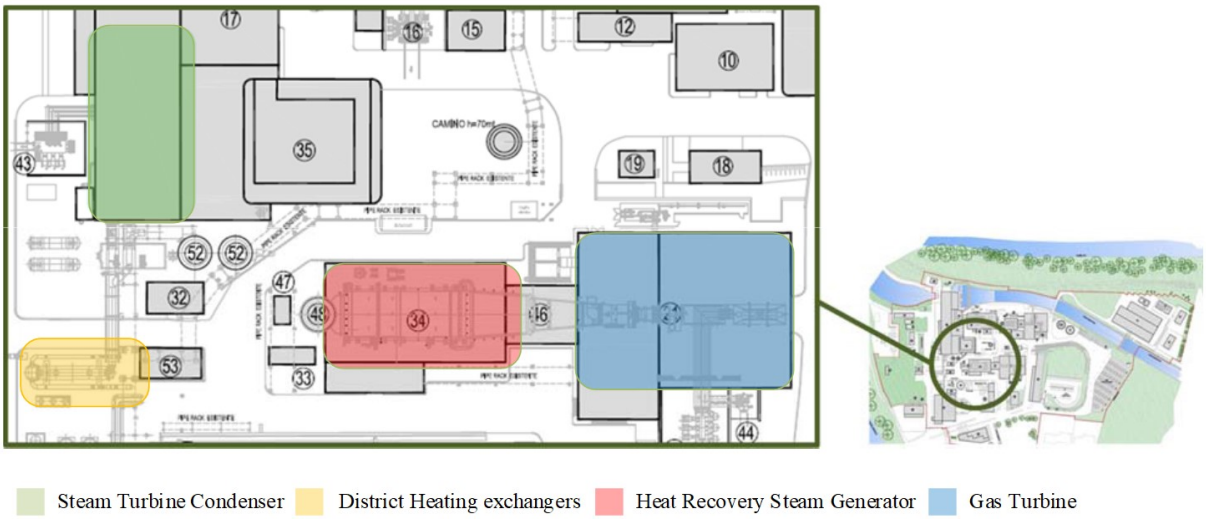

Figure 12 Location of the units.

3.1.1 Operating range

In Figure 13, the design operating range of CCGT unit, also known as Iron diagram, is depicted.

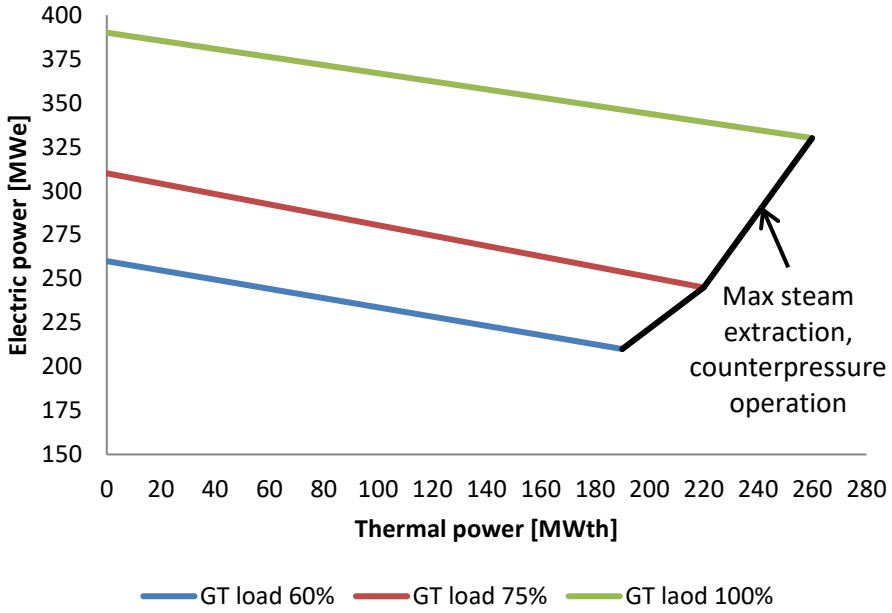

Figure 13 Moncalieri CCGT, design operating range at ambient temperature of 15 °C.

The Iron diagram simply shows the range in which the GT can be operated, and it enables the designer and operators to perform various techno-economic analyses for several options and find the related costs. Looking at the top left at the maximum gas turbine load, the unit will produce about 390 MW_{el} and no useful heat (this means that a lot of low temperature heat is discharged from the condenser to the river). As thermal energy is extracted from the ST bodies, by progressively opening valves at extraction points along the turbine, the electric power output decreases and thermal energy availability rises, and the GT operating point moves along the top line, marked as maximum gas turbine load. Eventually, a maximum thermal power and electric power of 260 MW_{th} and 330 MW_{el}, respectively, is reached on the right-hand side of the diagram [13].

If gas turbine load is now decreased and maximum steam is extracted from steam turbine, then the operating point starts moving down and to the left along the line marked counter-pressure (or back pressure) operation. Both thermal and electric power reduce until the lowest point in the diagram at about 190 MW_{th} of heat and 200 MW_{el} of electricity is reached. The gas turbine is now operating at its lowest allowed environment load (stated by the CO authorized limit). If the amount of heat taken is reduced, limiting steam extraction, then electricity generation rises, with the operating point moving to the left and up until the left hand vertical axis is reached and generating 260 MW_{el} without any heat production. Oblique lines, known as iso-fuel lines, represent all possible couplings of thermal / electric power, considering constant the load of the gas turbine and varying the amount of steam extracted. In turn, the extraction condensing turbine can work anywhere within the lowest and upper limits of the iron diagram, as infinite number of operating condition's lines exists in this envelope. The slope of the constant gas turbine load line, namely Z factor, in this case is almost constant (4÷5 MW_{th}/MW_{el}), and it specifies how much heat is gained for every unit of electricity lost [14].

4 Key Performance Indicators – KPI

For estimation of the techno-economic performance of the layouts, key performance indicators (KPI) are used. They are a quantifiable measure of whatever is valued in the proposed solution. They include economic, environmental and technical indicators. In this chapter, KPIs are described and quantified. A description of a KPI was given by Intrafocus:

"A Key Performance Indicator is something that can be counted and compared; it provides evidence of the degree to which an objective is being attained over a specified time" [15]

For this project, the following key performance indicators were chosen to analyse the layouts previously mentioned; in turn, some of the KPIs have been modified accordingly with the characteristics and available data of each layout.

4.1 Technical KPIs

Net electrical output is the total electricity provided to the grid with parasitic losses within the combined cycle subtracted from it.

For Layout 1 equation found in Chapter 5.4.1. has been used. While for Layout 2&3 the equation 4.1 was used.

$$\mathrm{E_{el}} = \int \left(E_{GT} + E_{ST} - E_{para}\right) dt \tag{4.1}$$

Net thermal power is, in the case of combined heat and power plants, the total district heating produced by the plant.

$$\mathrm{E_{th}} = \int \left(E_{DH}\right) dt \tag{4.2}$$

Net electrical efficiency is estimated as the ratio between the net electrical output and total fuel energy supplied and it stands for the power conversion quality of the combined cycle.

$$\eta_{el} = \frac{E_{el}}{\int \left(m_{fuel} \cdot LHV_{fuel}\right) dt} \tag{4.3}$$

Net thermal efficiency describes the efficiency of producing district heat, and it is the thermal power over the total fuel energy input.

$$\eta_{th} = \frac{E_{th}}{\int \left(m_{fuel} \cdot LHV_{fuel}\right) dt} \tag{4.4}$$

The net plant efficiency is fundamentally the sum of the net electrical and thermal efficiencies and gives an estimation of the global efficiency for cogenerative power plant.

$$\eta_{CC} = \eta_{el} + \eta_{th} \tag{4.5}$$

The thermal energy storage utilization factor refers to the ratio of the time that TES is in use to the total time that it could be used over a year.

$$TES_{utilization} = \frac{\sum E_{TES,day}}{365 days \cdot E_{TES,max}} \tag{4.6}$$

For Layout 1 two distinct methods were identified. For each method, the total charge differential throughout the year is summed up and then compared against a case where complete charging from 15% to 100% (1), or from 0% to 100% (2) would take place each day of the year.

The load and mass flow ramp-ups show how fast the ramping up of these parameters occurs over the desired time period. Equation 4.7 and 4.8 were used for Layout 2&3.

$$\frac{\Delta \text{load}}{\text{dt}} \tag{4.7}$$

$$\frac{\Delta \text{massflow}}{\text{dt}} \tag{4.8}$$

For Layout 1 the ramp-up for the heat pump was estimated as follows,

$$\frac{\Delta P_{HP}}{dt} \tag{4.9}$$

4.2 Economic KPIs

The economic feasibility and profitability of the project is measured with net present value, which refers to the cash inflows over the lifetime of the plant [16].

$$NPV = -\mu C_{INV} + \sum_{t=1}^{n} \left(\frac{I_{tot} - C_{O\&M}}{(1+i)^t} \right) \tag{4.10}$$

Capital charge factor:

$$\mu = \frac{i(1+i)^n}{(1+i)^n - 1}$$

Total annual income:

$$I_{tot} = sp \cdot P$$

The discounted payback time refers to the time required to break even from undertaking the initial capital investment, by discounting the future cash flow [17].

$$PBT = \frac{\ln(B - C_{O\&M}) - \ln[(B - C_{O\&M}) - i \cdot C_{inv}]}{\ln(1+i)} \tag{4.11}$$

The levelized cost of electricity is the average minimum price at which electricity must be generated from the power plant to break even over the lifetime of the project. For layout 1 equation 4.12 was used, while for Layout 2 and 3 equation 4.13.

$$LCoE = \frac{\alpha \cdot C_{inv} + \beta \cdot C_{decom} + C_{O\&M} + C_{labour}}{E_{el,net}} \tag{4.12}$$

$$LCoE = \frac{\alpha \cdot C_{inv} + \beta \cdot C_{decom} + C_{O\&M} + C_{labour} - hcr \cdot E_{th,net}}{E_{el,net}} \tag{4.13}$$

Where

$$\alpha = \frac{(1+i)^{n_{cons}} - 1}{n_{cons} \cdot i} \cdot \frac{i \cdot (1+i)^{n_{oper}}}{(1+i)^{n_{oper}} - 1} + k_{ins}$$

$$\beta = \frac{(1+i)^{n_{dec}} - 1}{n_{dec} \cdot i \cdot (1+i)^{n_{dec}-1}} \cdot \frac{i}{(1+i)^{n_{oper}} - 1}$$

Internal rate of return is calculated as a discount rate that makes the net present value equal to zero. Thus, the formula is solved for r and the solution is IRR.

$$IRR = r \; when \sum_{t=1}^{n} \left(\frac{B - C_{O\&M}}{(1+r)^t} \right) - C_{inv} = 0 \tag{4.14}$$

4.3 Environmental KPIs

Specific carbon dioxide emissions refer to the CO_2 emissions per unit of electrical or thermal power produced by the combined cycle.

$$x_{CO_2} = \frac{CO_{2\ specific\ emission}}{E_{net}} \tag{4.15}$$

Specific water consumption is the amount of water consumed per unit of electrical output generated by the power plant.

$$x_{H_2O} = \frac{H_2O_{\ specific\ consumption}}{E_{el,net}} \tag{4.16}$$

5 Layout 1: Power-Oriented Combined Cycle

In this chapter, the first layout is described with more details about components and control strategy defined.

The power-oriented layout (POCC) applies to combined cycles mainly devoted to electrical power generation by introducing a new Integrated Inlet Conditioning system (IIC) with thermal storage, to increase power production during high ambient temperature period. In fact, due to heating, ventilation and air conditioning (HVAC) systems diffusion, a peak of electrical consumption is required when the higher temperature reduces the capability of the production system. Moreover, the essential role of POCCs in a market with a higher share of renewable energy sources is spinning reserve and back-up capacity for grid stabilization. In such a case, it is beneficial to maintain the full capacity even in the less favorable conditions.

Figure 14 depicts the power-oriented combined cycle, with thermal energy storage, ambient heat exchanger, gas turbine heat exchanger and heat pump, along with valves and pumps required to maintain sufficient flow during the different operating modes. All of the new components are installed before the compressor inlet, and hence this system can be relatively easily installed in already existing power plants compared to making changes within the cycle itself.

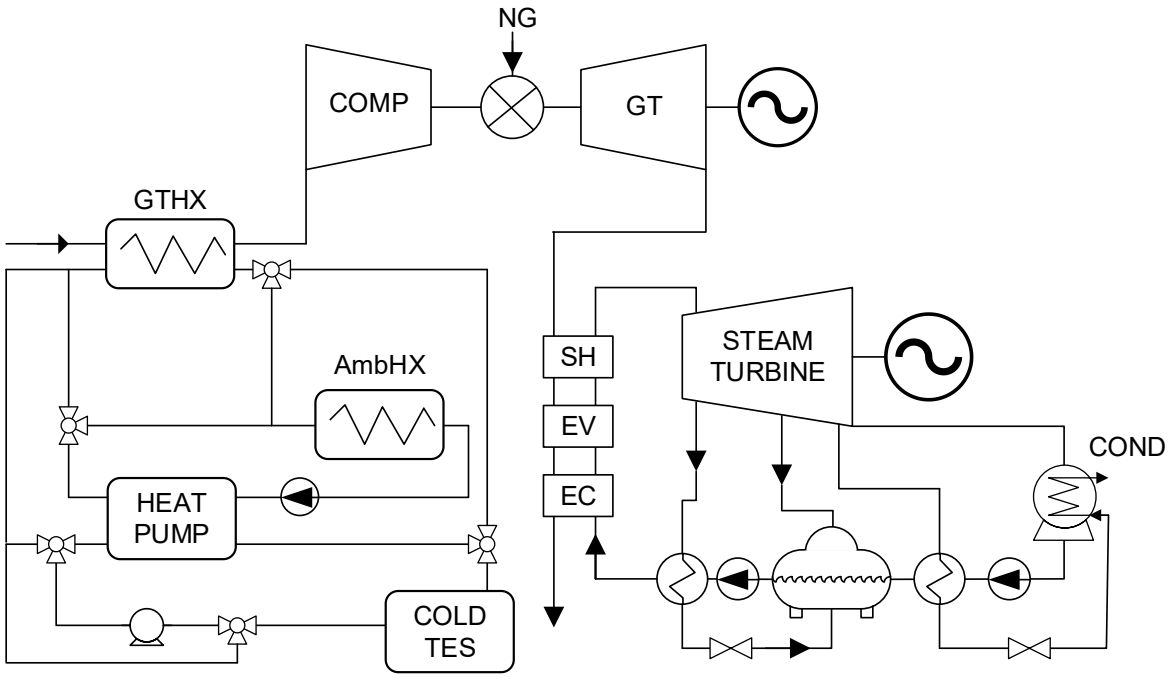

Figure 14 Power oriented combined cycle

Until the last ten years, the main focus of this technology was directed to inlet cooling systems as cost-effective way to add machine capacity (+10-15% for heavy-duty frames, up to 25% for aeroderivative frames) during the period when peaking power is required in operational environment with warm and dry weather [18]. With the increased push to flexible operations, a secondary solution was introduced: to heat the intake air to decrease its density and reduce the minimum load and increase part-load efficiency. Anti-ice systems are often adopted introducing thermal or GT cycle losses (e.g. discharge compressor air recirculation). Until now,

no integration of the cooling and heating processes was done, which is one of the main PUMP-HEAT objectives. The Integrated Inlet Cooling system was designed to cope with the increase of RES share in the European grid, acting also as a smart load in a grid balancing perspective. Thanks to the introduction of the TES, in fact the cooling energy provided by the mechanical chiller can be stored and used during the late afternoon ramp and electrical peak (decoupling of the HP electrical consumption and its thermal effect).

5.1 Inlet Conditioning with TES

The main drivers for the selection of the best strategy are two: the electricity prices and the ambient temperature. In particular, the electrical price of electricity mirrors the abundance of scarcity of this resource compared with the actual consumption rate. One of the main challenges is to overcome the present GT-oriented strategy of cooling [19] / heating control systems, by taking into account the conditioning effect over the whole combined cycle. In fact, while combined cycle power has the same negative correlation of gas turbine to the ambient temperature, combined cycle heat rate curves vs inlet temperature are not monotonic as the one for the gas turbine, thanks to bottoming cycle higher performance, so an optimum [20] (usually around 25 °C) must be found, taking into account also IIC performance. Indeed, the maximum of the efficiency does not correspond to a maximum in the power output this will be exploited to reduce the power output with a positive effect over the efficiency.

During low electricity prices period, off-peak period, TES is charged as shown in Figure 15 (left).

1) The HP is fed by CCs electricity, reducing the electricity delivered to the grid

2) GT inlet is heated by heat pump condenser heat reducing the electrical output

It must be noticed that the HP can work also as Grid Controller Load, charging the Cold TES even with the CC not running.

During high electricity prices period, peak period, the objective is to increase the CCs power output discharging the cold TES and cooling down the GT intake. The flow schematic for this operating mode is depicted in Figure 15 (right).

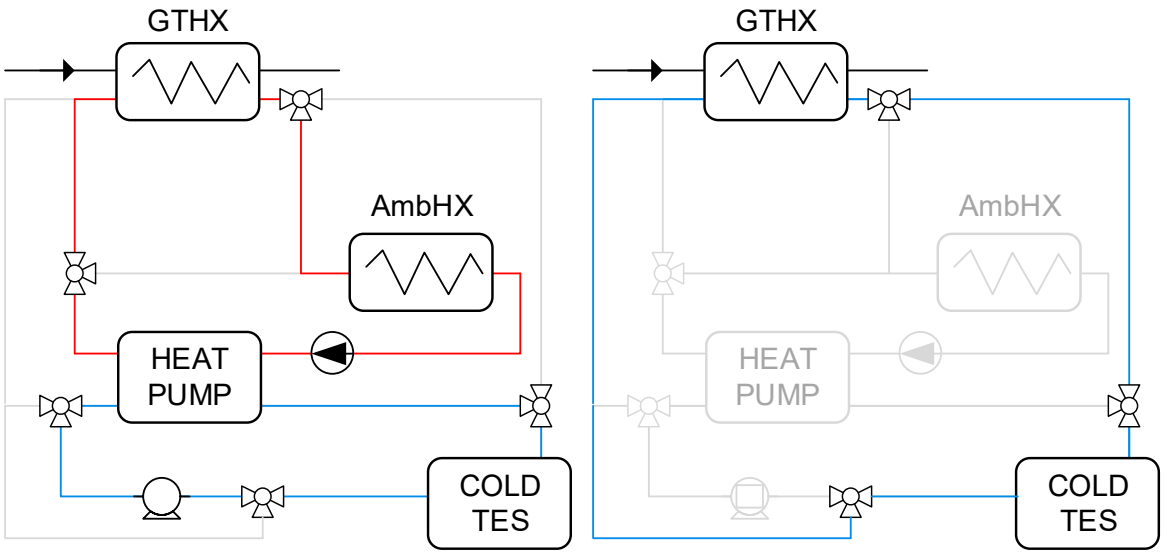

Figure 15 Charging flow diagram (left), discharging flow diagram (right).

If the ambient temperature is high, heating up the intake during off-peak period can require high temperature on the hot side of the heat pump leading to a decrease of the heat pump COP and so a reduction of the efficiency of the system, so the heat released from the HP can be directly discharged to the ambient.

A specific condition to be investigated is the effect of the *Continuous Cooling*, where TES in not used while HP is operated with the refrigerating effect directly fed to the GT intake. This is considered as the fourth operating mode.

If the ambient temperature is low, to avoid ice within the intake an inlet heating system must be adopted. This is already in place at Moncalieri, and was therefore modeled as an external system which increases the GT inlet temperature to the minimum 5°C.

As long as ambient temperature is above the minimum required, electricity price is used as the control switch which determines when either charging or discharging occurs. For continuous cooling, ambient temperature is an additional condition used as an on/off switch.

The expected benefits that adopting this IIC control strategy could bring are as follows

- during off-peak hours, the inlet heating can increase the efficiency up to 2%

- during peak hours, the HP is shut off and the TES is discharged to the inlet coil increasing the maximum power output, P_{max} (+10%).

The curves illustrated in Figure 16 represent the typical behavior of gas turbine combined cycle and are based on a 1+1 combined cycle of 400MW electric power. The preliminary analysis was performed evaluating the effect of air temperature, while all the other as well as the condenser pressure remain unchanged.

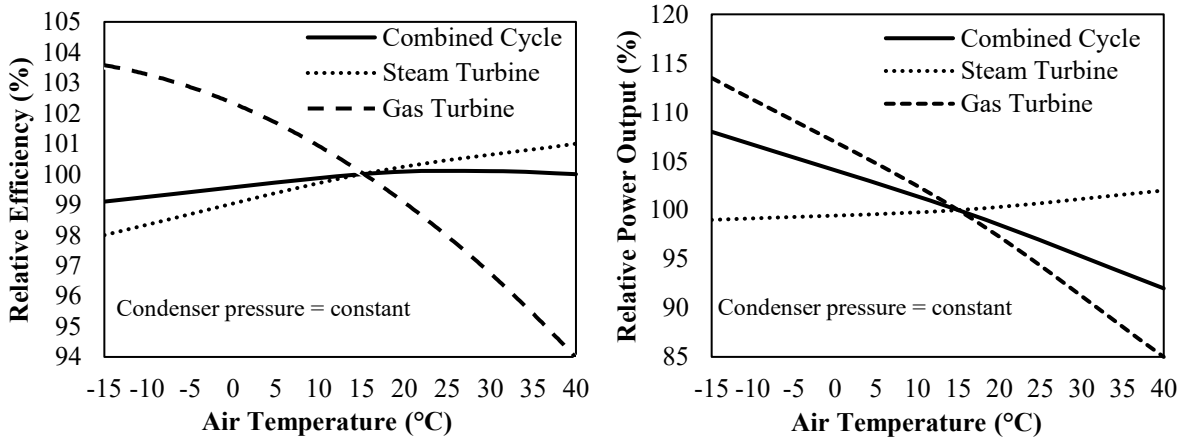

Figure 16 . Combined cycle performance vs Inlet temperature. (a) Efficiency, (b) Power output. [21]

An increase in the air temperature, as performed in the inlet heating condition, has a slight positive effect on the efficiency of the CC. Because the increased temperature in the gas turbine exhaust enhances the efficiency of the bottoming cycle, it more than compensates for the reduced efficiency of the GT unit [18]. The effect on the overall power output is a net reduction, regardless of the temperature level.

The proposed solution avoids the direct contact between the HP refrigerant and the external Heat Exchanger (the one located at the GT inlet and the ambient one) or the TES. As it relies

on an intermediate media fluid (ethylene glycol-based water solutions), it minimizes the risk of refrigerant dispersion while increasing the flexibility of the system. The HP refrigerant in fact will be then confined inside the HP enclosure where all the health and security prescription can be adopted. Moreover, the technical prescription related to the specific refrigerant (e.g. material compatibility) will apply only to the HP systems and its heat exchangers (evaporator and condenser). The effect of switching between different layouts and controlling of the energy delivered to the gas turbine inlet can be made by working on standard piping. This solution applies also to retrofit applications for power plants that already include heat exchanger in the filter house as anti-ice system.

During low electricity prices period, off-peak period, the GT Intake Heat Exchanger, GTHX, is placed in series/parallel with an ambient heat exchanger, AmbHX, which dissipate the amount of heat in excess. A three-way valve is adopted to control the temperature at the GT inlet. The cold loop of the heat pump then circulates through the TES, charging it.

During high electricity prices, peak period, The GT Intake Heat Exchanger is connected in closed loop with the TES and the circulating mass flow rate is controlled to obtain the desired GT inlet temperature.

One of the design aspects of this layout is to define a proper TES capacity to conveniently exploit daily price variations, and their impact over the charging and discharging period length. The GT inlet temperature set points must be selected taking into account the effect of such parameter over both combined cycle power output and efficiency. One of the main challenges is to overcome the present GT-oriented strategy of cooling/heating control systems, by taking into account the conditioning effect over the whole combined cycle. An optimum value of temperature (usually 25 °C) may be the IIC control set point during part load.

5.2 Continuous cooling

The Continuous Cooling solution applies to periods in which the electricity price is continuously favorable to production base load in high temperature condition. In this case the HP is not switched off and the GTHX is directly fed by the water mixture coming from the evaporator of the Heat Pump (blue line of Figure 17), while the hot loop heat is discharged to the ambient (blue line). The GT inlet temperature is controlled by controlling the heat pump power level. In this operating condition TES is assumed to be not used (or already discharged). The difference between the two approaches are reported in Table 1.

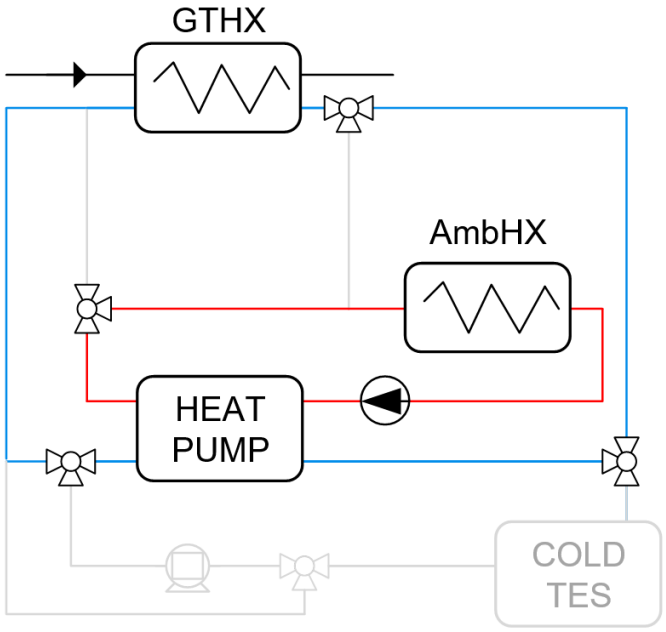

Figure 17 Continuous cooling flow diagram

Both of the systems depicted in Table 1 are implemented in this model, and it is not therefore directly clear how much of the benefit can be attributed to a single operational mode. Hence, a model run with only continuous cooling operation was conducted and the economic results can be found in Chapter 5.7.

Table 1 Comparison between TES and Continuous Cooling Solution [22]

	Advantages	Disadvantages
TES	• Low on-peak parasitic power required • Lower investment cost than direct chilling for peaks lasting less than 8 hours	• More off-peak power required • Higher capital cost than direct chilling for peaks lasting more than 8 hours • More complex system than direct chilling • Chilled air available for only part of the day
Continuous Cooling	• Provides chilled air 24 hours a day • Simple and reliable • No off-peak parasitic power required • Very efficient	• Higher on-peak parasitic power required • Refrigeration equipment is sized for peak load → increased capital cost

5.3 Component description

In this chapter, the main components related to the layout 1 are discussed in more depth. These components include namely latent thermal energy storage and heat pump. The additional heat exchangers are not considered a new component to a combined cycle as they are commonly used in power plants and were therefore not further discussed.

5.3.1 Thermal energy storage

Implementation of storage in the combined cycle power plant allows higher flexibility of plant operation. With energy storage, demand peaks can be shifted and smoothened so that less peak production capacity is necessary. This can lead to savings in economic terms.

According to Kalaiselvam and Parameshwaran [23], the energy storage application domain and energy demand define the characteristics which are required from the technology. The following characteristics were identified, among others.

Storage capacity is measured by the available energy in the storage system after charging. It is important to note that the depth of discharge influences the usable energy due to a minimum state of charge. Weakening of TES efficiency occurs due to frequent discharge-charge cycling and hence the amount of energy available will be, in the end, lower than storage capacity.

Energy density is a simple calculation of the total energy stored over the storage volume. *Power density* refers to the rated power output to the storage volume.

Response time is a characteristic measuring the discharging speed, or the time it takes to offset load demand requirements.

Self-discharge represents the rate of losses of stored energy during the times when TES is not used.

Efficiency measures the losses occurring unavoidably when operating an energy storage system on continuous basis.

Life expectancy is an evaluation of the system lifetime, with the important objective of guaranteeing the system reliability.

Operational economics describe the costs which occur when operating a storage system, which often includes auxiliary components such as pumps and heat exchangers.

5.3.2 Latent Thermal Energy Storage

Among the thermal energy storage (TES) systems, latent heat-based phase change materials (PCM) have shown potential in the recent decades due to their high storage density and small temperature swing. In fact, when a typical sensible heat storage has an energy density of 25 kWh/m^3, PCM-based TES systems may reach an energy density of 100 kWh/m^3 (see Figure 18) [24]. In addition, PCM's phase change temperatures can be changed according to the operational requirements. However, there is significant challenge with discharging and charging. The thermal conductivity of phase change materials is typically between 0.2 $\frac{W}{m\,K}$ and 0.7 $\frac{W}{m\,K}$. Another difficulty is related to safety; organic compounds pose a fire hazard due to their flammability. That is why here mainly inorganic salt hydrates are considered as a possible material for the POCC.

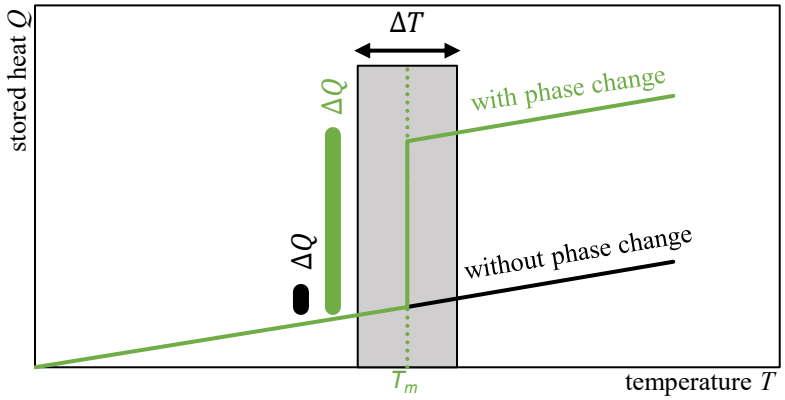

Figure 18 T-Q diagram for sensible and latent TES [24].

In basic terms, latent TES (LTES) involves material which experiences phase change during storing and discharging of thermal energy. Isothermal, or quasi-isothermal conditions govern the phase change from liquid to solid and vice versa. A heat transfer medium (HTM), which surround the PCM, is used to transfer heat between the PCM and application. The PCM processes for both storing and discharging of energy are shown in Figure 19, where heat release (a) and heat absorption (b) can be distinguished. The heat stored by PCM can be expressed by the equation

$$Q_{PCM} = m[(c_p \Delta T)_{sensible} + H + (c_p \Delta T)_{latent})]$$

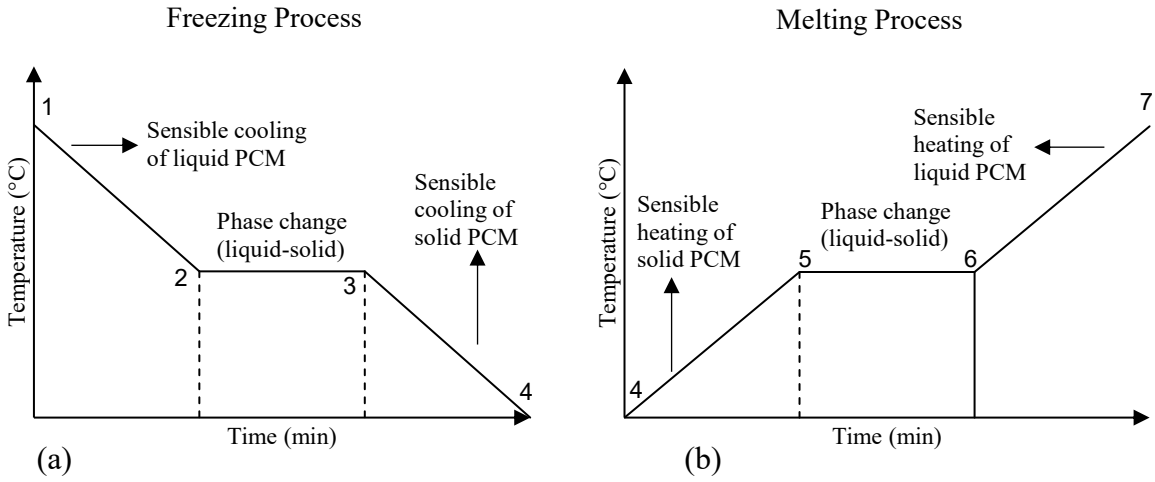

Figure 19 . Heat storage processes of phase change materials. (a) Freezing process, (b) Melting process

There are various types of LTES storage, such as submerged heat exchanger and direct contact storage material. However, for the purpose of this project, TES with encapsulated storage material was chosen. In this design, encapsulated phase change materials are used. The size of the encapsulations determines the heat transfer surface and the packing factor of the storage material. The advantages of this second type of design are non-contamination of the HTF and ease of maintenance for switch and change of the materials. The disadvantages are however the cost and the challenges in designing the diffusers for evenly distributed flow.

Figure 20 depicts the concept of an encapsulated storage material TES design.

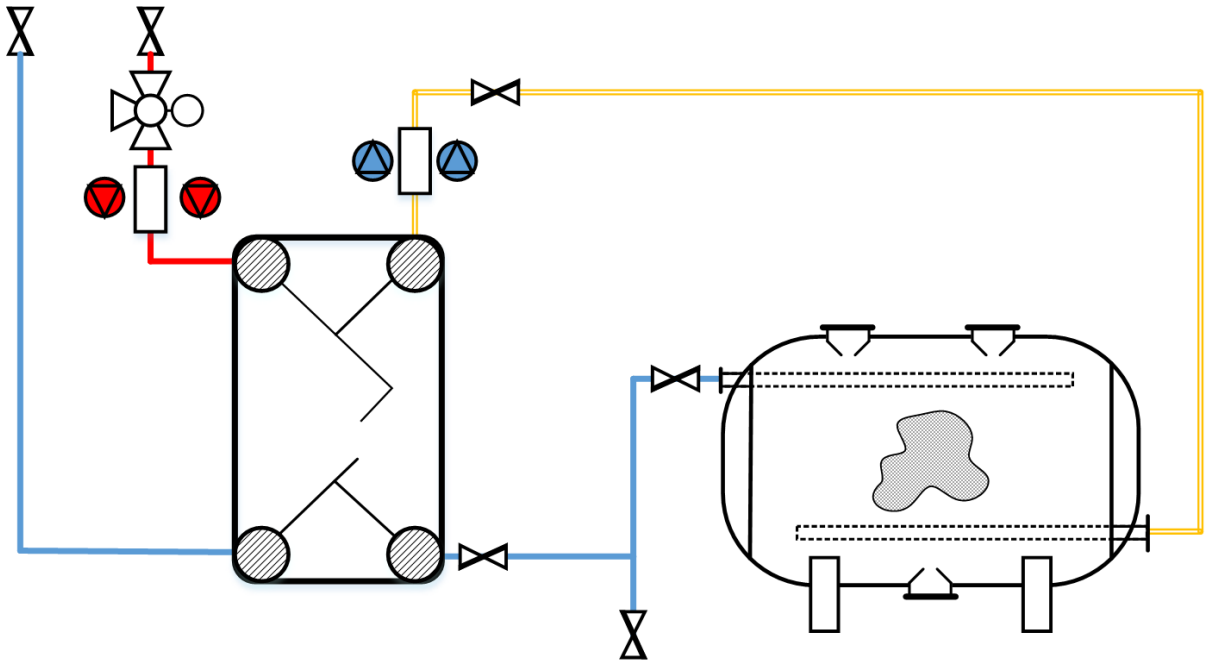

Figure 20 Thermal energy storage with encapsulated material.

5.3.2.1 Thermal Energy Storage simulation

For the modeling of the POCC system, it is important to acknowledge some aspects related to how the function for TES behavior was created. Here, the methodology of calculating PCM in operation is described.

The thermal energy storage behavior was based on a numerical model of a unit suited specifically for precooling of gas turbine inlet gas. A specific downscaled design of the thermal energy storage unit was made, from which correlations capturing the physical phenomena during charging and discharging processes were derived and then applied in the model for a larger scale system (depending on the case been investigated). The numerical model of the TES was built simulating a 5 m^3 tank with 1.9 m diameter filled with phase change material (PCM) based capsules in a compact arrangement (packing factor of 73.9%). The tank was discretized into eleven thousand columns where each column consists of 40 quarter capsules. An example of the analyzed model and capsule geometries are provided in Figure 21.

Each column consists of 19500 mesh cells at mesh quality above 0.54. Assumptions are made to enhance the convergence of the model: isotropic material properties; negligible buoyancy force; laminar flow; negligible capsule thermal resistance. Enthalpy method is used here for the phase change simulation, where the material property of the PCM is based on T-History method as described by Chiu J. and Martin [25]. The performance curves for both charge and discharge are modeled based on two operating conditions each with three mass flows (Table 2). These flows represent the nominal, 50% and 200% of the downscaled mass flow. The operating conditions are set with constraints on the minimum outlet temperature of the heat transfer fluid (HTF) during charge and on the maximum outlet HTF temperature during discharge.

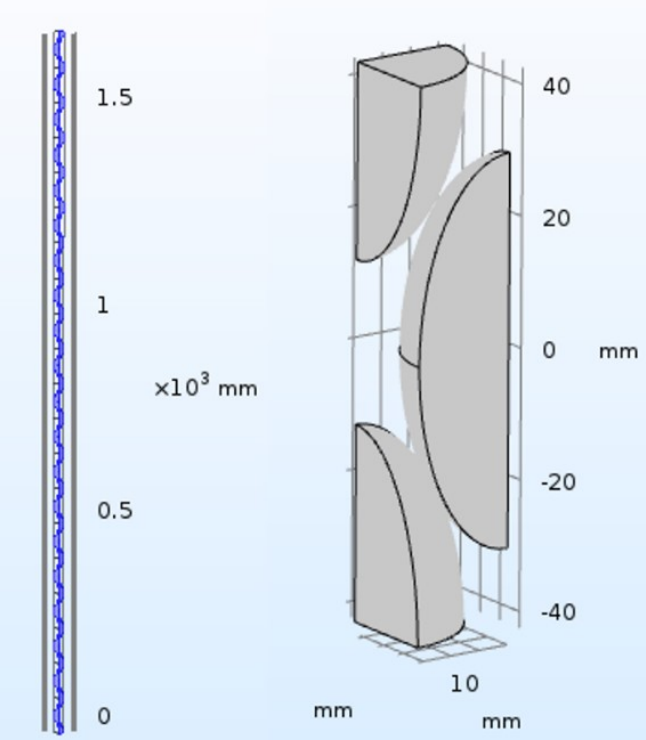

Figure 21 TES Model Geometry: Discretized Column (left), Capsule Geometry (right)

Table 2 TES modeling parameters

	Charging (Case A)	Charging (Case B)	Discharging (Max P)	Discharging (Min P)
T $TES_{initial}$ (°C)	7.8	7.8	1.8	1.8
T HTF_{inlet} (°C)	-7.5	-7.0	20.0	8.0
Constraint: T HTF_{out} °C	> -5	> -5	< 15	< 6.3
Mass flow $_{nominal}$ (kg/s)	8.58	10.3	4.06	9.54
Mass flow $_{50\%}$ (kg/s)	4.29	5.16	2.03	4.77
Mass flow $_{200\%}$ (kg/s)	17.2	20.7	8.14	19.1

The simulated PCM behavior in TES is illustrated in Figure 22. A constant mass flow rate of 5 kg/s was used with a temperature of 25°C. The initial TES temperature was 0°C.

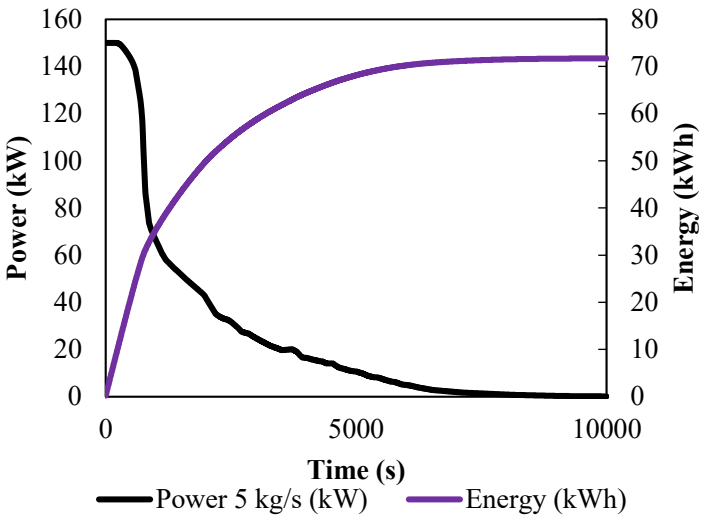

Figure 22 Power and energy capacity of TES with encapsulated PCMTF4.8.

The results from these simulations were combined to create an interpolation function within MATLAB, more in detail described in Chapter 5.4.

5.3.3 Heat Pump

For the case of POCC, a so-called warm temperature heat pump may be used as it is only necessary to perform cooling down to about -7°C, and heating up to 40°C. This is a commonly found range in heat pumps. Although various types of cooling techniques exist, namely absorption chilling and evaporative cooling, mechanical refrigeration cooling was chosen by the preliminary study that this thesis is based on. Mechanical chillers are a mature technology readily available and modifiable for any application. The capacity of the heat pump is based on a cooling demand, which in the case of Moncalieri during continuous cooling is cooling down the ambient air to match a certain desirable condition. In Turin, the ambient temperature rarely goes above 35°C, but temperatures above 25°C occur commonly in the summer. An optimal performance of the combined cycle requires, depending on the gas turbine nominal conditions, a temperature of 15°C approximately. During charging of the cold TES, the temperature drop may be far larger, yet the mass flow may be chosen to be lower and thus, the same HP capacity would be needed.

In terms of the refrigerant, ammonia was preliminarily shown to be the most reasonable for this case study. It has a low global warming potential along with a low price.

5.4 Modeling

In this chapter, details about each component in the model are given. Since MATLAB alone cannot be used to model a fully transient unit, the code was complimented with parts of code from TRNSYS. These codes mainly model the off-design performance of units which were first sized in MATLAB. The syntax for these codes can be found in Appendix A.1.

5.4.1 Combined Cycle load and efficiency

The performance curve given by IREN was used to calculate the power output. Only the 100% curve was used since the mass flows of air and fuel were kept constant throughout the year. For this reason, no KPI regarding load ramping was considered. According to the equation provided, only inlet temperature to the gas turbine affects power generation. This is a simplification as it does not consider ambient pressure or condenser temperature. The latter is dependent on the river temperature and is seasonal.

The exact equation used for power generation is as follows:

$$P_{CC} = P_{CC,nominal} \cdot (0.0000166994 \cdot (T_{GTin})^3 - 0.000152752311 \cdot (T_{GTin})^2 + 0.000112032405 \cdot T_{GTin} + 1.024691307344)$$

Where

$P_{CC,nominal}$: Combined cycle nominal power generation in MW

T_{GTin}: GT inlet temperature in °C

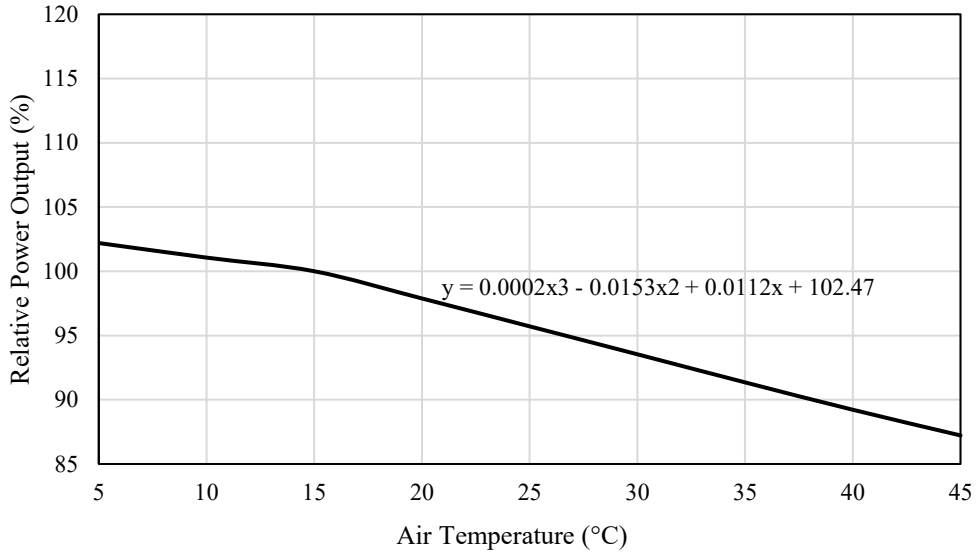

Figure 23 Combined Cycle power output curve.

For the efficiency, a constant mass flow of fuel of 14.62 kg/s was considered as given in the full electric mode flowsheet from IREN. In addition, an LHV of 47.031 MJ/kg was given in the flowsheet.

Although no ramping up or down needs to be considered due to assuming constant load, quick heating and cooling of the GT inlet temperature does occur. Within a time step of 15 minutes,

GT inlet can be at maximum heated by 24°C and cooled by the same amount. However, the average increase and decrease of temperature is well within 1°C/15 minutes.

5.4.2 Pressure drop

No pressure drop function was used during the modeling, i.e. no component for compressor due to simplification of the model. As load is constant, the pressure drop can therefore be considered constant.

5.4.3 Heat pump

The heat pump was modeled as two heat exchangers which interact through a simple COP calculation. For all operating modes, an initial COP was chosen (4.5), after which the next time step uses the temperatures at outlets of evaporator and condenser of the previous time step to calculate the new COP. Since this is the maximum theoretical COP, it was estimated that a reasonable maximum COP for these operating conditions would be 5. In a single time step of 15 minutes, the heat pump power can at maximum be increased by a variable amount of MW. Here the maximum ramp-up was chosen as 1.25 MW/15 minutes (0.083 MW/min). In terms of mass flows, the ramping up is 500 kg/s in 15 minutes (33 $\frac{kg}{s}/min$) in continuous cooling, and between 13 and 33 $\frac{kg}{s}/min$ in charging and discharging. Ramp-down wasn't considered as a constraint (assumed to be slower than ramp-up) and is therefore not estimated. The following equations were used in the heat pump model.

$$COP_{cooling} = \frac{T_{evap,out}}{T_{cond,out} - T_{evap,out}} \tag{5.1}$$

$$COP_{heating} = \frac{T_{cond,out}}{T_{cond,out} - T_{evap,out}} \tag{5.2}$$

$$P_{eva} = P_{HP,el} \cdot (COP - 1) \tag{5.3}$$

$$P_{cond} = P_{HP,el} \cdot COP \tag{5.4}$$

5.4.3.1 Water-Glycol mixture

The water-glycol mixture was considered to be 35% by volume and has been given the following specific heat equation, where T is temperature in °C.

$$C_{p,WG} = (0.0006 \cdot T + 08652) \cdot 4.1868\ [kJ/kgK] \tag{5.5}$$

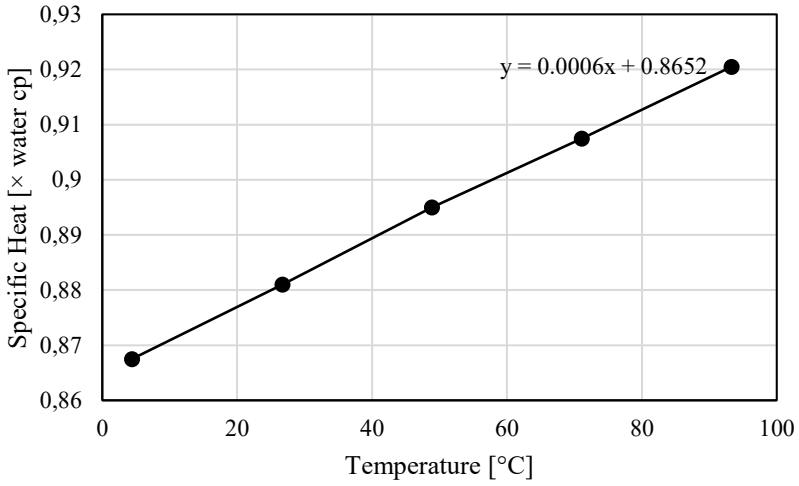

Figure 24 Water-glycol mixture specific heat.

5.4.4 Gas Turbine Heat Exchanger

The heat exchanger component (Unit 315, *economizer*) was recreated from TRNSYS component library into MATLAB syntax. Initially, the nominal conditions were chosen, and the component was sized accordingly. Table 3 contains variables considered when sizing the component.

Table 3. Gas turbine heat exchanger design parameters.

Design variable	Value
Ambient pressure	101 325 Pa
Air inlet	15°C
Air outlet	7.5°C
Liquid-side pinch temperature	2°C
Gas-side pinch temperature	3°C
Inlet WG mixture	0°C
Outlet WG mixture	25°C
Air mass flow	666 kg/s

5.4.5 Ambient Heat Exchanger

The same methodology for sizing the Ambient Heat Exchanger was used, i.e. same function. However, different input variables were used as shown in Table 4.

Table 4. Ambient heat exchanger design parameters.

Design variable	Value
c_p air in	1.006 kJ/kgK
c_p air out	1.006 kJ/kgK
c_p WG mixture in	3.6978 kJ/kgK
c_p WG mixture out	3.6727 kJ/kgK
Air mass flow	666 kg/s
Inlet WG mixture	25°C
Outlet WG mixture	20°C

The design mass flow of WG mixture was calculated with the following equation

$$MF_{WG} = \frac{P_{HP,el} \cdot COP_{dsgn}}{C_{p,WG,in}T_{in,AmbHX,dsgn,WG} - C_{p,WG,out}T_{out,AmbHX,dsgn,WG}} \quad (5.6)$$

The design mass flow of air was calculated with this formula

$$MF_{WG} = \frac{MF_{WG} \cdot (C_{p,WG,in}T_{in,AmbHX,dsgn} - C_{p,WG,out}T_{out,AmbHX,dsgn})}{C_{p,air,out}T_{out,AmbHX,dsgn,air} - C_{p,air,in}T_{in,AmbHX,dsgn,air}} \quad (5.7)$$

Finally, the same function as described in the previous chapter about GTHX was used to estimate the heat exchanger UA value and efficiency in design conditions.

5.4.6 Pumping power

Power consumption for pumps is taken directly from the TRNSYS unit *pump*. The constants considered in the model are

Pump efficiency: 85%

Water-Glycol density: 871 kg/m^3

Pressure drop in HXs: 1 bar

5.4.7 TES transient function

Four CFD simulations were originally run, two for discharging and charging each. In each simulation, an inlet temperature was chosen and kept constant while mass flow was changed three times to get a representative data set. The data from the CFD calculations was used to create an interpolation function which takes as inputs the state of charge, mass flow, time step, inlet temperature, and operation mode (charging/discharging). The outputs, state of charge and temperature, are calculated with the interp1 function. Since the time step in the simulation was 5 seconds, it was necessary to keep the POCC model time step as low as possible. It is a trade-off between model accuracy and the time it takes to run the model. It was later noticed that 15 minutes is an acceptable time step, which gives reasonable results while keeping the simulation time feasible. However, at lower levels of state of charge, the output given by the function cannot be used due to the shape of the discharging curves. Thus, a minimum state of charge (15%) was chosen. Furthermore, no thermal losses were considered in the TES.

For charging, data from two sets of calculations were used. The first one, shown in Figure 25, had a constant inlet temperature of 265.68 K, while the second one (Figure 26) was calculated with a temperature of 266.15 K. For the first case, three distinct mass flows were used; 4.29, 8.58, and 17.16 kg/s, while for the second case, the mass flows were 5.16, 10.33, and 20.66 kg/s. In the interpolation function (interp1), the mass flow can be varied, and the outputs state of charge and temperature thus calculated.

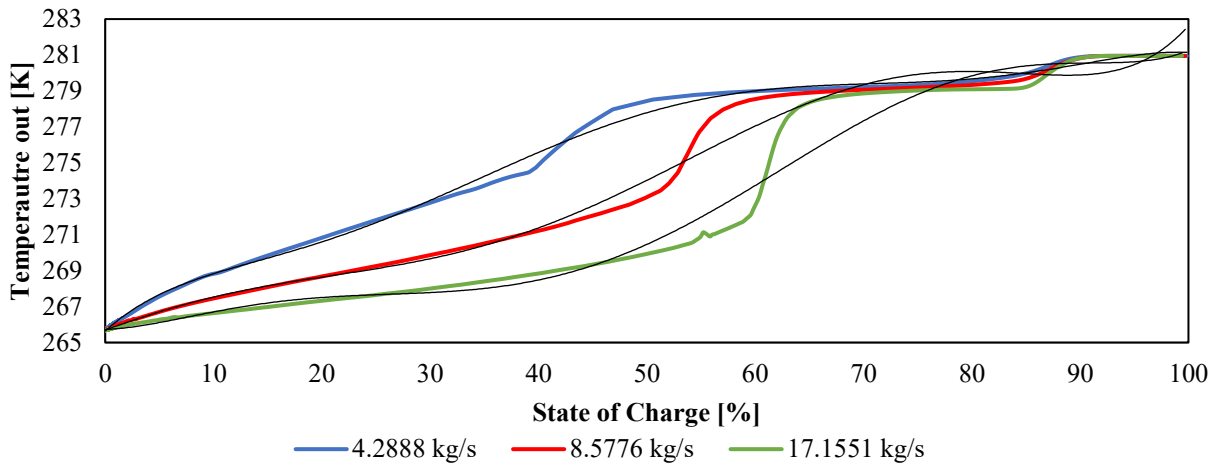

Figure 25 Charging polynomial functions at 265.68 K inlet temperature.

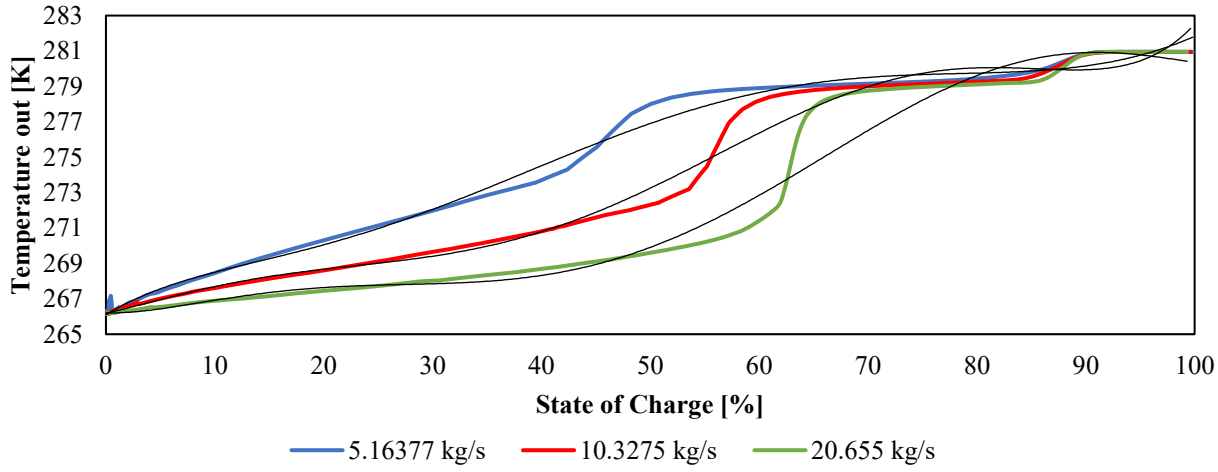

Figure 26 Charging polynomial functions at 266.15 K inlet temperatures.

The polynomial functions for charging cases are as follows, with mass flow in an ascending order. First, for the 265.68 K case:

$$SoC_{MF1} = 8^{-10x^6} - 2^{-7x^5} + 2^{-5x^4} - 0.0006x^3 + 0.0054x^2 + 0.1403x + 266.19$$

$$SoC_{MF2} = -2^{-10x^6} + 1^{-7x^5} - 1^{-5x^4} + 0.0008x^3 - 0.0203x^2 + 0.376x + 266.1$$

$$SoC_{MF3} = 6^{-10x^6} - 2^{-7x^5} + 2^{-5x^4} - 0.0009x^3 + 0.0152x^2 - 0.0101x + 266.21$$

Then, for the 266.15 K case:

$$SoC_{MF1} = -7^{-10x^6} + 2^{-7x^5} - 3^{-5x^4} + 0.0015x^3 - 0.0348x^2 + 0.5465x + 265.64$$

$$SoC_{MF2} = 7^{-10x^6} - 2^{-7x^5} + 1^{-5x^4} - 0.0003x^3 - 0.0009x^2 + 0.2113x + 265.7$$

$$SoC_{MF3} = 9^{-10x^6} - 2^{-7x^5} + 2^{-5x^4} - 0.001x^3 + 0.0151x^2 + 0.0233x + 265.73$$

Similar to the charging calculations, CFD simulations for discharging were performed with varying inlet temperature and mass flow. The inlet temperatures used were 281.15 K (Figure 27) and 293.15 K (Figure 28).

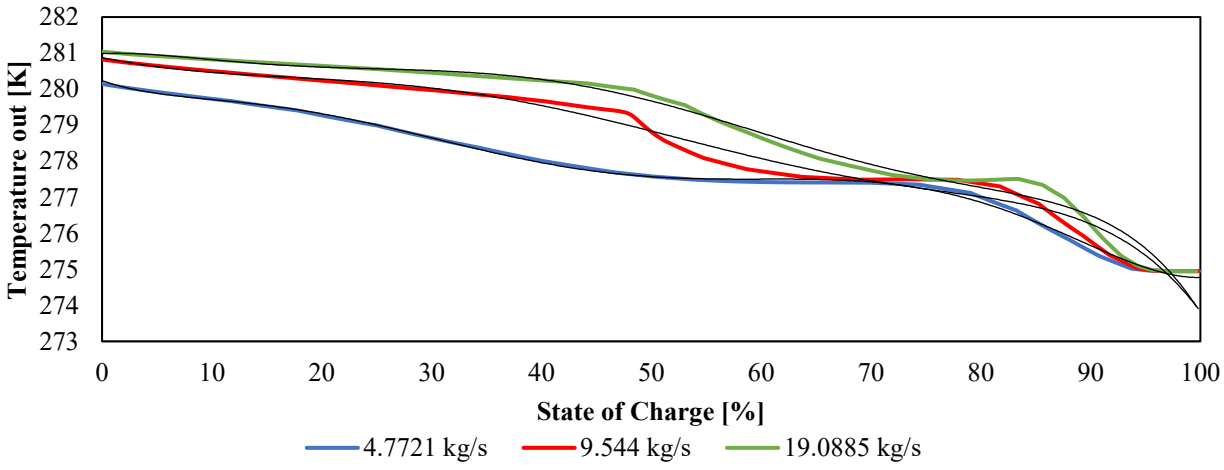

Figure 27 . Polynomial functions for discharging at 281.15 K.

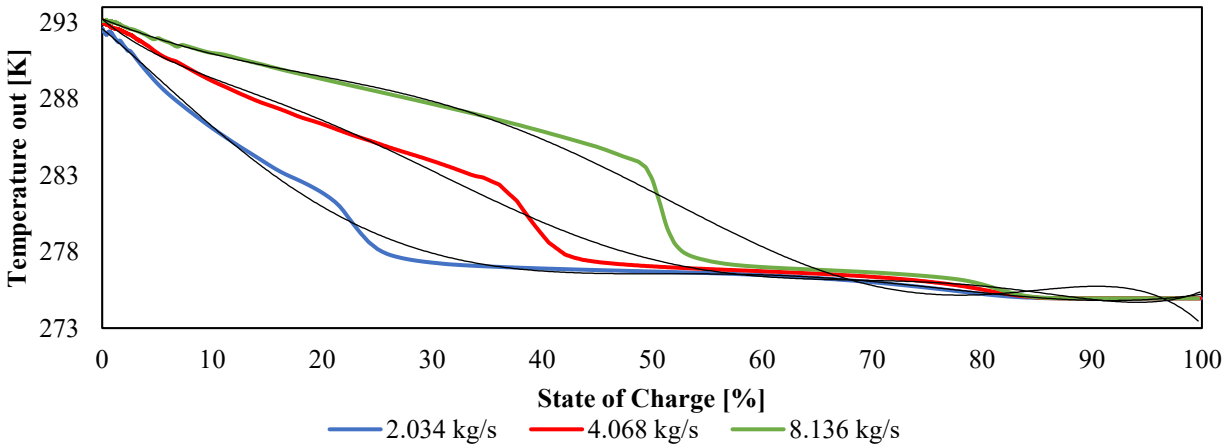

Figure 28 Polynomial functions for discharging at 293.15 K.

The polynomials for the 281.15 K case are, with mass flow in an ascending order

$$SoC_{MF1} = -3^{-10x^6} + 9^{-8x^5} - 9^{-6x^4} + 0.0003x^3 - 0.0057x^2 + 0.0136x + 280.99$$

$$SoC_{MF2} = -1^{-10x^6} + 3^{-8x^5} - 1^{-6x^4} - 3^{-5x^3} + 0.0024x^2 - 0.0615x + 280.87$$

$$SoC_{MF3} = 4^{-10x^6} - 1^{-7x^5} + 1^{-5x^4} - 0.0005x^3 + 0.0093x^2 - 0.1056x + 280.23$$

Now, for the 291.15 K case

$$SoC_{MF1} = -6^{-10x^6} + 1^{-7x^5} - 1^{-5x^4} + 0.0001x^3 + 0.0051x^2 - 0.283x + 293.23$$

$$SoC_{MF2} = 1^{-9x^6} - 3^{-7x^5} + 3^{-5x^4} - 0.0015x^3 + 0.0333x^2 - 0.5939x + 293.21$$

$$SoC_{MF3} = -3^{-10x^6} + 1^{-7x^5} - 2^{-5x^4} + 0.0008x^3 - 0.0102x^2 - 0.6053x + 292.59$$

5.5 Operation Modes

5.5.1 Continuous cooling

- Mass flow is kept constant in both hot and cold loop
- Heat pump while-loop
  - HP electric consumption is increased in each cycle until desired GT inlet temp is achieved or maximum nominal HP power is reached
  - Evaporator power and outlet temperature are calculated based on HP power
    - In the first time step, ambient temperature is assumed as the fluid temperature entering evaporator and condenser
    - Following time steps use the outlet temperatures from GTHX and AMBHX as inputs
    - c_p is calculated continuously
- Ambient heat exchanger while-loop
  - Air mass flow in the AmbHX is multiplied by 1.1 until the desired outlet temperature is achieved. Here the design condition (5°C pinch point) is used as the desired T_{out}.

5.5.2 Charging

- Temperature into TES is fixed at -7.47°C
- TES while-loop
  - An initial "minimum" HP electric power is given (1 MW)
  - An initial cold loop mass flow is given, and it is increased until one of these conditions are met
    - HP power reaches maximum power
    - HP power reaches maximum ramp-up compared to previous time step
    - State of charge equal to 100% is reached
- GTHX-AmbHX while-loops were created with two separate operating modes
  - 1: A maximum GT inlet temperature is chosen, and any excess heat is dissipated directly in the AmbHX
    - Hot loop mass flow is decreased from design until maximum allowed temperature is reached
    - GTHX and condenser outlet flows are then mixed as they enter AmbHX
  - 2: The originally proposed PHCC setup where heat is released at GT inlet with no upper temperature limit
  - For both modes, an initial air mass flow in the AmbHX is given and it is increased until WG outlet temperature equals ambient temperature + design pinch temperature (5°C) or lower

5.5.3 Discharging

- Maximum discharge mass flow is chosen
- Mass flow into TES is increased until
  - Desired conditions at GT inlet are reached
  - State of Charge equals minimum or lower (15%)
  - Temperature into TES is lower than or equal to temperature out of TES

5.5.4 Anti-ice system

- An electric consumption is estimated equal to the heat required to increase air temperature to the minimum of 5°C

The precise conditions for each operation mode is presented in Table 5. In order to utilize the integrated TES and HP as much as possible, a daily logic was deemed necessary since a large electricity price variation takes place throughout the year in Turin. For each 12 hours, minimum, maximum, and mean electricity price was calculated. This was decided due to the observation made by looking at the Italian electricity market data; two distinct peaks of electricity price occur almost every day. In each time step, the current electricity price is compared against the daily value to choose the operation mode. In the case of conditions both for continuous cooling and discharging occurring at the same time, discharging is prioritized. Therefore, no overlapping between operation modes is possible.

Table 5. Operation mode conditions.

Operation Mode	Ambient temperature	Electricity price
Charging	-	Daily minimum
Discharging	>15°C	Daily maximum
Continuous cooling	>15°C	< Daily mean
Anti-ice	< 5°C	-

5.6 Economic considerations

5.6.1 Capital Expenditure (CAPEX)

For the general *combined cycle*, a cost function given by the U.S. Energy Information Administration was used [26]. The following costs are in [€/kW]. 1.24245 is the foreign exchange ratio in 2018 in €/USD. The cost includes all capital costs related to a combined cycle power plant.

$$C_{CC} = 978 \cdot P_{CC,nominal} \cdot 1.24245 \tag{5.8}$$

where

$P_{CC,nominal}$: Combined cycle generating capacity in MW

For the additional components required by the POCC, the following cost equations were considered. For the *heat exchangers*, cost functions were derived from the ones already existing within DYESOPT. Maximum heat transfer during operation was defined as the HX power.

$$C_{GTHX} = 0.063 \cdot P_{GTHX,max} \tag{5.9}$$

$$C_{AmbHX} = 0.063 \cdot P_{AmbHX,max} \tag{5.10}$$

Pump cost depends on the number of pumps, pump power and efficiency. In this case, two additional pumps were installed, while the aforementioned efficiency used was 85%. The pump power was defined as the maximum power that the pump had to deliver during the simulation.

$$C_{pump} = n_{pump} \cdot 940 \cdot P_{pump}^{0.71} \cdot \left(1 + \frac{0.2}{1 - \eta_{pump}}\right) \cdot 1.24245 \tag{5.11}$$

Piping cost is defined by mass flow in pipes. An arithmetic mean of mass flows during the POCC operational modes was defined as $\dot{m}$.

$$C_{pipe} = 658 \cdot \dot{m}_{pipe}^{1.2} \cdot 1.24245 \tag{5.12}$$

TES cost function [€/MWh].

According to Yann Kaplan from PCM manufacturer Clauger, a TES with 100 kWh storage capacity has a price of 1437 €/kWh. It is not realistic to assume a cost which behaves linearly and therefore two different exponential cost equations are proposed (Figure 29).

$$C_{TES} = 143700 \cdot \left(\frac{E_{TES}}{E_{TES,Ref}}\right)^{exp} \tag{5.13}$$

where

exp is varied with values 1, 0.9, and 0.8.

E_{TE}: TES capacity in kWh

$E_{TES,Ref}$: Reference TES capacity (100 kWh)

These costs can be evaluated as a sensitivity.

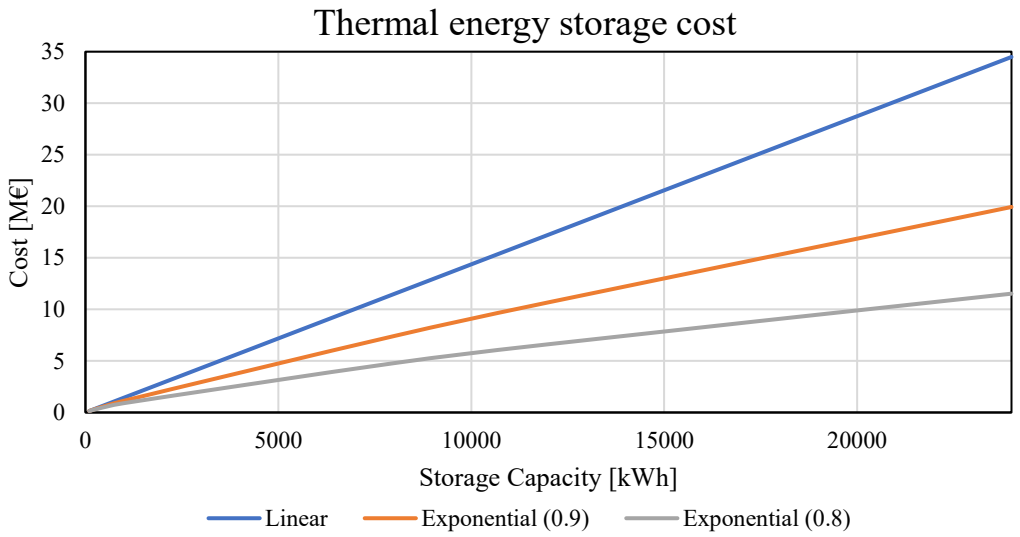

Figure 29 Thermal energy storage cost curve.

Heat pump capital investment was proposed by Song et al [27] [€/kW].

$$C_{HP} = 1580 \cdot \left(\frac{P_{HP,el}}{P_{HP,el,Ref}}\right)^{exp} \tag{5.14}$$

where

$P_{HP,el}$: Heat pump electric power in kW

$P_{HP,el,Ref}$: Reference heat pump electric power (1 kW)

Similar to TES cost, HP cost can be varied with the same exponents as a sensitivity (Figure 30).

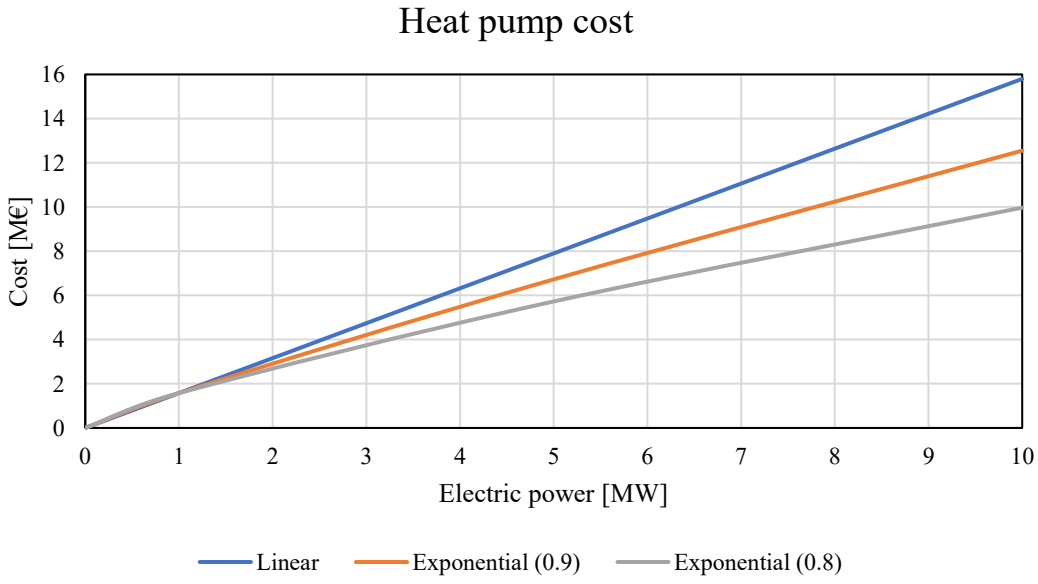

Figure 30 Heat Pump cost curve.

Civil works costs

$$C_{civil} = 21.2 \cdot 10^6 \cdot \left(\frac{P_{CC,nominal}}{129.4}\right)^{0.8} \cdot 1.24245 \tag{5.15}$$

Total equipment costs

$$C_{equip} = C_{CC} + C_{GTHX} + C_{AmbHX} + C_{pump} + C_{pipe} + C_{TES} + C_{HP} \tag{5.16}$$

Installation costs (C_{inst}) were calculated as 20% of the total equipment costs, taken directly from DYESOPT. Therefore, the total plant cost ends up being

$$C_{plant} = C_{equip} + C_{civil} + C_{inst} \tag{5.17}$$

Furthermore, the contingency costs ($C_{conting}$) are 10% and engineering costs (C_{eng}) 5% of the plant costs. Decommissioning costs (C_{decomm}) are 5% of plant costs. All these costs are as well taken from DYESOPT.

The total investment costs caused by the power plant are

$$C_{inv} = C_{plant} + C_{conting} + C_{eng} \tag{5.18}$$

Finally, the total capital costs are

$$CAPEX = C_{inv} + C_{decomm} \tag{5.19}$$

5.6.2 Operation and Maintenance Expenditure (OPEX)

The current cost of natural gas in Italy is 0.0177 €/kWh [28]. The cost is varied for the best case with multipliers 0.75 and 1.25.

Power block maintenance costs are considered as 4% of civil works costs and 3% of combined cycle equipment costs.

$$0.04 \cdot C_{civil} + 0.03 \cdot C_{CC} \ [€/yr] \tag{5.20}$$

Labor costs include the salaries of two technicians and two plant operators, and any costs related to labor force such as employee insurance.

$$C_{labor} = 998\,310\ [€/yr] \tag{5.21}$$

5.7 Thermo-economic analysis

Reference plant KPIs can be seen in Table 6 while the costs are presented in Figure 31 in millions of euros. The reference plant, in this case, refers to a power-oriented combined cycle power plant where only the anti-ice system and normal operation are included. Otherwise the principle is the same; the power plant is operated at 100% load and produces maximal power output without thermal power.

Table 6. Reference plant KPIs.

KPI	Value
Technical	
Total electricity	3498 GWh_{el}
Mean power output	399.32 MW_{el}
Mean efficiency	58.07 %
Economic	
NPV	771 M€
PBT	16 years
LCOE	52.71 €/MWh_{el}
IRR	2.74 %

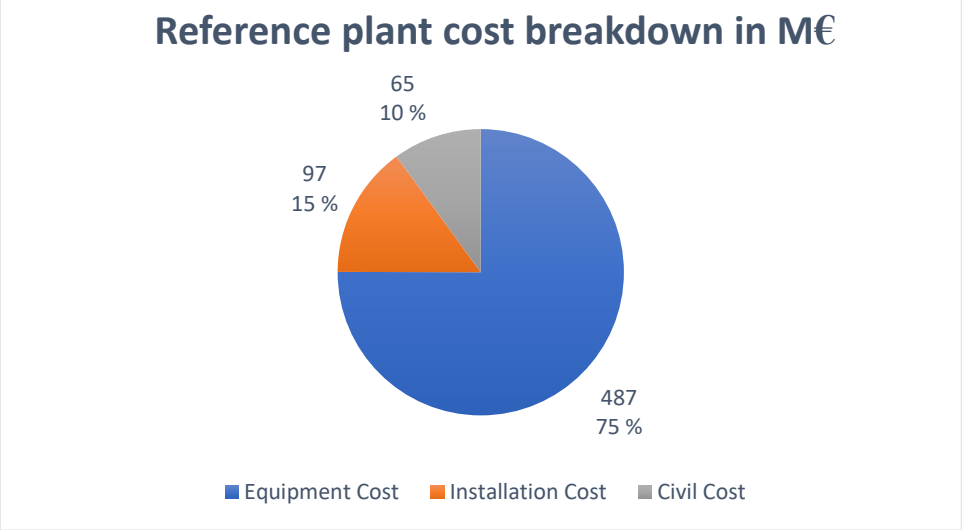

Figure 31 Reference plant capital cost breakdown.

The common parameters for all the cases ran are presented in Table 7. To be noted is that a new maximum heated air temperature (20°C) at the GT inlet was given, as opposed to the one suggested in the PHCC concept (around 40°C). This limit leads to a significantly higher electricity output during charging as heat is dissipated in AmbHX instead of GTHX and no overheating occurs. The difference in power output with inlet temperature of 40 and 20 degrees is approximately 35 MW_{el}, not considering parasitic losses and heat pump power. If no limit on GT inlet is imposed, the net annual power production is in fact decreased slightly when compared to the reference plant. The ambient temperature switch for continuous cooling was decided to be above 15°C. A separate sensitivity analysis for using only this operation mode was later conducted.

The mass flows given define the upper limit. The minimum state of charge was chosen due to the interpolation function giving unreasonable values below a certain point, i.e. at SoC under 15%. Finally, a parameter affecting significantly the unit performance is the targeted temperature at GT inlet during discharging and continuous cooling. Changing this is a trade-off between short-term peak power output and long-term cooling effect the TES is able to provide.

Table 7. Common simulation parameters.

Parameter	Value
Design COP	4.5
Max COP	5
Design CC mass flow	500 kg/s
Design discharge mass flow	500 kg/s
Design charge mass flow	500 kg/s
Design AmbHX air mass flow	1800 kg/s
Max GT inlet charging temp	20°C
Target inlet temperature	7.5°C
Max ramp-up	1.25 MW_{el}/time step
Charging time	4 hours
Discharging time	4 hours
Minimum state of charge	15 %
Continuous cooling T_{amb}	15°C

The following cases were simulated as listed in Table 8. For cases 1 and 2, the thermal energy storage capacity was kept constant to see the difference a varying heat pump capacity can make in the system. In cases 3 and 4, a similar sensitivity analysis was done with TES capacity while keeping HP power. In this way, the near-optimal layout containing both TES and HP was decided. A separate case, Case 5, considers using solely a heat pump to provide the cooling capacity during low electricity prices and high ambient temperatures.

Table 8. Simulated cases.

Case 1	
Heat pump electric power	5 MW_{el}
TES capacity	12 MWh
Case 2	
Heat pump electric power	7.5 MW_{el}
TES capacity	12 MWh
Case 3	
Heat pump electric power	5 MW_{el}
TES capacity	6 MWh
Case 4	
Heat pump electric power	5 MWel
TES capacity	18 MWh
Case 5	
Heat pump electric power	5 MW_{el}
TES capacity	-

Subcases are considered as well for the most profitable, i.e. best cases only, with HP and TES cost as sensitivities. The cases are referred to with letters A, B, and C, where A uses 1, B equals 0.9 and C uses 0.8 as scaling exponents for costs.

5.7.1 Technical performance

In this chapter, more details are given to the way TES and HP capacities affect various key values in the POCC system. These include mainly the power output and state of charge.

The visual presentation of how each operation mode affects the most important performance indicator, power output, can be found in Figure 32. As expected, charging causes a significant drop in power generation for a lengthy period. The drop in generation could be even lower if not limiting the heated GT inlet temperature to 20°C. This limitation is fundamental for making the plant more profitable if other values such as higher part-load efficiency during charging are not considered. Discharging, on the other hand, allows for a relatively steady power output for just under two hours. The TES capacity along with design mass flow are the governing factors when it comes to discharge time. Continuous cooling gives a stable increase in power output for as long as the condition of low electricity price occurs. The effect of HP ramp-up limit is seen in the gradual change of power output compared to the steep change during discharging.

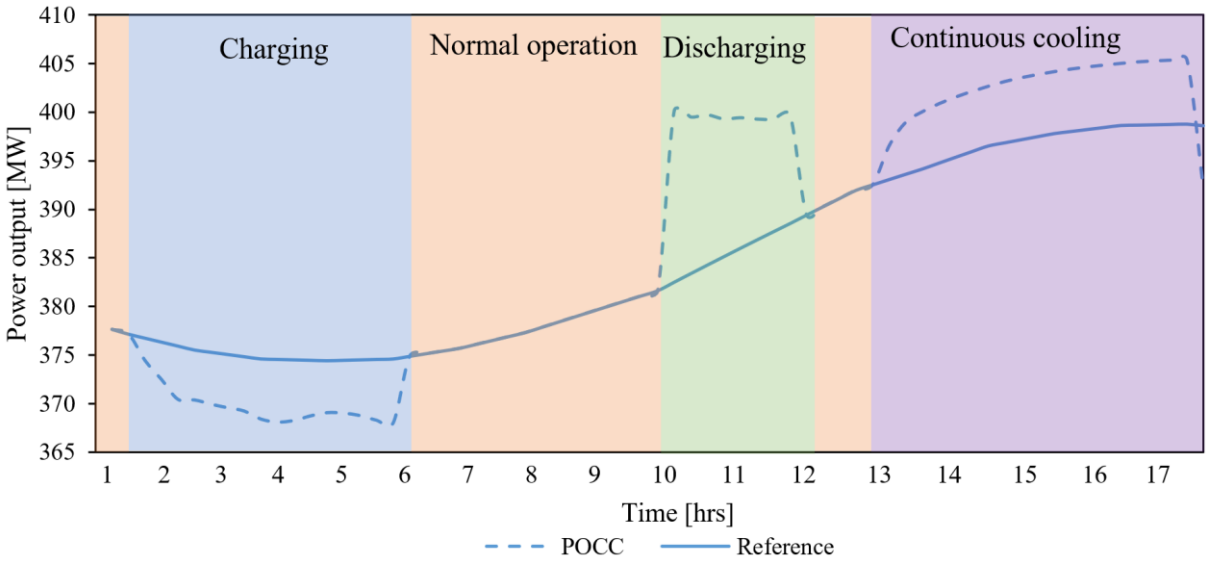

Figure 32 Operation mode effect on power generation.

The state of charge depends strongly on TES capacity as illustrated in Figure 33. The heat pump electric power, on the other hand, does not show a significant effect as the 7.5 MW HP (Case 2) state of charge largely overlaps with the state of charge of same capacity TES with a smaller heat pump (Case 1). The case with the largest capacity (Case 4) shows significant delay in reaching full charge, and sometimes the full charge may not be reached. On the other hand, it also shows a slower discharge rate even when discharge occurs at 80% state of charge.

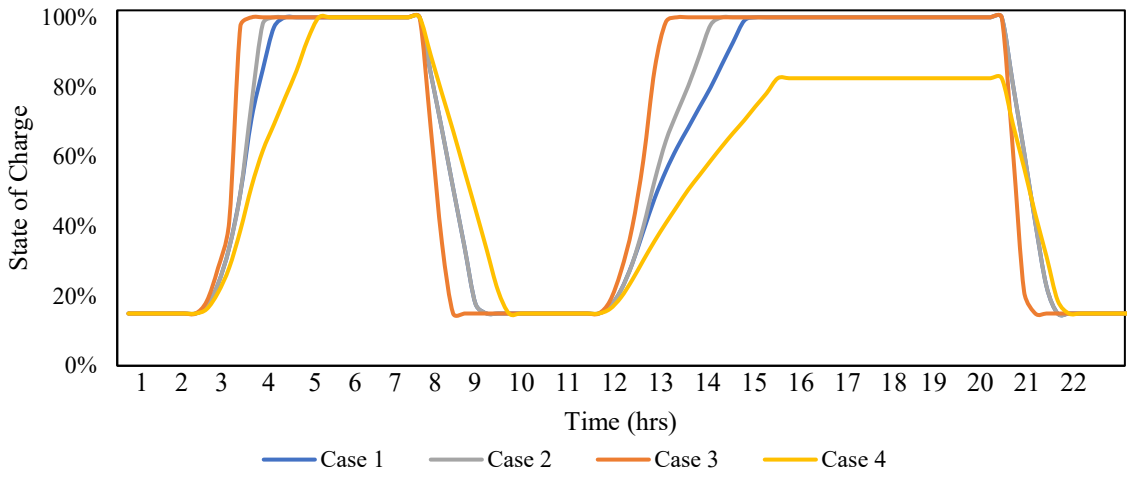

Figure 33 State of charge for all cases.

A comparison between the cases in both state of charge and power output is shown in Figure 34. An increased TES capacity leads to slower charging and discharging, granted that same mass flow is used. The difference in heat pump power between cases 1 and 2 (5 vs 7.5 MW) is not large enough to show a significant effect on TES behavior, while a much slower charge for Case 4 compared to Case 3 (18 vs 6 MWh) occurs.

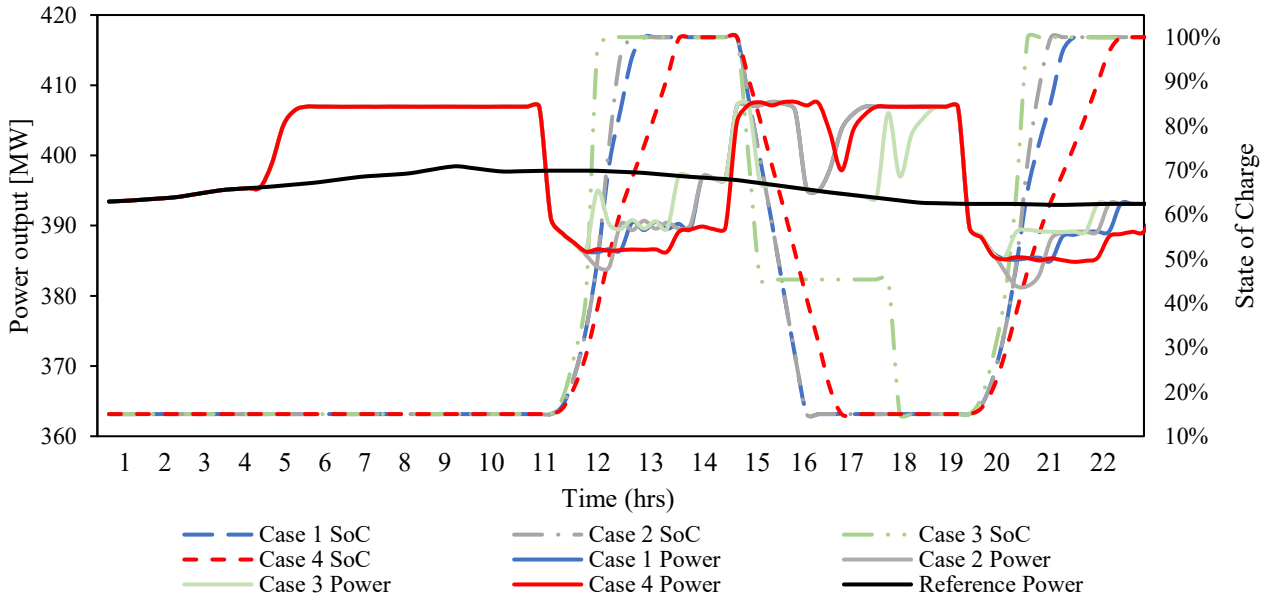

Figure 34 POCC technical performance.

A significant variance in power generation compared to the reference plant occurs throughout the year, with a largely positive net effect as illustrated in Figure 35. During peak summer temperatures, the difference is naturally the largest. The effect the limit on temperature has on power generation is shown in Figure 36. If no limit is imposed, the temperature can go up to 41°C. At this condition, the power output is as low as 355 MW, not considering parasitic losses. In order to maximize the benefit from TES, the ambient heat exchanger must be sized in such a way which allows for all the excess heat generated during charging to be dissipated into the ambient. This condition means that any time the ambient temperature is above 20°C the whole hot loop mass flow is sent to AmbHX. Without limit the net effect on power is negative, while

with the limit an increase is achieved. This limit on temperature is the most important factor when evaluating the POCC system with integrated TES and HP. An analysis without TES was later performed, with the results presented later in chapter Continuous Cooling performance.

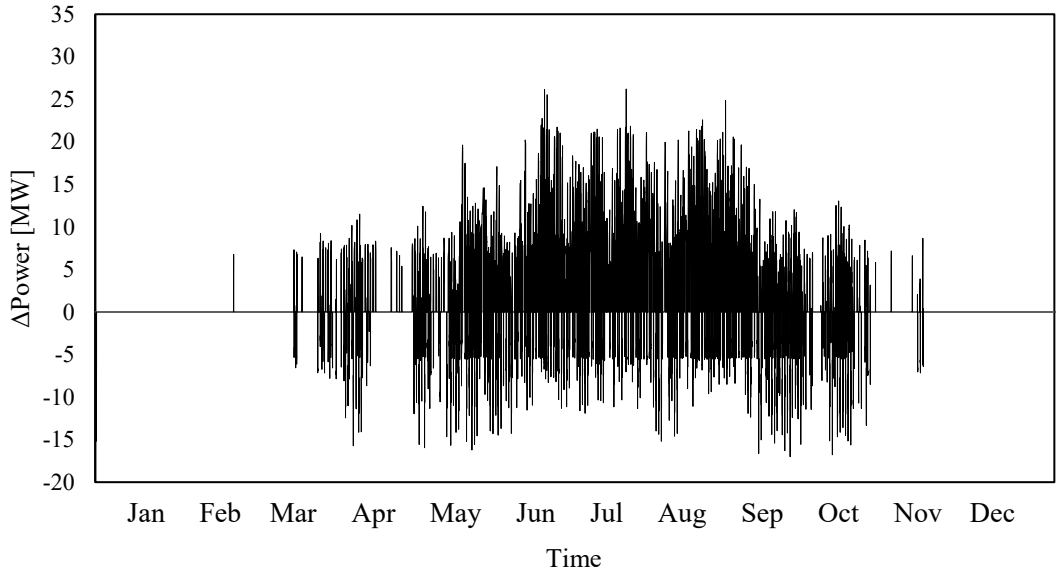

Figure 35 Power difference between Case 3 and Reference plant.

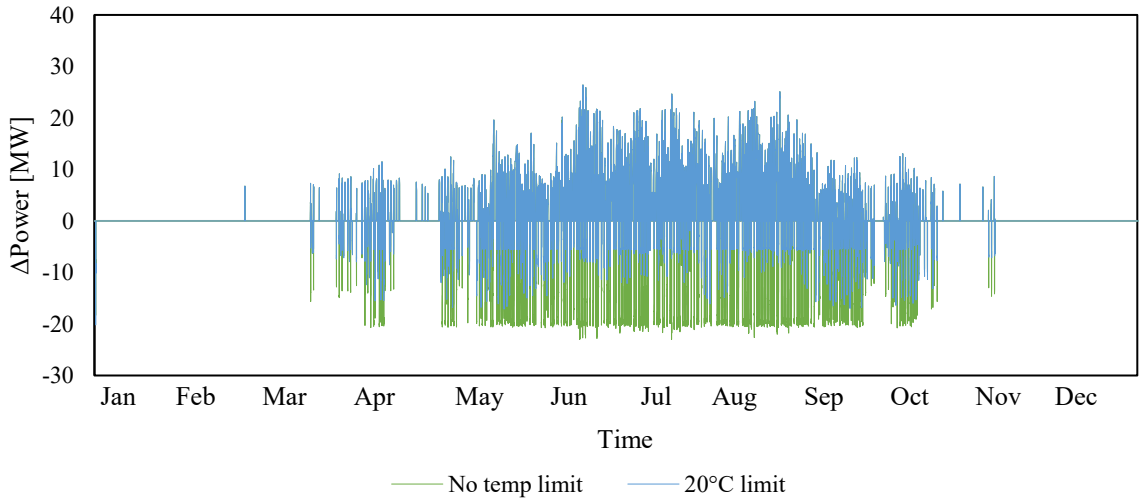

Figure 36 Power difference (Case 3), varying GT inlet temperature.

The transient behavior of the heat pump in terms of temperature levels is illustrated in Figure 37. A larger cooling effect requirement leads to a lower COP and higher electric consumption. The gradual increase of heat pump electrical consumption, and its effect on the GT inlet temperature can be seen. At higher ambient temperatures, such as 25°C, the 5 MW_{el} heat pump was not able to cool the air down to the desired temperature of 7.5°C. An important thing about the modeling, which is clear from the graph, is that the heat pump for continuous cooling does not directly interact with the heat pump for charging. In other words, when a loop for CC ends and charging begins, all values required by the new operation mode are recalculated from zero. This is apparent from the near-instantaneous drop in HP power between the two operation modes. Complete control over HP transients was assumed to make this simplification.

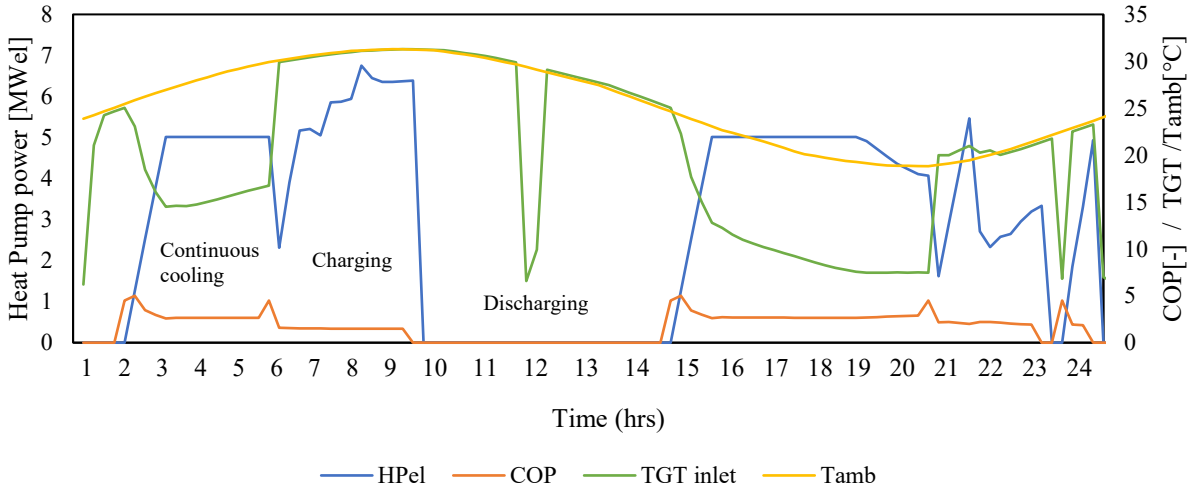

Figure 37 Heat pump transient operation during continuous cooling (Case 5).

5.7.1.1 Alternative techniques – double effect absorption chillers

Dharam Punwani [29] found that an increase of the inlet air temperature reduces both power output and thermal energy in GT exhaust gases and increases the heat rate. Hence, an effective way to control and cool down the turbine inlet air thus maximizing and making stable the power output irrespective of the ambient temperature, is the double effect absorption chiller. Such technology, that usually works with Aqua-Ammonia or Lithium Bromide Water as working fluids, was demonstrated to be an attractive alternative technology for electricity generation due to its enhanced capabilities. In particular, when compared with other technologies such as electric chillers or single-effect absorption chiller, a COP of about of about 1.2-1.4 was estimated [30], ca. 40% higher when compared to a single effect absorption chiller, and greater plant capacity with respect to electric chiller applications due to their lower parasitic losses, even though this comes at the expense of a certain pressure drop due to the design of the cooling system. From an economic prospective, the capital and maintenance costs required are relatively high. Nevertheless, despite the additional economic expenditures and pressure drops, the implementation of such technologies leads to an enhancement of the total capacity at less than 50% of the capital costs per MW of a gas turbines without any integrated inlet conditioning system. However, to properly assess the viability and the cost-effectiveness of implementing a double-effect absorption chiller in a specific facility several factors such as the weather conditions for the plant location, fuel costs and local electricity market should be analyzed in depth [29]. Hence, a thorough sensitivity with regards to such assumptions is recommended.

5.7.2 Technical KPIs

All of the selected cases exhibit an increased power production and efficiency as compared to the reference case. The technical KPIs are presented in Table 9. These key performance indicators may not alone be used to determine which case is the most desirable, yet it is clear from here that the maximal output is given by the configuration utilizing only the heat pump.

Table 10 contains all KPIs related to ramping up. These include the cold loop mass flow (TES), heat pump mass flow, and temperature change in the GT inlet. For the TES utilization factor, two calculation methods are presented: The first method (1) subtracts the minimum state of charge from the available storage capacity, while the second (2) considers the whole capacity as

usable. This is to show the difference that is caused by the lower limit of the state of charge. This limit is measurable with this KPI.

The TES utilization factor is greatly affected by the fact that ambient temperatures cause a large part of the year, approximately one fifth of the time, to be dominated by anti-ice operation. Although the electricity price condition for charging occurs roughly twice a day annually, the prioritization of anti-ice over TES operation causes a significant decrease in the utilization factor.

Table 9. Technical KPIs.

	Total electricity (GWh_{el})	Mean power (MW)	Mean efficiency (%)	TES utilization factor (%) (1)	TES utilization factor (%) (2)	Mean HP ramp-up (MW/min)
Reference	3498	399.32	58.07	-		-
Case 1	3508	400.41	58.23	161	99	0.052
Case 2	3508	400.49	58.24	161	99	0.062
Case 3	3509	400.53	58.25	121	103	0.054
Case 4	3507	400.33	58.22	106	90	0.047
Case 5	3523	402.20	58.49	-		0.032

Table 10. Ramp-up KPIs.

	$\Delta T_{GT,max}$ (°C/min)	$\Delta T_{GT,mean}$ (°C/min)	$\Delta MF_{TES,max}$ (kg/s /min)	$\Delta MF_{TES,mean}$ (kg/s /min)	$\Delta MF_{HP,max}$ (kg/s /min)	$\Delta MF_{HP,mean}$ (kg/s /min)
Case 1	1.64	0.08	33.3	6.6	33.3	20.9
Case 2	1.58	0.08	33.3	6.7	33.3	22.1
Case 3	1.56	0.08	36.0	10.1	33.3	23.9
Case 4	1.59	0.08	33.3	4.0	33.3	18.6
Case 5	1.02	0.58	-	-	33.3	33.3

5.7.3 Economic KPIs

The economic KPIs for each case can be seen in Table 11. From the comparison between cases, it was decided to use the payback time along with net present value as measurements to choose the best cases to run sensitivity analysis on. With the conditions presented in previous chapters, Case 3 with a 5 MW_{el} heat pump and 6 MWh thermal energy storage was deemed the best case with the proposed TES+HP layout. Case 5, with only the heat pump installed, was the case with the largest NPV and shortest payback time and was therefore also additionally studied. Note that the KPIs presented here use linear scaling for HP and TES costs, while further on cases with scaling factors are shown.

Table 11. Economic KPIs.

	NPV (M€)	PBT (years)	LCOE (€/MWh)	IRR (%)
Reference	771	16	52.71	2.48
Case 1	774	17	53.45	1.98
Case 2	774	17	53.57	1.90
Case 3	775	17	53.17	2.15
Case 4	773	18	53.72	2.08
Case 5	783	16	52.79	2.44

5.8 Sensitivity analysis

5.8.1 Electricity price

A multiplier in the range between 0.5 and 1.5 was used to vary the electricity price. The letters A, B, and C refer to cost scaling factors of 1, 0.9, and 0.8 respectively. This sensitivity tests the unit's rigidity in various electricity markets. The internal rate of return suggests that in the current Italian electricity market, the cases with linear scaling are not competitive against the reference case. However, as is expected, using a cost exponent to scale down the cost leads to increases in the IRR and Case 5B becomes cost effective in comparison. Nonetheless, as electricity price is increased, the reference case stays the most profitable case in terms of IRR.

Table 12. Sensitivity analysis with electricity price.

Reference	Normal price	1.25	1.5	0.75	0.5
NPV (M€)	771	1,375	1,979	167	-437
PBT (a)	16	8	5		
LCOE (€/MWh)	52.71				
IRR (%)	2.48	10.18	17.27	-8.55	-
Case 3A					
NPV (M€)	775	1,381	1,986	170	-436
PBT (a)	17	8	5		
LCOE (€/MWh)	53.17				
IRR (%)	2.15	9.65	16.53	-8.65	-
Case 3B					
NPV (M€)	776	1,382	1,987	170	-435
PBT (a)	16	8	5		
LCOE (€/MWh)	52.94				
IRR (%)	2.30	9.87	16.83	-8.56	-
Case 3C					
NPV (M€)	776	1,382	1,987	171	-435
PBT (a)	16	8	5		
LCOE (€/MWh)	52.82				
IRR (%)	2.38	9.99	17.00	-8.52	-
Case 5A					
NPV (M€)	783	1,390	1,998	176	-431
PBT (a)	16	8	5		
LCOE (€/MWh)	52.79				
IRR (%)	2.44	10.04	17.04	-8.38	-
Case 5B					
NPV (M€)	784	1,391	1,998	176	-431
PBT (a)	16	8	5		
LCOE (€/MWh)	52.58				

IRR (%)	2.49	10.13	17.16	-8.35	-
Case 5C					
NPV (M€)	784	1,391	1,998	176	-431
PBT (a)	16	8	5		
LCOE (€/MWh)	52.49				
IRR (%)	2.55	10.22	17.28	-8.32	-

In addition to the electricity price, fuel costs were also varied with multipliers 1.25 and 0.75.

Table 13. Sensitivity analysis with fuel price.

FP 1.25	Reference	Case 3A	Case 3B	Case 3C	Case 5A	Case 5B	Case 5C
NPV (M€)	430	435	435	436	443	443	443
PBT (y)	-	-	-	-	-	-	96
LCOE (€/MWh)	60.33	60.76	60.54	60.42	60.36	60.14	60.05
IRR (%)	-2.79	-2.99	-2.88	-2.82	-2.72	-2.68	-2.63
FP 0.75							
NPV (M€)	1,111	1,116	1,117	1,117	1,124	1,125	1,125
PBT (y)	10	10	10	10	10	10	10
LCOE (€/MWh)	45.09	45.57	45.34	45.23	45.23	45.01	44.92
IRR (%)	6.95	6.50	6.69	6.79	6.83	6.90	6.98

5.8.1.1 Cost breakdown

For the best two cases (3 and 5), a breakdown of capital costs is presented here in Table 14. The costs given were calculated with linear scaling. The equipment-level costs are shown in the following graphs (Figure 38).

Table 14. CAPEX breakdown. (M€)

Cost type	Reference	Case 3	Case 5
TES	-	8.6	-
HP	-	7.9	7.9
Equipment	487.5	491	490.4
Installation	97.5	101.5	99.7
Civil works	65	65	65
Total	649.9	674	662.9

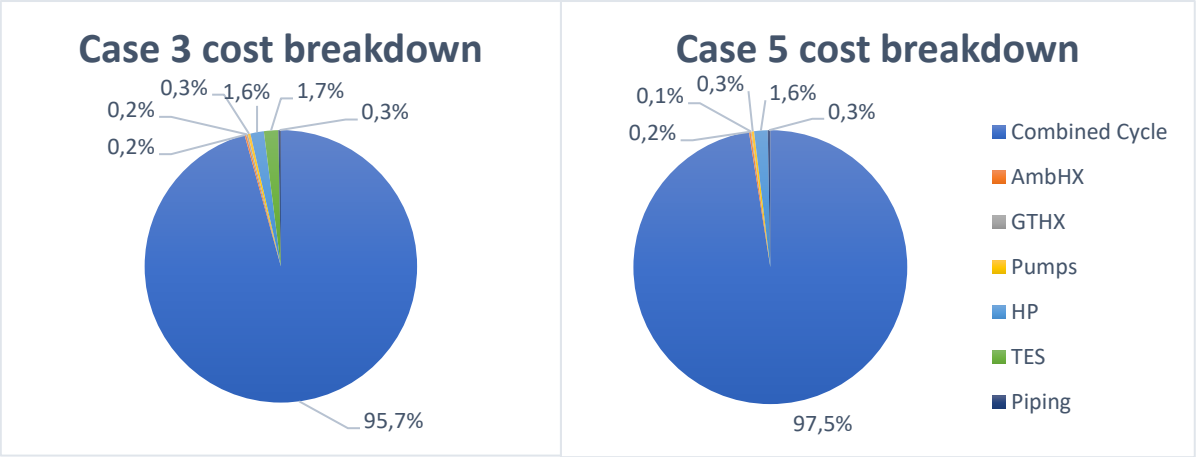

Figure 38 Case 3 (left) and Case 5 (right) equipment cost breakdown.

5.8.2 Continuous Cooling performance

It was seen in the analysis above, that the heat pump alone can bring technical and economic benefits for combined cycle performance when aiming for power-oriented operation. In this chapter, a sensitivity analysis regarding the optimal operating conditions is discussed.

Continuous cooling technical performance is shown in Figure 39. As can be seen, the higher temperature leads to a decrease in power output as heat pump maximum power is reached and COP decreased. Otherwise, the heat pump is able to keep a steady 15°C condition at GT inlet, ensuring a stable production.

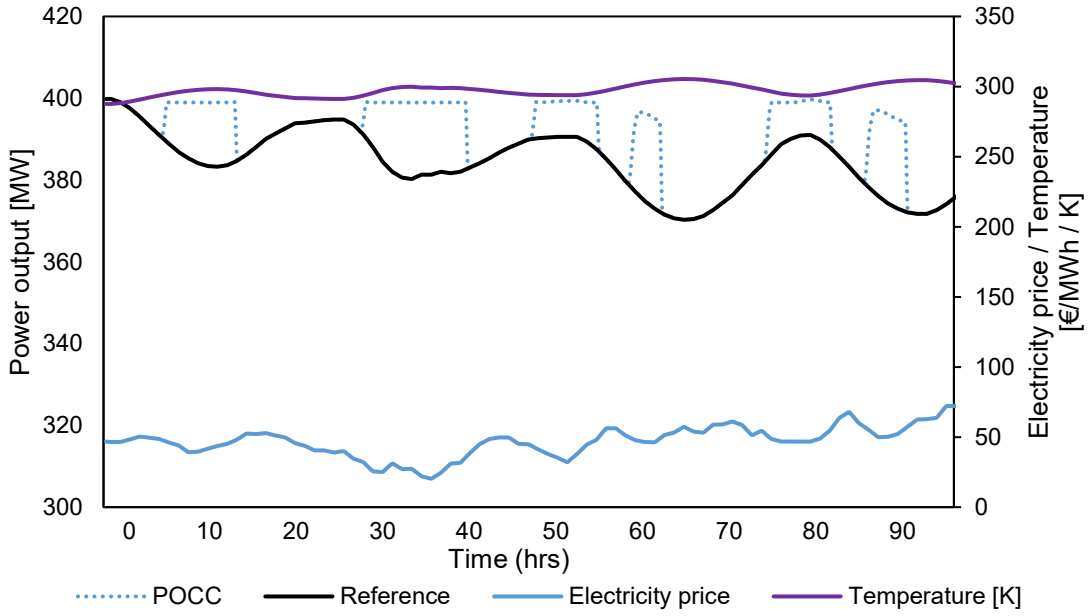

Figure 39 Continuous cooling power output.

There is a significant difference in operation when changing the switch temperature between 15 and 25 degrees Celsius. First, the condition where the ambient temperature is above 15 and electricity price is below mean daily electricity price occurs more often (20% of the year) than

the condition with 25 degrees (3% of the year) and can therefore be utilized more often. Secondly, as shown in Table 15, remarkably more benefit from the system is gained. Economic benefits follow accordingly, as NPV is increased with the larger electricity output. In this analysis, a heat pump of 5 MW_{el} capacity was used.

To be noted is that the first cases were ran with the condition of cooling the GT inlet temperature to 15°C (1). Additional benefits are reaped with decreasing the cooled air temperature all the way down to 7.5°C (2), considering a buffer of 2.5°C for the anti-ice system to not start. However, when using the 25°C switch temperature, the heat pump is not able to provide such a large cooling effect to reach these benefits while at 15°C, the cooling effect is attainable for a 5 MW_{el} heat pump. Increasing the heat pump capacity will accommodate for this, although lower economic improvement can then be expected with increased CAPEX. Thus, it is recommended to use the switch condition of 15°C and aim for cooling the GT inlet as close to 5 °C as possible, while avoiding problems due to icing. This allows for maximum profitability even when compared to the system integrated with thermal energy storage.

Table 15. Continuous Cooling KPIs.

	15°C (1)	25°C (1)	15°C (2)	25°C (2)
Total electricity (GWh_{el})	3 516	3 503	3 523	3 504
Mean power (MW)	401.35	399.88	402.20	399.93
Mean efficiency (%)	58.37	58.16	58.49	58.16
NPV (M€)	779	772	783	772
PBT (y)	16	17	16	17
LCOE (€/MWh)	52.90	53.10	52.79	53.09
IRR (%)	2.57	2.47	2.62	2.47

6 Layouts 2 and 3: Cogenerative combined cycle

This chapter discusses the second and third layouts, here combined due to their strong similarities.

6.1 Introduction

PHCC solution for cogeneration addresses multi-product power plants and the integration with heat produced by electrical HP (general layout in Figure 40). The main application envisaged to benefit the most from the PHCC concept is associated with a DHN, and the integration with warm temperature HP (up to 120 °C). Like the PO CCs, also CHP CCs sell electricity to the market. However, there is often a mismatch between the national electricity price and local DHN heat demand, which led, in the last years, to an increase of TES application in DHN. Additionally, the thermal demand is very often driving the cogenerative CC electrical load set-point: therefore, cogenerative CCs are not contributing to the electrical grid stabilization as they could. This inherent reserve of flexibility will be untapped thanks to the PHCC concept.

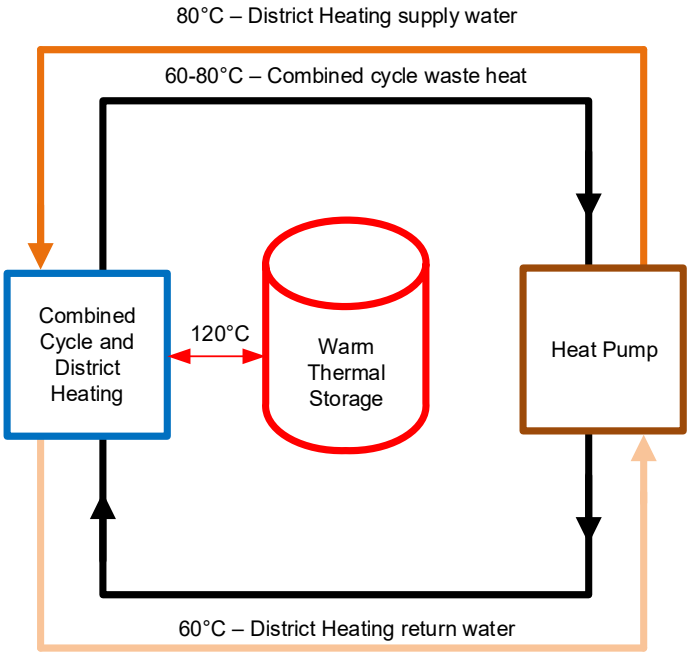

Figure 40 PHCC concept solution for CHP CC.

In fact, when energy mismatch is largely present between sources and users in terms of location and time, energy storage is one of the effective means to overcome this gap. Thermal energy storage (TES) is a solution that has gained increasing attention due to the ability to store lower grade energy at a competitive cost. A growing momentum is shown in both stratification enhancement for sensible heat storage and phase change material (PCM) design for thermal storage. PUMP-HEAT aims to couple the economic effectiveness of the TES with the balancing capacity over the grid, making the PHCC able to be economically profitable on both heat and electricity markets. In fact, during low price periods – HIGH RES production – PHCC allows to reduce electrical production still satisfying the heat demand.

6.1.1 Heat recovery from Heat Recovery Steam Generator feed water

The concept of GTCC units is born from the idea that flue gases discharged from the gas turbine contain an important amount of energy, potentially wasted. Therefore, the higher is the amount of energy recovered from flue gases, the higher is the global efficiency of the plant. The idea of condensing (or almost condensing) HRSGs comes out from the above concept, cooling flue gases at the lowest temperature acceptable. The lowest level of temperature is a function of the amount of water in flue gases (in order to avoid condensing problems). The flue gases design temperature is around 90 °C, but considering the real operating conditions, this value is actually higher. For existing CCs, the proposed solution is to use the already existing layout with the additional benefit of a lower temperature water entering the HRSG.

The water discharged by the water condenser (cold reserve) and/or by the district heating exchanger (hot reserve) is pumped through dedicated pumps to the heat recovery steam generator. Water temperature varies from a maximum value when the plant is operated in full cogeneration mode (higher amount of water from the hot reserve) to a minimum value when the plant is operated in full electric mode (water coming from the cold reserve). Considering operation in reference condition (15 °C), from the heat balance the above two values varies from 30 to 70 °C in the case of RPW2GT. The full flow diagram for this unit is shown in Figure 11.

Figure 41 outlines the cogenerative PHCC layout with series configuration (Layout 2) while Figure 42 illustrates the layout with parallel configuration (Layout 3). The main difference between these two layouts is in temperatures and mass flows. Both of the layouts aim to decrease extractions from the working cycle, extending the combined cycle operating range as previously illustrated in Figure 1.

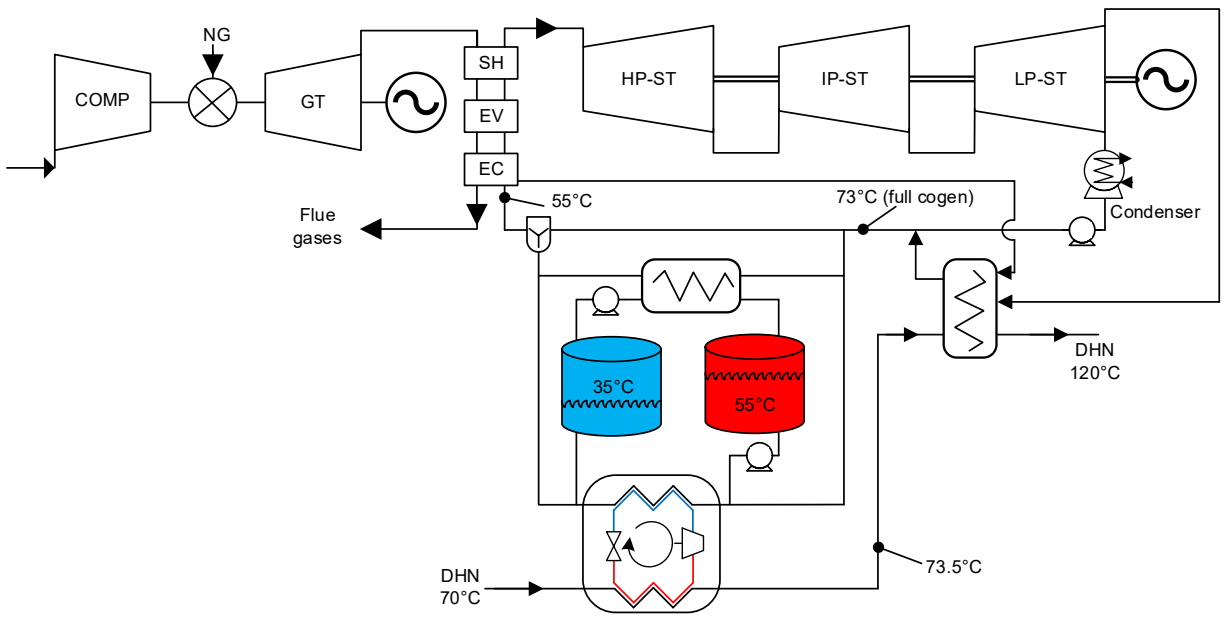

Figure 41 Cogenerative PHCC layout with series configuration (Layout 2).

The series configuration increases the incoming district heating return water temperature, allowing for less extractions later in the cycle. In this configuration, the total mass flow in the DHN passes through the heat pump condenser. These temperature levels allow for the commonly used refrigerant ammonia to be used.

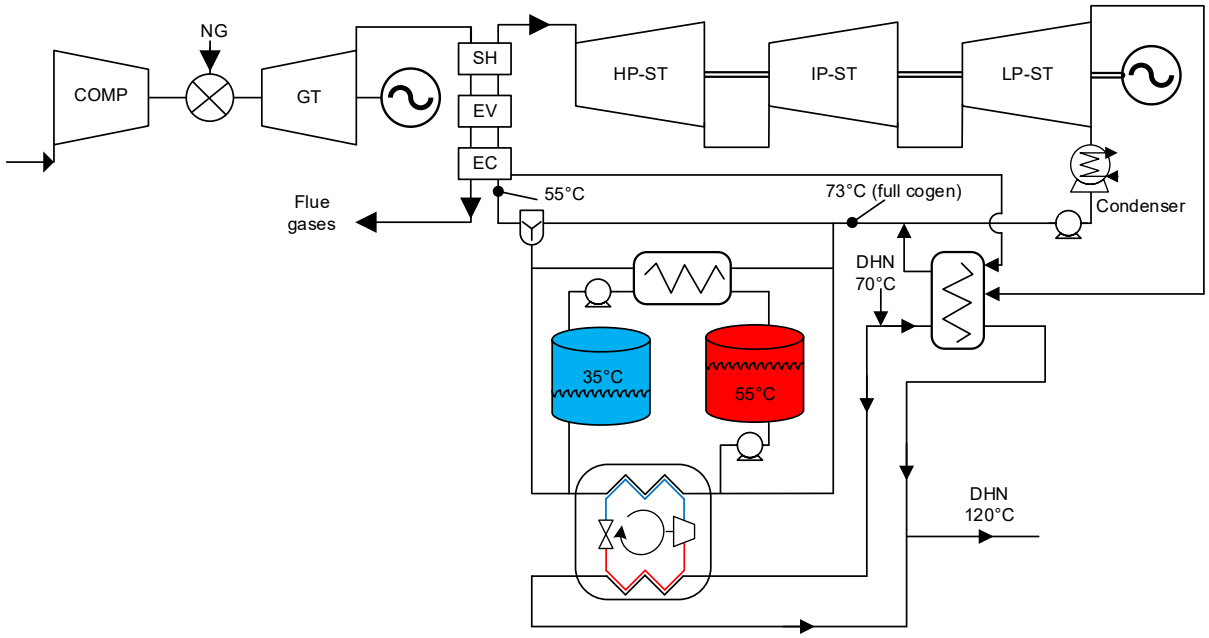

Figure 42 Cogenerative PHCC layout with parallel configuration (Layout 3).

In the parallel configuration, enough mass flow is passed through heat pump condenser to increase the temperature of district heating return water to the required supply temperature of 120°C.

6.1.2 Bottoming Cycle Constraints

The integration of the heat pump into the bottoming cycle of Moncalieri power plant has been assessed and the following constraints have been identified.

6.1.2.1 Minimum steam flow rate

At the maximum electrical power, the existing plant has been sized respecting the constraint of a minimum steam flow rate for the low-pressure stage of the LP steam turbine section. Any heat recovery strategy must take this constraint into account. For Moncalieri's plant this minimum flow rate has been set at 6.6 kg/s.

6.1.2.2 Minimum exhaust temperature at stack

The HRSG inlet cold water is the mix of the condensate coming from steam cycle condenser, and the condensate coming from the district heater. Such a stream could be cooled down by the HP. With the lowering of the water temperature at the inlet of the HRSG the heat exchange with the exhaust gas improves in the preheater, thus a lower temperature at the exhaust stack occurs. At the stack, the residual exhaust temperature must be sufficient so that the exhaust density is sufficiently lower than the density of the surrounding air in order to have the right speed upwards and to avoid exhaust gases to fall to the ground. This depends on the local conditions,

prevailing winds, and the possibility of thermal inversion. Usually the latter possibility is occasional and therefore, in case the thermal inversion occurs, the heat extraction could be bypassed, totally or partially. In the case of an existing plant, technical characteristics of the stack should indicate the lowest temperature limit of the exhaust. For new plants, the adoption of a Flue Gas Condenser can be considered since the design phase, therefore systematically increasing the amount of energy recovered without environmental concerns.

6.1.2.3 Feed Water Heater Recirculation flow rate

The design features of the HRSG preheater limit this flow rate. In fact, the HRSG preheater components are designed to preheat feed-water by recovering the heat from the exhausts, optimizing the reference working point of the plant. In the case of Moncalieri, the reference case is the Full Condensing operation. The preheater is designed to recover as much as possible the heat from the exhausts downstream of the low-pressure evaporator and to heat the incoming water to the degasser with the right sub-cooling (8°C), to allow the bubbling and facilitate the extraction of incondensable gases from water. There is a system for regulating the water temperature at the inlet of the degasser, which leads the opening of the bypass valve for preheating to comply with sub-cooling, vs the pressure of the third level. Obviously, the activation of this bypass worsens the system efficiency. With reference to the heat exchange performance, the equivalent section of the water pipes in the pre-heating bench harps is designed to ensure the optimal speed for heat exchange. Taking into account these points and the operating points of the plant at reduced loads too, the pre-heating component is sized. To maximize the exhausts heat recovery, the water entering the boiler is recirculated in the preheating until its temperature reaches 55°C (considering natural gas as a fuel of the gas turbine, otherwise, the presence of sulfur in the exhausts would create acid condenses below the acid dew point which is a function of the percentage of the presence of sulfur). A constraint regarding the recirculation flow rate is to not exceed twice the reference flow of the preheating component.

6.2 Steady-state design

In this chapter the steady-state approach for Layout 2 and 3 is presented and described with details.

6.2.1 Topping cycle

6.2.1.1 Gas Turbine

The steady-state model of the gas turbine estimates the thermodynamic set points such as temperature, pressure, enthalpy as well as the mass flows involved in each stage of the cycle. The gas turbine unit here proposed physically consists of four main components: a compressor, combustion chamber, turbine and electrical generator.

The GT cycle is intended to operate at the nominal operating conditions shown in Table 16. The steady-state cycle is designed for a base load operation at ISO standard conditions, i.e. 15 ˚C, 1.013 bar at sea level and 60% of relative humidity.

Table 16 GT nominal operating conditions

Nominal operating conditions	Value	Unit
GT power	268.50	MW_{el}
Compression ratio	18	-
Combustion temperature	1480	˚C
Fuel	Natural Gas	
Fuel composition	[0.90] methane, [0.08] ethane, [0.02] propane	
Initial fuel temperature	15	˚C
Lower Heating Value	47.011	MJ/kg
Exhaust mass flow	662.74	kg/s
Exhaust temperature	575.4	˚C

A multistage axial compressor was assumed with a given nominal pressure ratio equal to 18 (Π_{compr}). Some assumptions have been considered for the steady-state modelling of the compressor and they are summarized as follows:

- Adiabatic, non-isentropic process.
- The variation in heat exchange and kinetic and potential energy were neglected.
- Air-filter dissipation considers a relative pressure drop factor ($x_{AF,loss}$).
- Internal dissipation is estimated considering an isentropic efficiency.

The main equations involved in the calculations of the parameters in each stage of the compression process are listed below

$$P_{in} = P_{atm} \cdot \left(1 - x_{AF,loss}\right) \tag{6.1}$$

$$P_{out} = P_{in} \cdot \Pi_{compr} \tag{6.2}$$

$$h_{out} = h_{in} + \frac{h_{out} - h_{in}}{\eta_{is}} \tag{6.3}$$

$$E_{compr} = m_{in} \cdot \frac{(h_{out} - h_{in})}{\eta_{mec}} \tag{6.4}$$

The isentropic efficiency used in the equation 6.3 is estimated considering polytropic efficiency, pressure ratio, gas constant and isobaric specific heat capacity. Polytropic efficiency of turbine and compressor are assumed to be 89% and 91%, respectively, accordingly with the designed temperature levels.

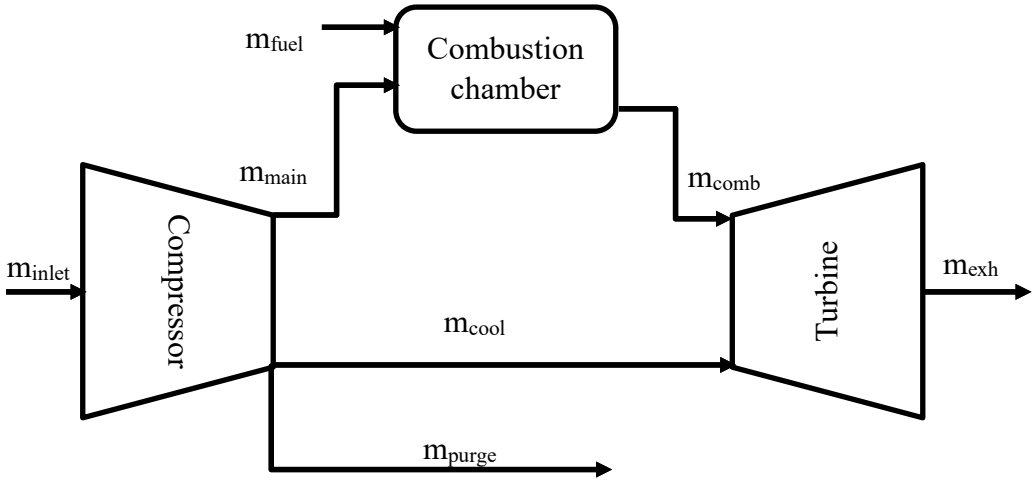

Figure 43 GT sub-components configuration and mass flows.

Figure 43 depicts the mass flows of the GT unit. The compressor outlet mass flow is split into the main mass flow and mass flow required to cool down the turbine blade and the purge mass flow. In this analysis, the last one it is assumed to be 3% of the compressor inlet mass flow.

Hence, once m_{cool} and m_{purge} are fixed, the main mass flow, i.e. the mass flow of compressed air, can be calculated as it is shown in equation 6.5.

$$m_{main} = m_{inlet} - (m_{cool} + m_{purge}) \tag{6.5}$$

For the steady-state combustion process some assumptions have been made and they can be summarized as follows

- Complete combustion of the fuel in the combustor.
- Constant average NG composition.
- Thermal losses and combustion air characteristics are neglected.

The fuel mass flow to the combustor is varied in such a way that the gas turbine inlet temperature is kept constantly at the desired temperature level, which is equal to the nominal design temperature of 1480 °C. To be noted that a constant fuel inlet temperature of 15°C was assumed.

The time step for an annual performance analysis, such as that considered here, is a 15-minute time step. As such, dynamic effects in the control of the combustion chamber can be ignored, and a quasi-static approach can be considered for calculation of the required mass flow.

The dynamic effects on the annual power plant performance due to the time step, in this analysis considered as a 15-minute time step, have been neglected and a quasi-dynamic analysis was performed for the estimation of the required mass flow.

Under these assumptions, the fuel mass flow can be calculated as it is shown in equation 6.6, where Δh_{air} is the desired raise in enthalpy difference, Δh_{fuel} is the enthalpy variation between the fuel inlet temperature and desired combustion outlet temperature and LHV_{fuel} is the fuel lower heating value.

$$m_{fuel} = \frac{\Delta h_{air}}{LHV_{fuel} - \Delta h_{fuel}} \tag{6.6}$$

For the steady-state model of the expansion process the same assumptions made for the compressor have been considered. The turbine outlet pressure is calculated as the ratio between combustor outlet temperature and the relative pressure drop of the exhaust duct and silencer of the gas turbine by using equation 6.7.

$$P_{exh} = \frac{P_{out,comb}}{1 - x_{dp}} \tag{6.7}$$

Hence, the shaft power and the net electrical output of the gas turbine were calculated as follows

$$E_{turb} = \eta_{mec} \cdot m_{comb} \cdot \left[h_{in} - \left[h_{in} - \eta_{is}\left(h_{in} - h_{is,out}\right)\right]\right] \tag{6.8}$$

$$E_{el,out} = \eta_{mec} \cdot \eta_{el} \cdot \left(E_{turb} - E_{compr}\right) \tag{6.9}$$

Finally, the exhaust gas composition was estimated using the well-known stoichiometric balance equation shown in equation 6.10, where the carbon content was calculated by using equation 6.11.

$$C_x H_y + \left(1 + x + \frac{y}{4}\right) O_2 \rightarrow x CO_2 + \frac{Y}{4} H_2 O \tag{6.10}$$

$$x_{C,fuel} = \frac{12x}{12x + y} \tag{6.11}$$

6.2.2 Bottoming cycle

6.2.2.1 Steam Turbine

For the steady-state steam turbine cycle, a multistage axial turbine was assumed, and the main purpose of this model is to estimate the thermodynamic states of the outlet steam as well as the power, extraction and mass flow of each stage of the steam turbine cycle. The same assumption made for the gas turbine cycle has been considered also in this case (∫ 6.2.1.1). The enthalpy across each sub-section was calculated by using equation 6.12.

$$h_{out} = h_{in} - \eta_{is} \cdot \left(h_{in} - h_{is,out}\right) \tag{6.12}$$

Hence, once the enthalpies and mass flows within the sub-sections of the steam turbine are known, a ST nominal shaft power equal to 132.4 MWe was calculated by using equation 6.13.

$$E_{ST} = \eta_{mec} \cdot m_{steam} \cdot (h_{in} - h_{out}) \tag{6.13}$$

6.2.2.2 Feed water pump

The scope of a feed water pump is to determine pump power required to raise the pressure level at each pressure stage of the boiler from condenser pressure to the required pressure. It is calculated as a ratio of the water mass flow and the hydraulic efficiency as a function of the pressure difference across the section as it is shown in equation 6.14.

$$E_{pump} = \frac{m_w}{\eta_{hydraulic}} \cdot \left(\frac{\Delta P}{\rho_w}\right) \tag{6.14}$$

Moreover, to determine the water needed by the condenser surface, the ratio between the energy balance equations of the steam and water have been used, as it is shown in equation 6.15.

$$m_{cond} = \frac{m_w \cdot \Delta h_{cond}}{c_{pw} \cdot \Delta T_{rise,cond}} \tag{6.15}$$

To be noticed is that an 11 °C temperature rise for cooling water in the condenser is considered. Moreover, 12 °C is the cooling water temperature (e.g. river temperature – a branch of the Po river) and 3 bars is the pressure drop in the condenser (cold side).

6.2.2.3 Heat Recovery Steam Generator

The steady-state model of heat recovery steam generator is mainly intended to calculate the mass flow with respect to pressure level in each of the sub-section of the HRSG, namely high-, intermediate- and low- stage pressure steam as well as to estimate the heat exchanger (HX) surface area needed. In turn, it is based on the combination of a pinch point analysis across each sub-section of the unit and the use of the effectiveness-NTU method for the calculation of the heat exchange area. Moreover, for the HRSG design, it has been assumed that no heat loss between the exchanger and the surroundings occurs as well as no mixing between the cold and the hot stream fluids (Figure 44).

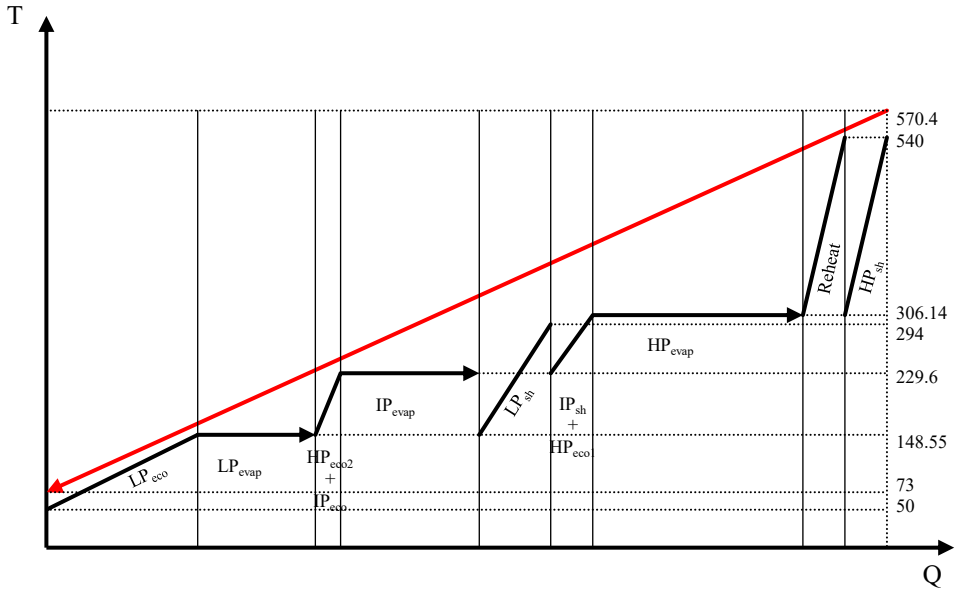

Figure 44 Pinch-point diagram for three-pressure level HRSG.

The mass flow rate of high-pressure steam ($m_{HP,st}$) is calculated as a function of GT exhaust flow rate m_{exh}, mass flow rate in reheat branch and enthalpy change in each of the respective heat exchanger by using equation 6.16. Likewise, the mass flow rate in the intermediate and low-pressure stage have been calculated.

$$m_{HP,st} = \frac{m_{exh}\Delta h_{g,HP} - m_{RH}\Delta h_{RH}}{\Delta h_{HP,sh} + \Delta h_{HP,evap}} \tag{6.16}$$

The enthalpy changes in each sub-section is estimated taking into account both the temperature variations and minimum approach temperatures of different streams in each heat exchanger section. In particular, the approach temperatures ($\Delta T_{min}/2$) considered for high pressure gases, low-pressure gases, evaporating water, condensing water are 15, 10, 2 and 2 (°C) respectively.

Table 17 ST Nominal operating conditions.

Nominal operating conditions	Value	Unit
ST power	132.4	MWe
HP stage pressure	93.56	bar
IP stage pressure	27.77	bar
LP stage pressure	4.58	bar
HPT inlet temperature	540	˚C
IPT inlet temperature	540	˚C
LPT inlet temperature	294	˚C
Condenser temperautre	50	˚C

Knowing exhaust and steam mass flows in each pressure stage of the HRSG, it allows to estimate the required heat exchangers' surface area and it can be calculated using effectiveness-NTU method, as it is shown below. The total minimum approach temperature in the HX is calculated by summing the $\Delta T_{min}/2$ for each stream across it. Hence, the effectiveness ε can be calculated as a function of the minimum approach temperature difference and heat exchanger temperature change (equation 6.17).

$$\varepsilon = 1 - \frac{\Delta T_{min,approach}}{\Delta T_{HX}} \tag{6.17}$$

Since the effectiveness is a function of the number of transfer units (NTU) and heat capacity rates (C_r)

$$\varepsilon = \int \left(NTU = \frac{UA}{C_{min}}, C_r = \frac{C_{min}}{C_{max}} \right) \tag{6.18}$$

and the economiser and super-heater sub-sections are assumed as cross flow heat exchanger, the NTU can be calculated by using equation 6.19, while for the evaporator, equation 6.20 is used.

$$NTU = -\ln\left[1 + \left(\frac{1}{C_r}\right)\ln(1 - \varepsilon C_r)\right] \tag{6.19}$$

$$NTU = -\ln(1 - \varepsilon) \tag{6.20}$$

Once the NTU is known, the heat exchanger area was extrapolated from function 6.18.

To be noticed is that the outlet temperature of exhaust gas from the HRSG is controlled in such a way it does not go over 73-75 °C to overcome problems that might lead to serious damages like corrosion of the equipment. Moreover, to maximize the exhausts heat recovery, the water entering the boiler is recirculated in the preheating system until its temperature reaches 55°C.

6.2.2.4 District Heating System

District heating coming from the network (return) has a nominal temperature of 70°C and passes across the low temperature heat exchanger. Its temperature is then increased up to 120°C by the means of a high temperature heat exchanger and using the extraction of steam from the cross-over pipe (the pipe that connects medium to low pressure steam turbine) and the heat recovered from the last stage of HRSG.

Table 18 DH nominal operating conditions.

Nominal operating conditions	Value	Unit
DHN capacity at full Cogen. mode	260	MW_{th}
DHN mass flow	1250	kg/s
DHN supply temperature	120	°C
DHN return temperature	70	°C

A MATLAB-based detailed model able to calculate for each of the heat exchanger both the extraction, capacity, temperature and pressure levels was built. From trial and error, as well as comparison with the available data from the operator (IREN S.p.A), it has been estimated that the low temperature heat exchanger accounts for 14% of the total extraction capacity while the high temperature heat exchanger 86%. Hence, the two heat exchangers can provide the district heating water with a nominal maximum power of about 260 MW_{th}, considering an increase of temperature of 50 °C (70-120 °C) and a mass flow rate of about 1.250 kg/s. Nevertheless, since the pumping station is made up of variable speed pumps, the amount of water passing through this equipment is adjustable.

6.3 Transient Model

In this chapter, the dynamic behaviour and modelling approach for Layout 2 and 3 is presented.

6.3.1 Methodology - Modelling

Since the objective of this thesis is techno-economic optimization of a combined cycle power plant, it is important to select a tool which can capture the major aspects of the simulated environment. In this case, these aspects include physical characteristics of heat exchangers, gas and steam turbines and condensers, to name a few components. The tool chosen for the second and third layouts is the Dynamic Energy System OPTimizer, DYESOPT, and it readily includes these features of a power plant. DYESOPT was developed at KTH Royal Institute of Technology in the solar research department, but it has since then been developed further to include gas turbine technology with Rankine cycle as the bottoming cycle.

The way that DYESOPT operates is shown in Figure 45.

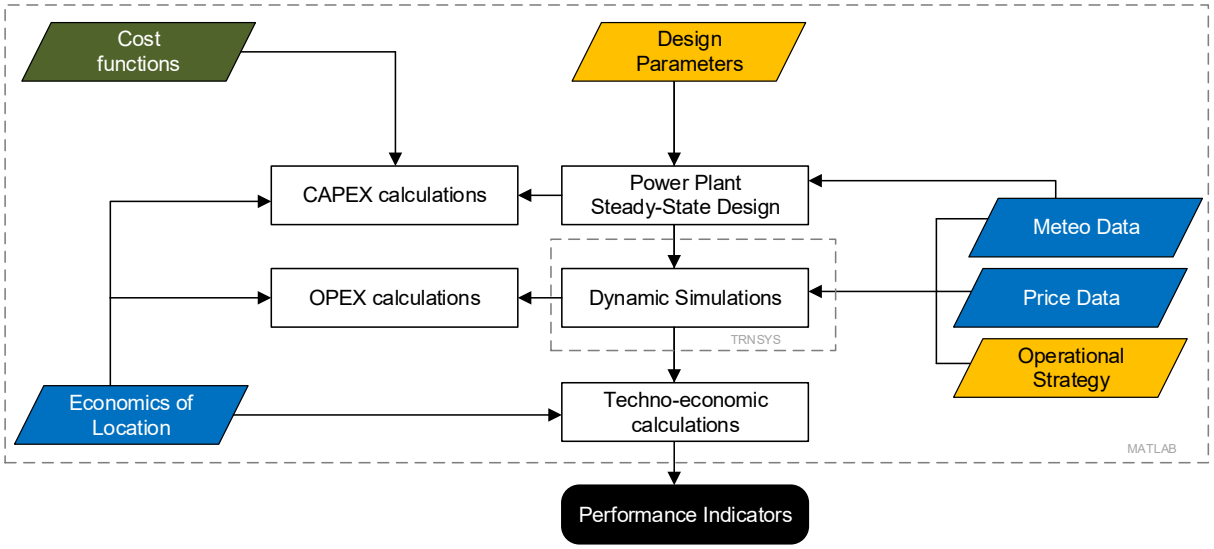

Figure 45 DYESOPT programming logic.

After an input of various boundary conditions such as cost functions and design parameters, MATLAB-based functions are used to design the power plant components in steady state. The sizing of the plant is directly connected to capital costs which are also calculated here. Afterwards, the designed power plant is created in TRNSYS where the dynamic simulations throughout the chosen time period is ran. TRNSYS (Transient System Simulation Tool) is a tool which enables simulating transient systems in a graphical environment. The power plant output is therefore measured when running in sub-optimal, i.e. part-load conditions. In order to accurately depict this, operational strategies and electricity and heat price data are inputs in the dynamic model. Dispatch strategy is described in this phase of the modeling. In the last step, the overall techno-economic calculations are performed in MATLAB and the output is measured with the chosen key performance indicators in order to choose the optimal power plant for a particular case.
As a result of this thesis, the current DYESOPT version is updated with a model which includes heat pump and thermal energy storage as an optional addition to a CCGT power plant.

A general model of a combined cycle power plant was used as a basis for the simulation. The new components added to the cycle are a hot water tank, a cold water tank, a heat exchanger and a heat pump. These were readily available in the component library provided by TRNSYS.

6.3.2 TRNSYS model input

- Nominal operating points and design parameters of the power plant. These values are estimated by means of the steady-state simulation in MATLAB and then taken by TRNSYS as "caseData" (i.e. fixed values). The power plant is assumed working all the year, i.e. 8760 hours.
- Meteorological data for the power plant has been gathered from the dataset provided by local operator (IREN S.p.A). These data collect both ambient temperature and pressure of the power plant location. Weather data with 15 min time step has been used for this analysis.
- Load dataset has been created for the turbine in order to match the electricity price and heat demand swings, thus resulting into a more representative turbine operational behavior with respect to the local energy market.

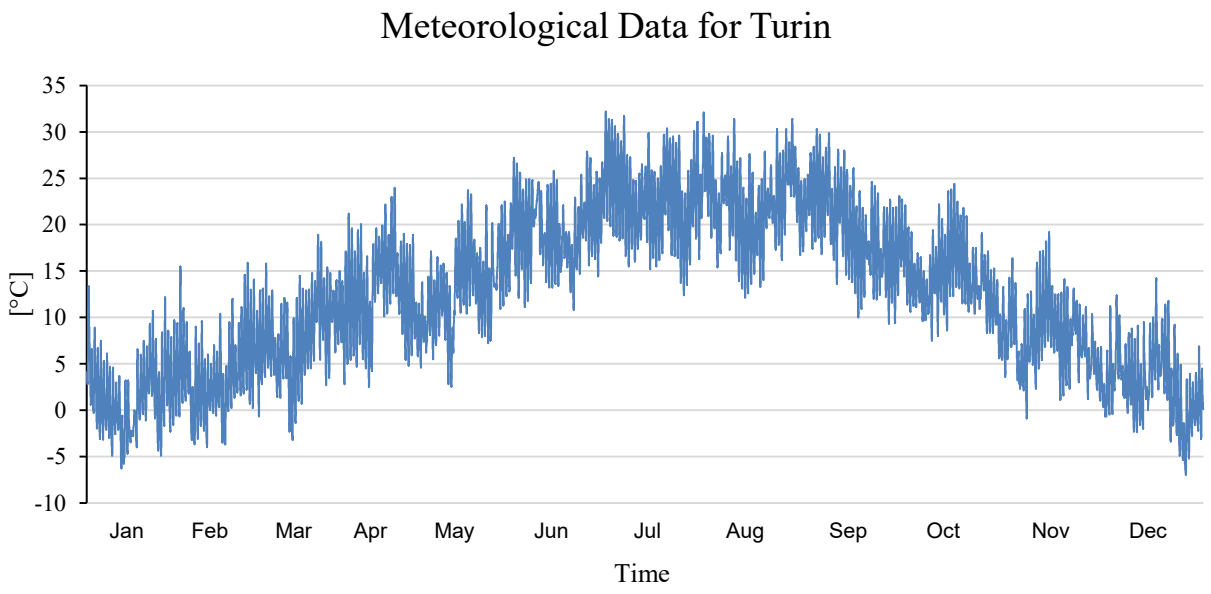

Figure 46 Meteorological Data for Turin, Italy

6.3.3 Load control

District heating data from 2017 for the unit RPW2GT (Figure 47) along with the electricity price (Annex A.2) from the same year were used to create a load control common for both the reference plant and the two layouts. For the PHCC unit, an additional logic with heat demand as the key factor was created. Below, the methodology followed when creating the operating strategy is presented.

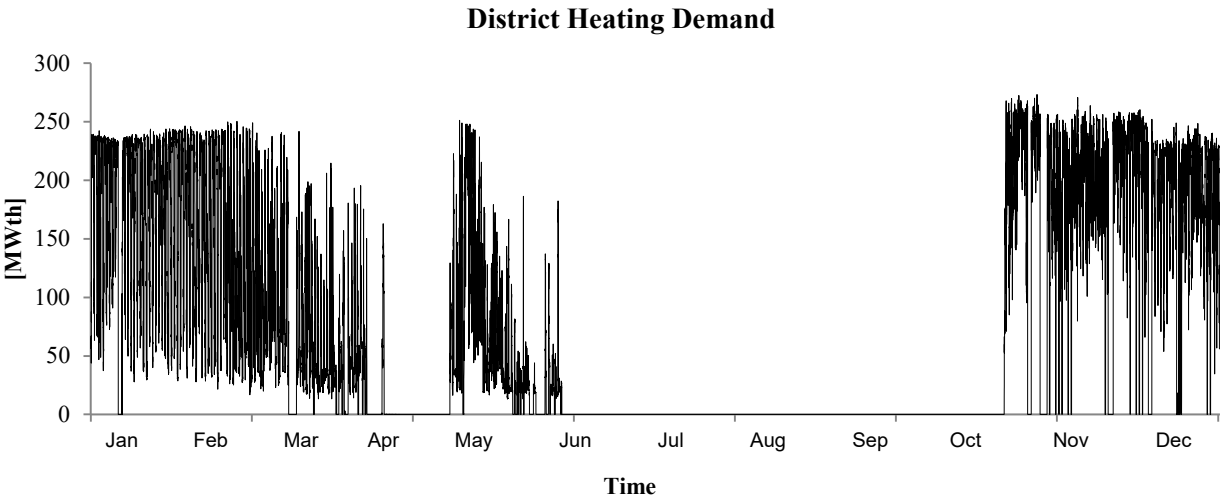

Figure 47 District heating demand (RPW2GT)

Step 1.

A preliminary load was defined by the electricity price / heat price ratio by visually approximating a reasonable operating range. If the ratio is above 1.5, then the load is 100 %. Below 0.5 the load is 45 %. In the range between 0.5 and 1.5 the load varies accordingly so that at ratio = 1, the load is 75 %.

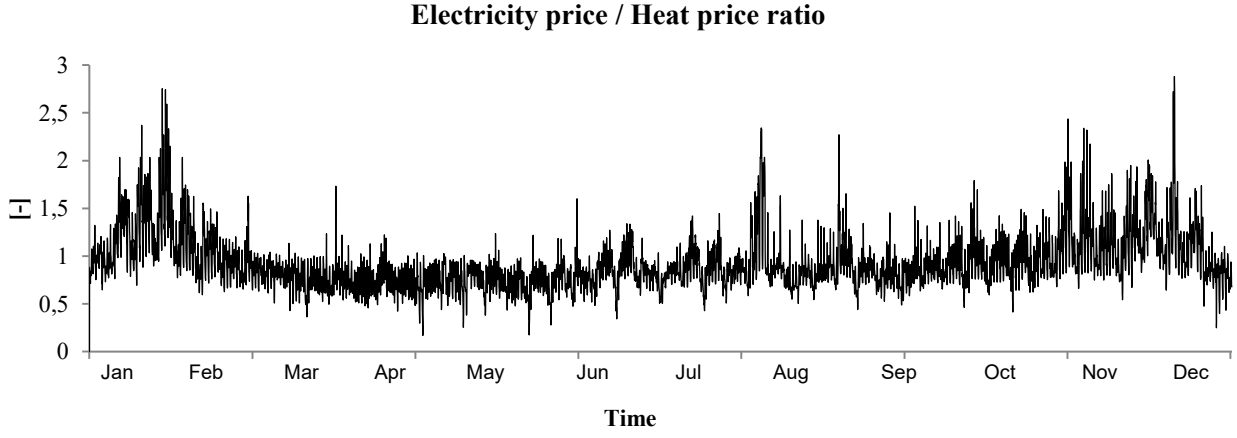

Figure 48 Electricity price vs heat price ratio.

Step 2.

The heat demand / electricity price ratio ($HDEP_{ratio}$) was also taken into account; in turn, the load was increased accordingly with the excess of heat estimated from this ratio. The purpose of this was to consider the current heat demand in Turin, which in reality affects the operational strategy. The fraction of the ratio to the maximum ratio was then added to the load calculated in the first step as it is shown in equation 6.21.

$$Load_{Step2,i} = Load_{Step1,i} + \left(\frac{HDEP_{ratio,i}}{HD_{max}}\right) \cdot Load_{Step1,i} \qquad (6.21)$$

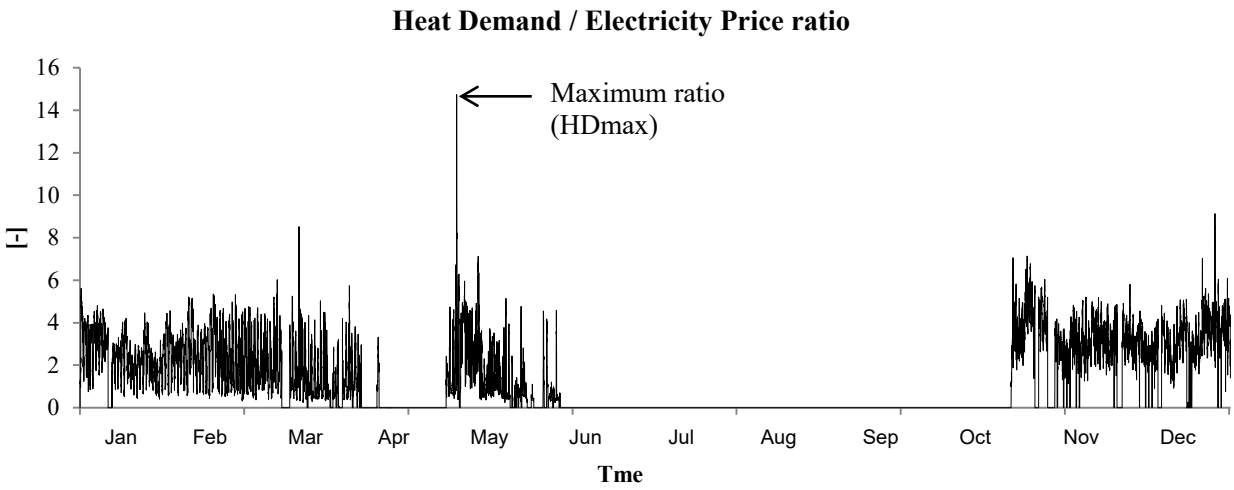

Figure 49 Heat demand vs electricity price ratio.

Step 3.

Then, the combined cycle load was worked out by considering the excess of thermal energy that is currently provided by a thermal energy storage or an external heat source (this can be noted from the data provided by IREN). Thus, the load estimated at Step 2 was decreased assuming this external heat source. I.e. both the reference plant and PHCC plant will use the load presented here. However, the PHCC plant produces additional heat on top of the reference case by the means of HP and TES. The values exceeding the maximum load were rounded down to 100%.

Finally, the load has been multiplied by a multiplication factor of 1.25 to let the power plant to be run at higher minimum load and at more constant full load, thus resulting in a minimum load no lower than 57% and a power plant operating a full load 24% of the time, as it is shown in Figure 50.

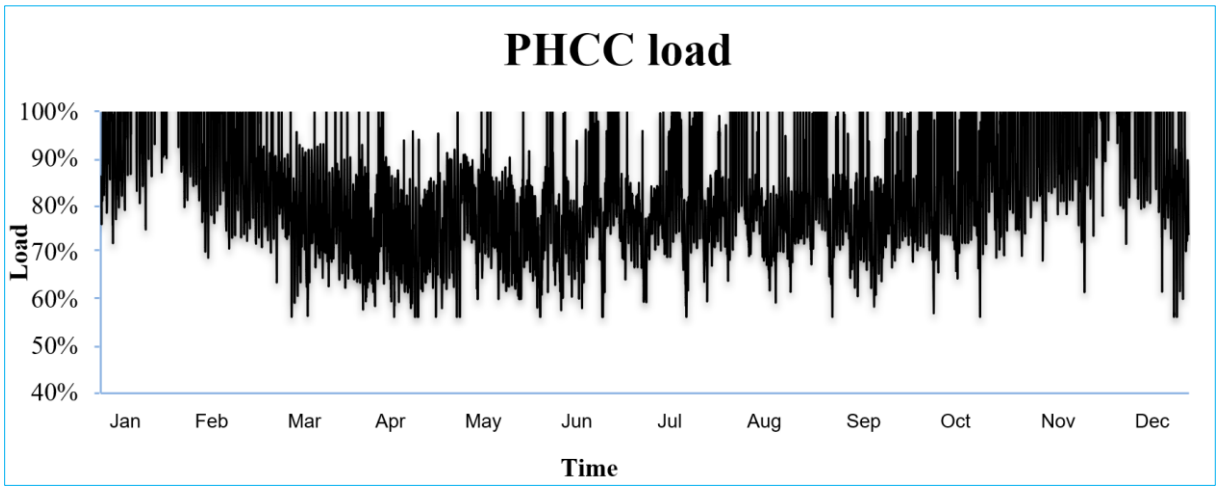

Figure 50 Power plant load (Layout 2 and 3).

In Table 19 are shown the load operating hours throughout the year.

Table 19 Reference load operating hours.

Load	Full	Half	Minimum
Operating hours (hr/yr)	2123	2050	501

6.3.4 Turbomachinery performance

6.3.4.1 Gas turbine

For the modeling of steam turbine stages, the Type 427 in TRNSYS component library has been used. This component calculates the outlet conditions from the inlet state by using an isentropic efficiency which can be specified by the user. In this study, η_{so} is calculated in the steady-state simulation in MATLAB and kept at 91.982%, even though the enthalpy difference across the turbine might vary sensitively with the turbine load variations. However, the rotational speed is usually maintained relatively constant as per power production practices, since the turbine is desired to be synchronous to the grid, thus the possible inefficiencies due to the load variation have been neglected and the turbine inlet temperature was kept constant. In this way, the model calculates for inputs such as combustion air inlet temperature, inlet pressure, combustion mass flow, inlet enthalpies and isentropic efficiency and given parameters like mechanical efficiency and ambient pressure, the outlet temperature and mass flow as well as the associated outlet pressure and enthalpy.

6.3.4.1.1 Gas turbine control

To ensure stable and controllable power output from the GT at desired load, some parameters are actively controlled, namely the combustion chamber outlet temperature and the compressed air mass flow.

The combustor mass flow control has been explained in 6.2.1.1. The compressed air mass flow, instead, is constrained between an upper limit given by full opening of the guide vanes and a lower limit to prevent rotating stall of the unit, thus meaning that the minimum volumetric flow rate is kept no lower than 50% of the flow rate at standard condition can withstand. At full opened guide vane, the compressor operates as a constant volume flow and the maximum allowed mass flow m_{max} is calculated by using equation 6.22, where m_{iso} is the nominal mass flow of the unit at standard operating conditions (ISO). T_{ISO}, Ta, P_{ISO}, P_a are the temperatures and pressures at ISO conditions and the current ambient conditions, respectively [31].

$$m_{max} = m_{iso} \cdot \frac{T_{iso}}{T_a} \cdot \frac{P_a}{P_{iso}} \tag{6.22}$$

6.3.4.2 Steam turbine

For the modeling of steam turbine stages, the Type 318 in TRNSYS component library has been used. This component estimates the inlet pressure of the turbine stage from the outlet pressure, the steam mass flow rate and reference values of inlet and outlet pressure and mass flow rate using law of the eclipse. It calculates the outlet enthalpy from the inlet enthalpy and outlet pressure using an isentropic efficiency [32]. In this study, the isentropic efficiency has been calculated in detail in the steady-state simulation in MATLAB but kept constant at the nominal point in the dynamic simulation in TRNSYS, i.e. without varying the inner efficiency

coefficients associated with each of the steam turbine stages. The generator efficiency was kept as equal to 99%.

Table 20 ST Isentropic efficiency

Isentropic Efficiency	Value	Units
HP steam turbine stage	86.63	%
IP steam turbine stage	89.99	%
LP steam turbine stage – 1st extraction	92.28	%
LP steam turbine stage – 2st extraction	92.30	%

6.3.4.2.1 Electrical generator off-design model

For the electrical generator off-design model, the mechanical and electrical efficiencies have been calculated as a function of the generator load by the means of a quasi-dynamic model in MATLAB. The generator electric power output E_{el} has been estimated from the mechanical shaft input E_{shaft} as shown in equation 6.23, where η_{mec} and η_{el} are, the mechanical and electrical efficiencies, respectively [31].

$$E_{el} = \eta_{mec}\eta_{el}E_{shaft} = \eta_{mec}\eta_{el}(E_T - E_c) \tag{6.23}$$

The overall efficiency variation is depicted in Figure 51, which shows the efficiency versus the generator load.

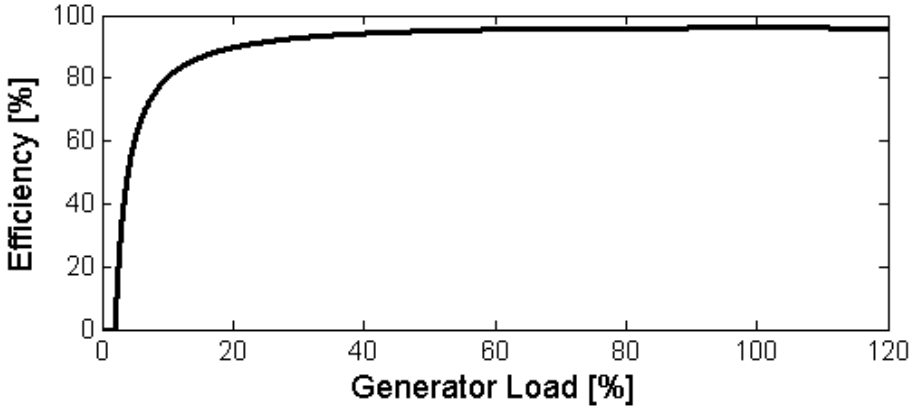

Figure 51 Generator off-design efficiency values [31].

Therefore, the off-design mechanical efficiency can be calculated taking into account the generator load (f_{load}) as it is shown in equation 6.24, where the subscript "o" refers to the nominal mechanical efficiency.

$$\eta_{mec} = 1 - \frac{1}{f_{load}}(1 - \eta_{mec}^{o}) \tag{6.24}$$

Similarly, the off-design electrical efficiency is estimated considering the nominal electrical efficiency as it is shown in equation 6.25.

$$\eta_{el} = 1 - f_{load}(1 - \eta_{el}^{o}) \tag{6.25}$$

6.3.5 Heat pump

For the water-water heat pump, the Type 668 in TRNSYS component library has been used [33]. This component models a single-stage heat pump. The catalogue data for the capacity and power has been modified accordingly to the data provided by MAYEKAWA heat pump manufacturer in order to estimate the COP with respect to the entering load and source temperature and be representative for an ammonia-based heat pump. Figure 52, shows the COP catalogue of the heat pump for the different source temperature levels. As expected for a higher load temperature, the solution presents lower COP.

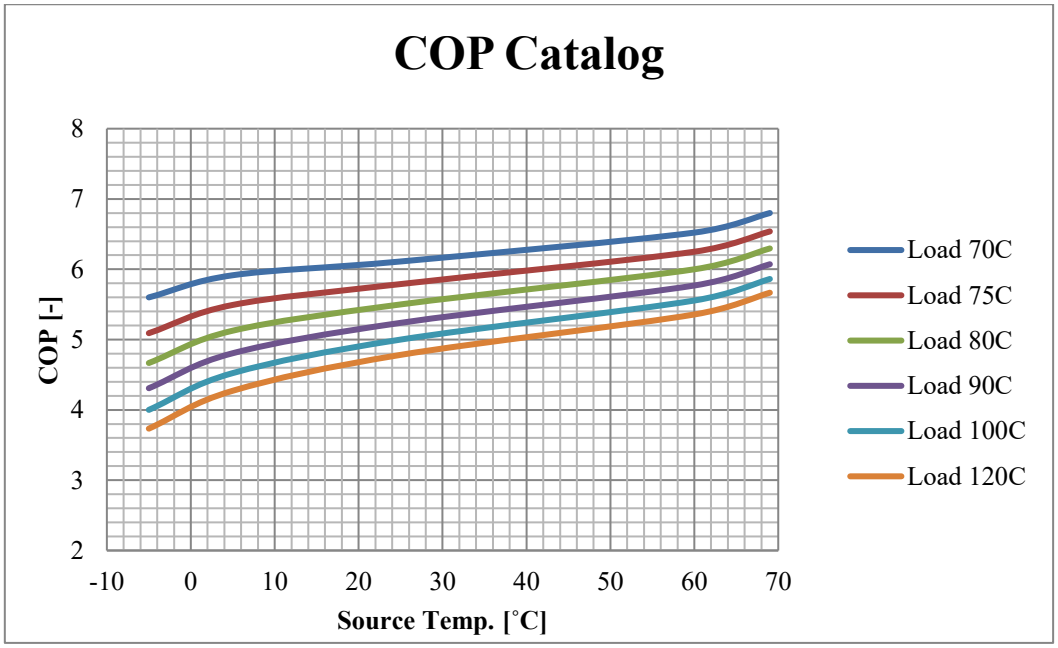

Figure 52 COP catalogue for Ammonia Heat Pump.

6.3.6 Thermal energy storage

For the modeling of water tank, the Type 39 in TRNSYS component library has been used. This component models a fully mixed tank with a constant cross-sectional area that contains a variable quantity of fluid [32]. It allows the level of the water in the tank to vary, according to the high and low level limits specified by the user. In this study, the minimum fluid volume was set to 10% of the tank volume while the maximum was set as the maximum volume capacity of the tank. In turn, the volume of the tank was set as an input parameter that can be varied depending on the analysis or sensitivity to be carried out. The cross-sectional area was estimated by using basic calculations based on a fixed diameter (d = 15 m) and the volume.

Table 21 TES parameters.

Parameter	Value	Unit
Wetted loss coefficient	6.0	kJ/ (hr m2 K)
Dry loss coefficient	4.0	kJ/ (hr m2 K)
Fluid specific heat	4.19	kJ/kgK
Design temperature, hot tank	55	°C
Design temperature, cold tank	35	°C

6.3.7 District heating condensers

The district heating condensers have been modeled in TRNSYS by the means of a calculator which uses the inputs computed by the steady-state simulation in MATLAB to work out the equations written in the calculator. These functions are then carried out by using the dynamic outputs from the cycle and/or the PHCC configuration. In turn, the amount of energy and mass flow that each condenser can extract was calculated as follows

$$Q_{DHcond} = DHD \cdot \left(\frac{Q_{DHcond,steady-state}}{maxDHD}\right) \tag{6.26}$$

$$massflow_{DHcond} = \frac{Q_{DHcond}}{H_{DHcond,steady-state} - H_{DHcond,out}} \tag{6.27}$$

Hence, the total heat production was calculated summing up the heat coming from the basic cycle with the heat produced by the heat pump when PHCC configuration is operated.

$$Total\ Heat = Heat_{CC} + Heat_{PHCC} \tag{6.28}$$

In a cogeneration heat and power plant, the only release option / heat pump high temperature interface that has been explored is the district heating one. However, heat pump can be connected in two different configurations, as it has been described in Chapter 6.1, hence a control logic was created to switch among the two possible DH condenser configurations, namely series and parallel configuration, Figure 53 and Figure 54, respectively.

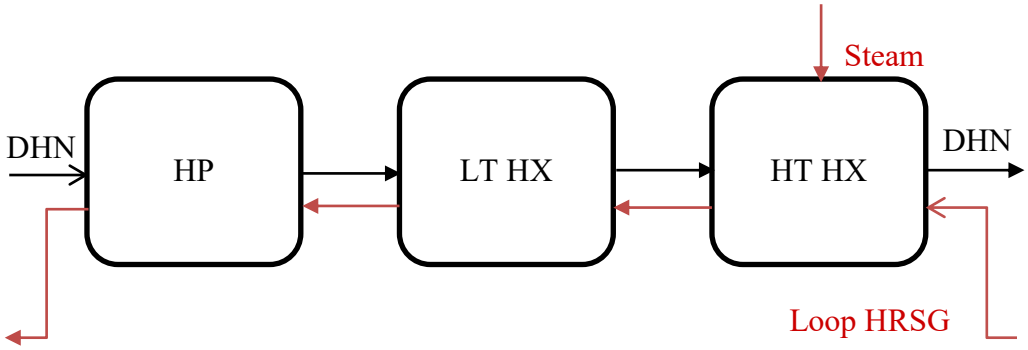

Figure 53 Series configuration

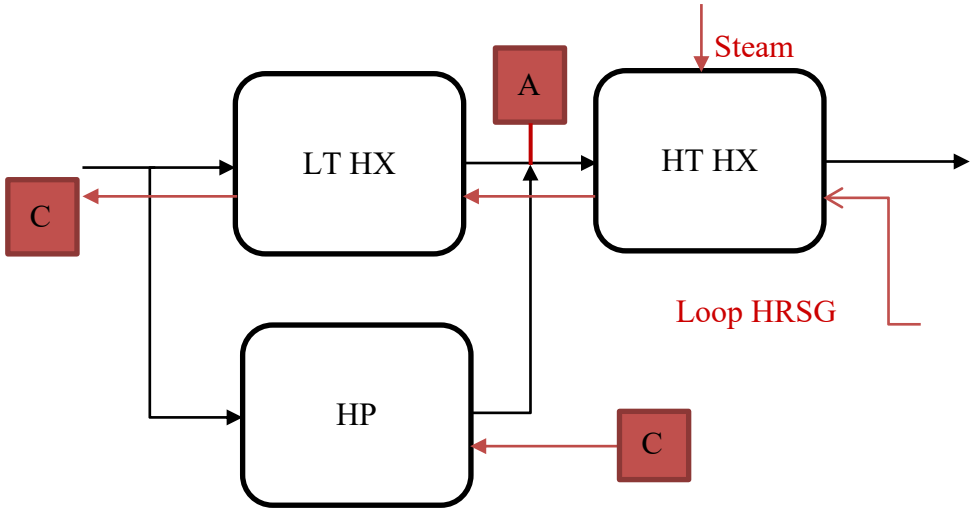

Figure 54 Parallel configuration

In the series configuration the heat pump is installed in series with the low temperature heat exchanger of the district heating network (DHN). Instead, the parallel configuration has the heat pump installed parallel to the low temperature heat exchanger of the DHN. The intermediate temperature, (A) in Figure 54, can be a free variable reaching at maximum the DHN delivery level.

To note that the pumps related to the PHCC were implemented in the TRNSYS model and the power consumed from this additional pumping system was added to the one of the combined cycle, thus resulting in slightly variation in the total electricity production due to the different parasitic losses when operating the PHCC mode either in parallel or series configuration.

6.4 Economic considerations

In this chapter the economic performance for Layout 2 and 3 is analysed and further discussed.

6.4.1 Capital Expenditure (CAPEX)

The capital expenditure costs accounts for all the investments required by the project and they include equipment purchasing costs and the related installation costs, pumping system costs and civil engineering costs required to manage the power plant as well as the facility's indirect costs. These cost functions mainly depend on the size of the units and related operating conditions. In this paragraph, the costs functions used to work out the economic performance are described and briefly explained.

The existing cost functions in DYESOPT were used to estimate the costs of the different components, equipment units and fuels. Since these equations refer to 2010 as reference year, in order to obtain the nominal cost in euros for the current year, the following equation has been implemented in the simulation tool [34].

$$C_{current\ year,€} = k \cdot C_{2010,\$} \cdot (1+i)^{y} \tag{6.29}$$

Where i is the mean inflation rate, which is equal to 2.1% [35], k is the foreign exchange ratio of the period 2010-2018 and is equal to 1.24245 €/USD and y is the number of years from 2010, the reference year of the cost functions, to 2018, the current year.

Table 22 Investment parameters.

Investment parameters	value	unit
Interest rate	6	%
Capital insurance rate	1	%
Construction period	2	year
Depreciation period	25	year
Decommissioning period	1	year

The investment parameters listed in Table 22 have been used in the following calculations. The costs for the components of the gas turbine cycle, i.e. the topping cycle, have been estimated by summing up the different cost of each of the sub-section of the GT, namely compressor, turbine, combustion chamber and the associated auxiliary services. The GT costs have been described with details in Appendix A.2.

$$C_{GT} = C_{comp} + C_{turb} + C_{comb} + C_{aux} \tag{6.30}$$

Accordingly, the costs associated to the steam turbine cycle, i.e. the bottoming cycle, are estimated by sum heat recovery steam generator, steam turbine, condenser, district heating condenser system, water treatment facilities and deaerator unit costs.

$$C_{ST} = C_{HRSG} + C_{turb} + C_{cond} + C_{waterTreatment} + C_{deaeretor} \tag{6.31}$$

In turn, the total equipment cost of the combined cycle is determined by taking into account both the units from the basic GTCC and the heat pump and thermal energy storage costs added by implementing the PHCC configuration.

$$C_{equip} = C_{GT} + C_{ST} + C_{gener} + C_{electronic} + C_{HP} + C_{TES} \tag{6.32}$$

To note that the investment cost for the thermal storage was estimated using the function shown in Figure 55, that refers to the cost for the building of insulated steel heat storage for CHP facilities. This cost includes equipment, installation, insulation and auxiliary costs [36].

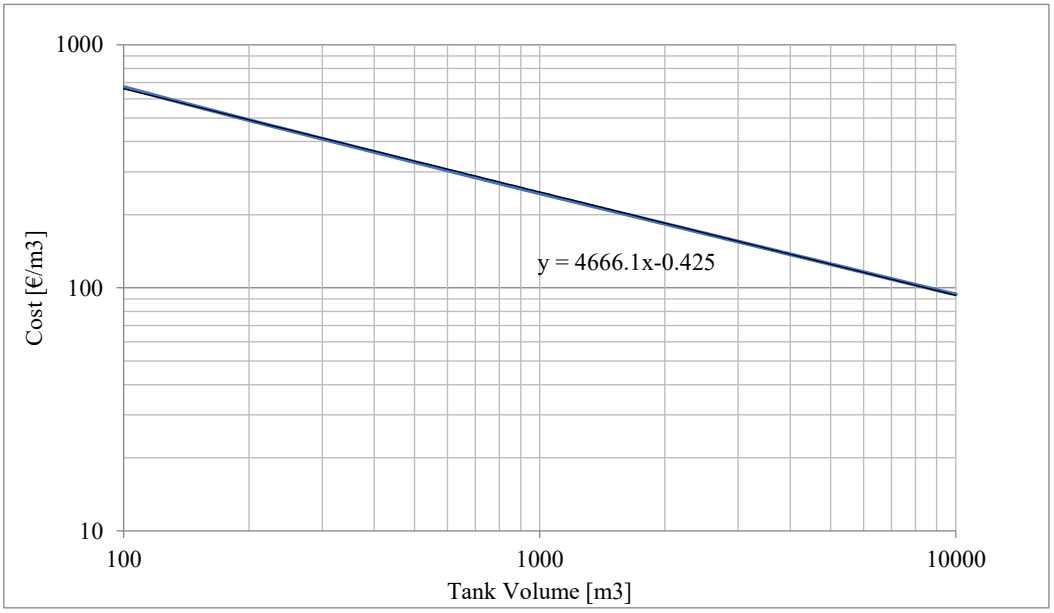

Figure 55 Investment Cost function water tank

Furthermore, the investment cost for the heat pump was estimated multiplying the capacity of the heat pump in kilowatt by the reference cost of 1580 €/KW [27].

$$C_{HP} = 1580 \cdot P_{HP} \tag{6.33}$$

Then, installation costs are estimated by multiplying the equipment costs by a fraction of the total equipment costs, in this case set to 20% of these costs. This value is taken as default parameters from DYESOPT.

$$C_{installation} = 20\% \cdot C_{equip} \tag{6.34}$$

In turn, the total power plant cost was calculated by adding to equipment and installation costs the civil engineering costs and natural gas pipeline system costs required by the power plant.

$$C_{plant} = C_{equip} + C_{install} + C_{NGpipe} + C_{civil} \tag{6.35}$$

Moreover, total investment cost takes also into account the contingency, indirect engineering costs and decommissioning costs; these costs have been estimated considering that each of them

accounts for 15%, 3% and 5%, respectively. These percentages are taken as default parameters from DYESOPT.

$$C_{contingency} = 15\% \cdot C_{plant} \tag{6.36}$$

$$C_{indirect} = 3\% \cdot C_{plant} \tag{6.37}$$

Finally, the total capital expenditure cost (CAPEX) required by the CHP plant is estimated using equation 6.40. 5% of the total investment cost is taken as the amount of money necessary for the decommissioning of the power plant.

$$C_{inv} = C_{plant} + C_{indirect} \tag{6.38}$$

$$C_{dec} = 5\% \cdot C_{plant} \tag{6.39}$$

$$CAPEX = C_{inv} + C_{dec} \tag{6.40}$$

The total investment costs of the Reference CHP plant shown in equation 6.40, is estimated about 630,3 million of €. The capital costs breakdown for the cogenerative combined heat and power plant where the heat pump with thermal energy storage system (PHCC configuration) is not implemented is presented in Figure 56.

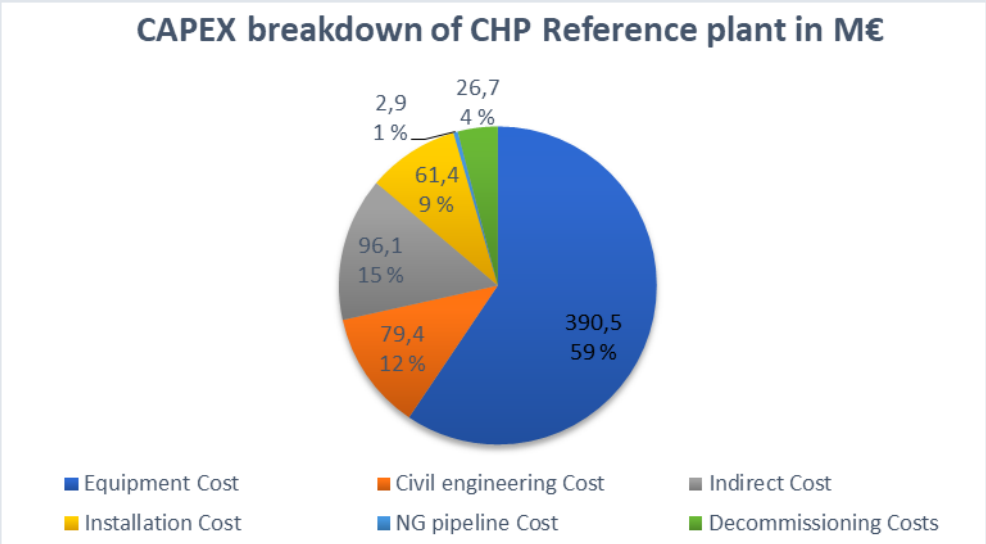

Figure 56 CAPEX breakdown of the CHP reference plant model

6.4.2 Operation and Maintenance Expenditure (OPEX)

The operation and maintenance costs do not include capital outlays and they refer to the cash flow associated to the operating time of the facility, namely depreciation period, on an annual basis.

For the CHP plant the operational cost is calculated considering water use cost and fuel use cost.

$$C_{Operational} = C_{fuel} + C_{water} \tag{6.41}$$

Where the cost of fuel and cost of water are calculated as follows, assuming a cost of fuel equal to 17.7 €/MWh (x_{fuel}) [28] and cost of water equal to 1.6 €/MWh (x_{water}) [37].

$$C_{fuel} = x_{fuel} \cdot \int m_{fuel} \cdot LHV_{fuel} \cdot dt \tag{6.42}$$

$$C_{water} = x_{water} \cdot \left(vol_{water}^{comr} + vol_{water}^{cycle}\right) \tag{6.43}$$

In this study, the water is supposed to be used for the feed-water pump and compressor washing on regular basis. The water needed for the condenser is assumed to be supplied from the nearby branch of Po river free of charge with regulated temperature rise levels.

While the maintenance cost was estimated by sum the cost for the power block maintenance and the service contract cost. For the power block maintenance of GT and ST cycle components, 3% of the equipment cost on an annual basis was chosen. For the annual civil maintenance costs, 4% of investment costs in gas piping and civil engineering elements was considered [31].

In addition, the labour cost was estimated about 998 310 € per year by using the cost function in DYESOPT; this includes salaries of two technicians and two plant operators and all the associated costs to the plant personnel such as employee insurance and related fees.

The O&M costs breakdown for the cogenerative combined heat and power plant where the heat pump with thermal energy storage system (PHCC configuration) is not implemented, is presented in Figure 57.

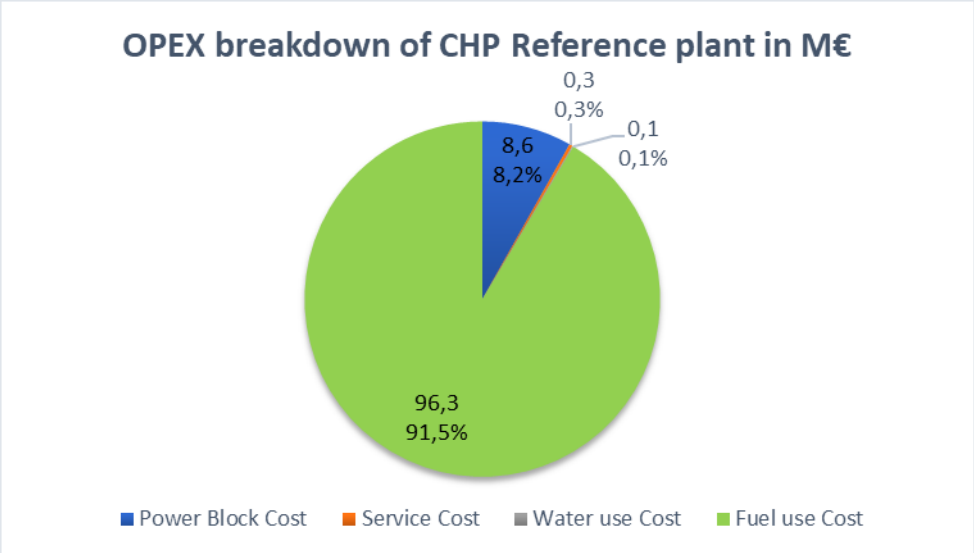

Figure 57 OPEX breakdown of CHP Reference plant model

6.5 Thermo-economic analysis

To figure out the best configuration and unit size for the PHCC configuration a sensitivity analysis was carried out changing the most critical-size parameters, namely TES volume and HP capacity, as well as on their investment costs. Moreover, on top of this analysis a further sensitivity has been carried out by changing the power plant load.

6.5.1 Control logic and modes definition

A control logic for the happening of charging, discharging and combined cycle directly to the HP (CC to HP) has been built as it is shown in Table 23, based on the best operational strategy with respect to the heat demand, thus aiming for heat addition when the district heating demand is relatively high and is economically convenient. In turn, 60% of maximum district heating demand was considered as a threshold for the operational control. However, changing this percentage might lead to either an increase or decrease of the PHCC operations. The maximum district heating demand (*maxDHD*) for the case study was assumed equal to 260 MW as referenced from the local operator (IREN S.p.A). Note that since the load control already takes into account the electricity price behaviour, it was not considered in the definition of the operational control logic of the PHCC layout.

Table 23 Control logic.

Case	Control logic
Charging	<60% of maxDHD
Discharging	>60% of maxDHD
CC to HP	>60% of maxDHD

Moreover, four different modes were investigated changing the most critical-units' size parameters as shown in the Table 24.

Table 24 Modes (configurations).

Unit	**Mode 1**	**Mode 2**	**Mode 3**	**Mode 4**	**Unit**
TES volume	1000	1000	2000	2000	m^3
HP capacity	2.17	4.34	2.17	4.34	MW_{el}

Reference plant KPIs are shown in

Table 25. The reference plant refers to cogenerative combined heat and power plant where the heat pump with thermal energy storage system (PHCC configuration) is not implemented.

Table 25 KPIs for Reference CHP plant model.

KPI	**Reference plant**	
	Values	**Unit**
Electricity Generation	2640.99	GWh_{el}/yr
Thermal Production	1286.3	GWh_{th}/yr
Alpha value	2.053	-

Electrical efficiency	50.9	%
thermal efficiency	24.8	%
Total efficiency	75.7	%
Specific CO2 emissions	375.2	kg/MWh_{el}
Specific water consumption	33.7	l/MWh_{el}
Total Investment Cost	630.3	M€
NPV	1198.9	M€
PBT	8	yr
LCoE	66	$€/MWh_{el}$
IRR	11.73	%

Otherwise, the resulting KPIs for a cogenerative CHP plant operating with the integration of the PHCC layout, are shown in

Table 26. In particular, the results for the two extreme cases, namely Mode 1 and Mode 4, are shown.

Table 26 KPIs for CHP plant model, Mode 1 and 4.

KPI	**Mode 1**		**Mode 4**		
	Series	**Parallel**	**Series**	**Parallel**	**Unit**
Electricity Generation	2638.874	2639.543	2637.16	2637.78	GWh_{el}/yr
Thermal Production	1292.7089	1292.7	1301.94	1301.94	GWh_{th}/yr
Alpha value	2.0414	2.0419	2.0256	2.0260	-
Electrical efficiency	50.81	50.83	50.76	50.77	%
thermal efficiency	24.9	24.9	25.1	25.1	%
Total efficiency	75.71	75.73	75.86	75.87	%
TES utilization (annual basis)	52	52	45	45	%
TES utilization (seasonal usage)	90	90	78	78	%
Specific CO2 emissions	375.5	375.4	375.7	375.6	kg/MWh_{el}
Specific water consumption	33.8	33.8	33.8	33.8	l/MWh_{el}
Total Investment Cost	634.9	634.9	639.2	639.2	M€
NPV	1201.2	1201.7	1205.6	1206	M€
PBT	8	8	8	8	yr
LCoE	66.2	66.2	66.5	66.4	$€/MWh_{el}$
IRR	11.636	11.643	11.58	11.59	%

Mode 4 was deemed the best configuration (2000 m3 for the TES and 4.34 MWe for the HP) since this case shows the highest NPV and a noticeable increase in thermal production, when compared with the other modes, with relatively negligible energy losses, and greater global efficiency.

On the other hand, this case shows lower TES utilization factor due to the bigger size of the unit. Moreover, the internal rate of return (IRR) for Mode 4 is lower than the one of the Reference CHP plant; however, the NPV is higher, meaning that even though the pace at which the project may give some return is slow, the project may also be adding a great deal of overall value to the facility. Then, the size of the units was chosen taking into account the state of charge of the TES in such a way it would have achieved certain charge level, trying to get charged as much as possible. Otherwise, too small a tank would have resulted in a TES not fully charged very often, i.e. the tank would have discharged very quickly.

Finally, the parallel configuration was chosen as the best configuration due to the slightly higher net electrical power output coming from the lower power required by the pumping system. This is linked to the necessity of a lower temperature difference, which affects less negatively the COP and so the electrical consumption when compared with the series configuration. In other words, in the parallel configuration the mass flow is split between the two pipelines resulting in lower parasitic losses, hence in lower power consumption and operating costs.

6.5.2 Technical performance

In this chapter, the visual presentation of the contribution of the PHCC layout with parallel configuration is shown in several graphs where the thermodynamic behaviour of the cycle with respect to the reference plant behaviour can be seen. In particular, different periods of the year both on monthly and weekly basis, namely January, May and November, are shown.

The following figures compare the thermal and electricity production of the different period of the year as well as the state of charge for the Mode 4, as representative of the option with the best techno-economic performance shared by the different solutions. In this way, it is possible to compare the impact of the PHCC parallel configuration on the thermal energy production and the electrical consumption, related to the energy provided to the HP compressor.

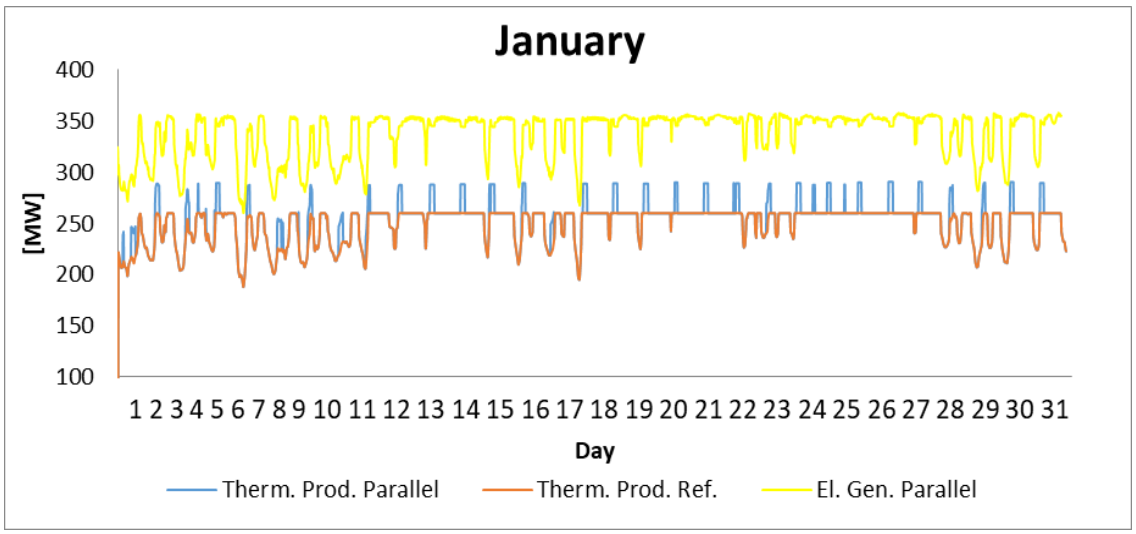

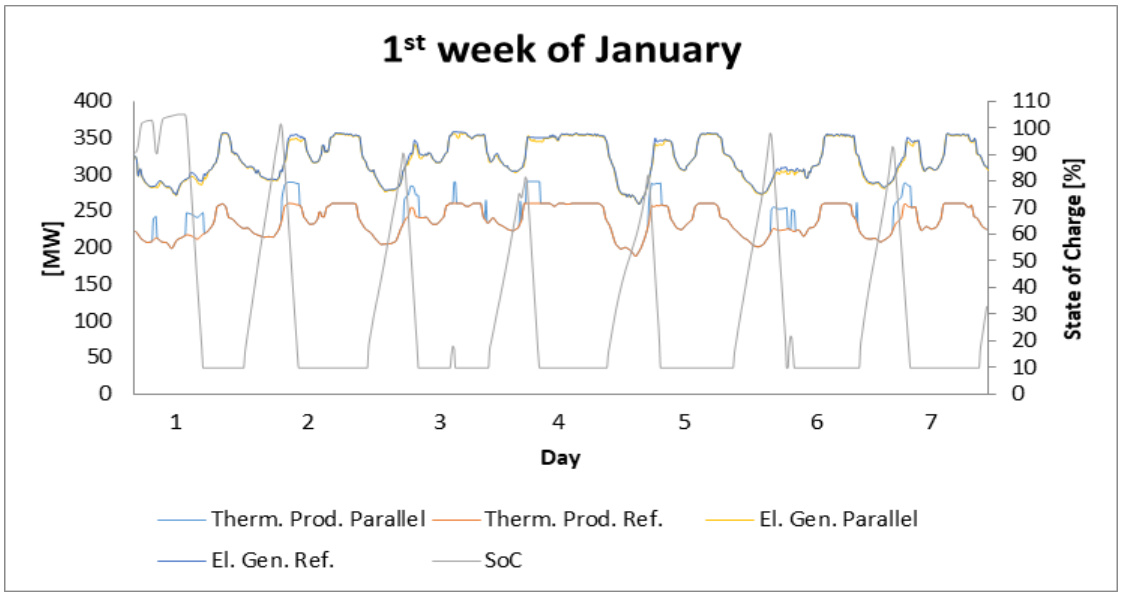

Figure 58 Monthly and weekly thermodynamic behaviour, January

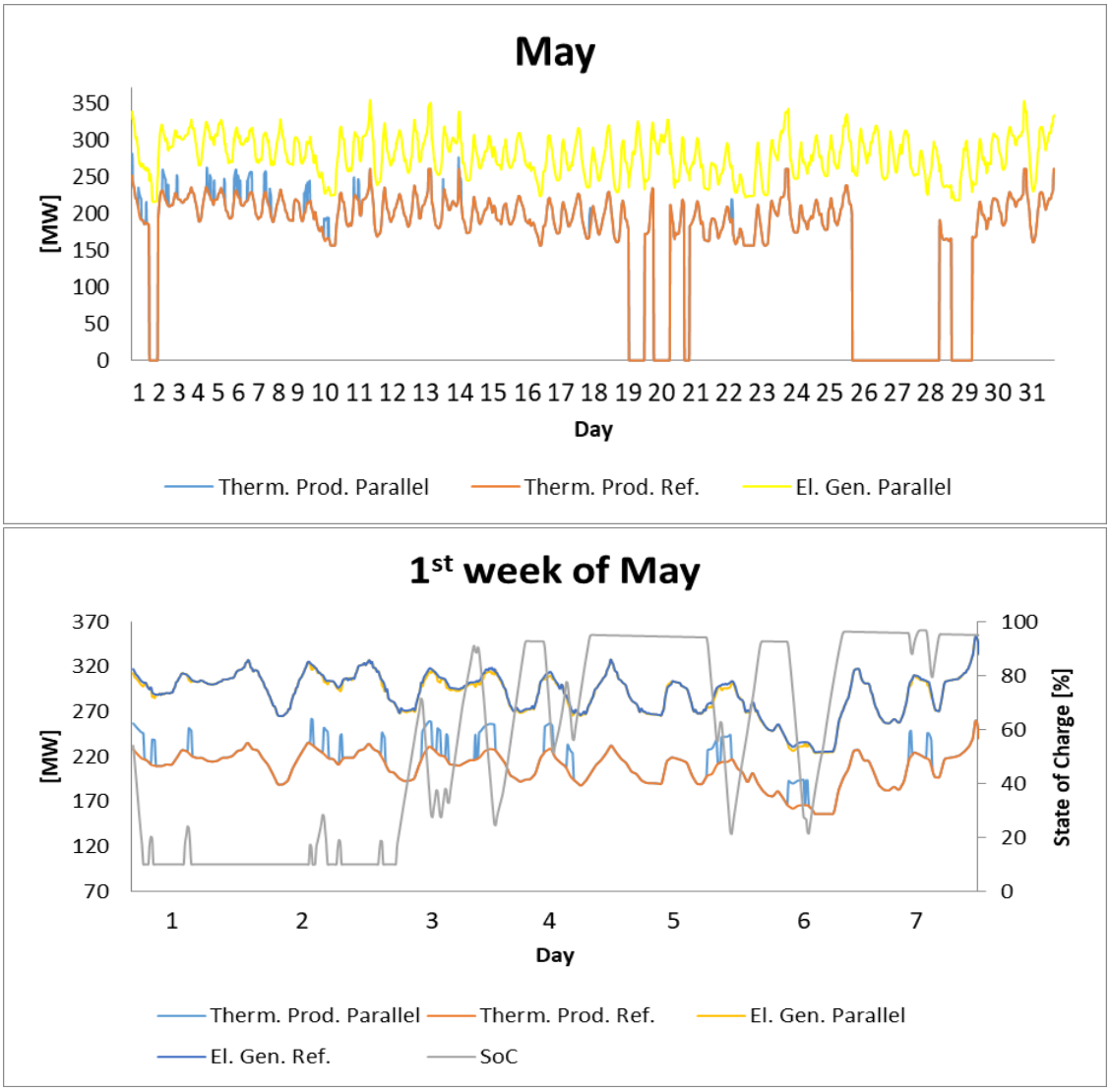

Figure 59 Monthly and weekly thermodynamic behaviour, May

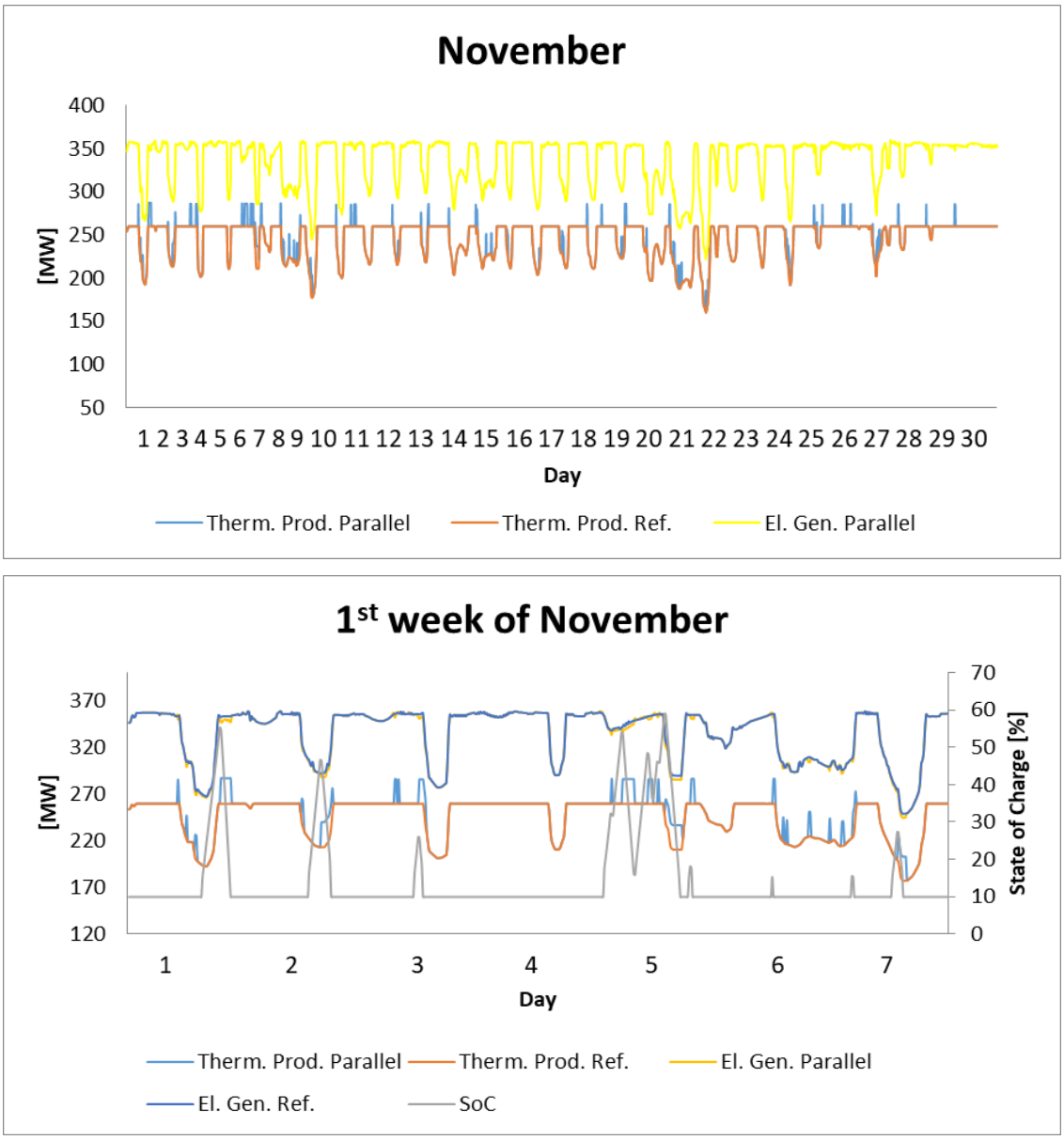

Figure 60 Monthly and weekly thermodynamic behaviour, November

As expected, the use of the heat pump either in direct connection with the combined cycle or coupled with the thermal storage system causes a noticeable drop in the electricity generation. However, due to the contribution of the PHCC configuration a significant variance in thermal energy production compared with the reference plant occurs throughout the year, with a relatively large positive net effect as shown in the figures above. In turn, the thermal production has been enhanced on average by 15 up to 20 MW_{th}.

Moreover, a plot with the thermal and electricity production behaviour on an annual basis is shown in Figure 61 and Figure 62, respectively. To note that in summer, the heat demand is lower or inexistent thus leading to a lower usage of the heat pump for heat production purposes, thus calling for the viability of such a proposed layout in colder regions.

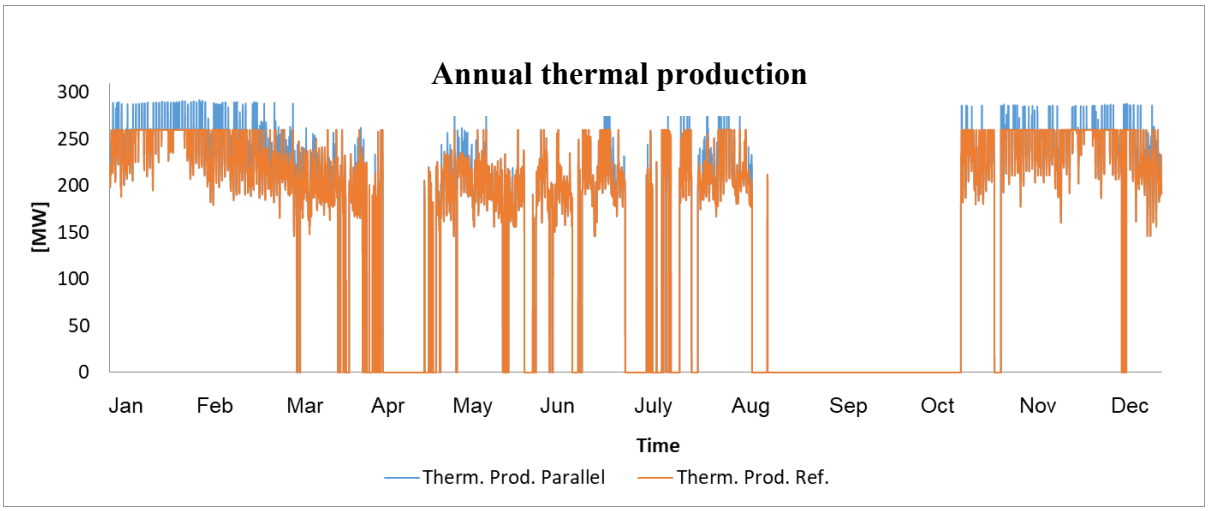

Figure 61 Annual thermal production.

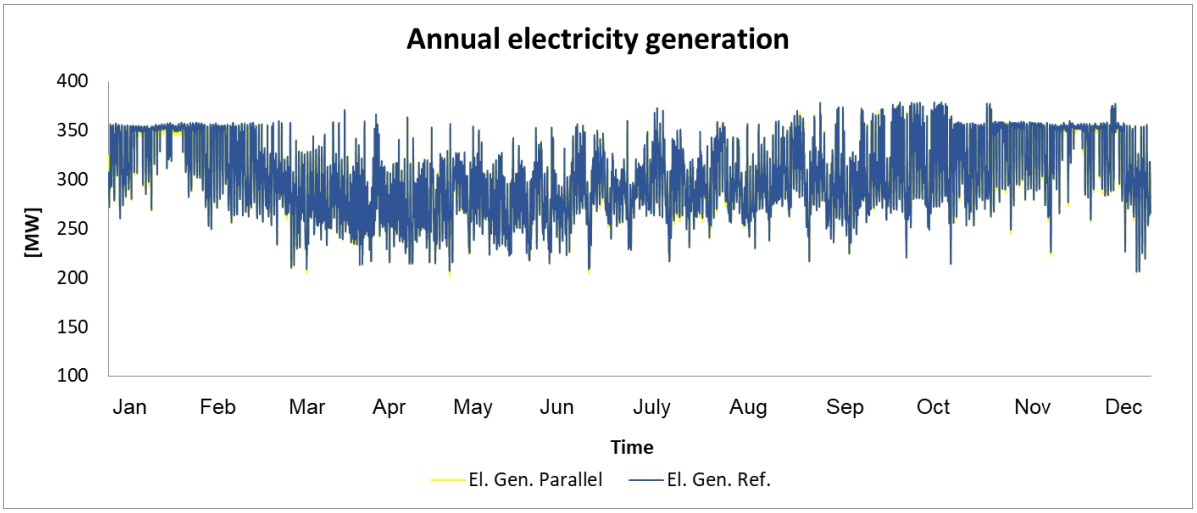

Figure 62 Annual electricity generation.

Finally, to test the impact of the load on the ramp-up, both the delta difference of the inlet mass flow in the compressor and the delta load between two subsequent timesteps (in this case 15 min per timestep) were evaluated. The maximum ramp-up was estimated as equal to 0.362 Δkg/s and 0.7% over time for the compressed air mass flow and load, respectively. Thus, the load was used to control the compressor mass flow in a similar fashion which is the key parameter used in this model to control the operational behaviour and performance of the power plant.

6.5.3 Economic performance

With the conditions presented in the previous chapter, Mode 4 with a 4.34 MW_{el} heat pump and 2000 m^3 water tank leads to a total capital investment of 639.2 million of €. The CAPEX breakdown for this case is shown in Figure 63.

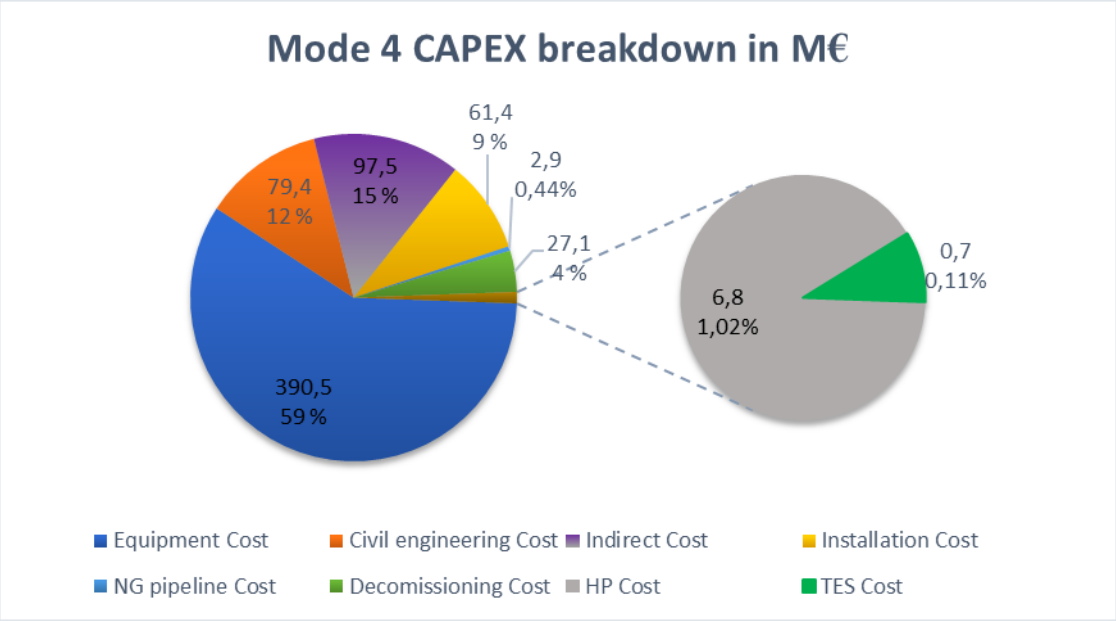

Figure 63 CAPEX breakdown best configuration, Mode 4.

A significant variance in the annual cash inflow compared with the reference plant model occurs throughout the year, with a noticeable positive net effect on the annual income as shown in Figure 64. In particular, when the heat pump is operating, the thermal production of the PHCC layout generates a total annual benefit of about 3,024.7 million €. The effect, however, is only appreciated during the winter months – thus calling for the economic feasibility of such a proposed layout in colder regions where the heat demand/consumption is less susceptible to variations.

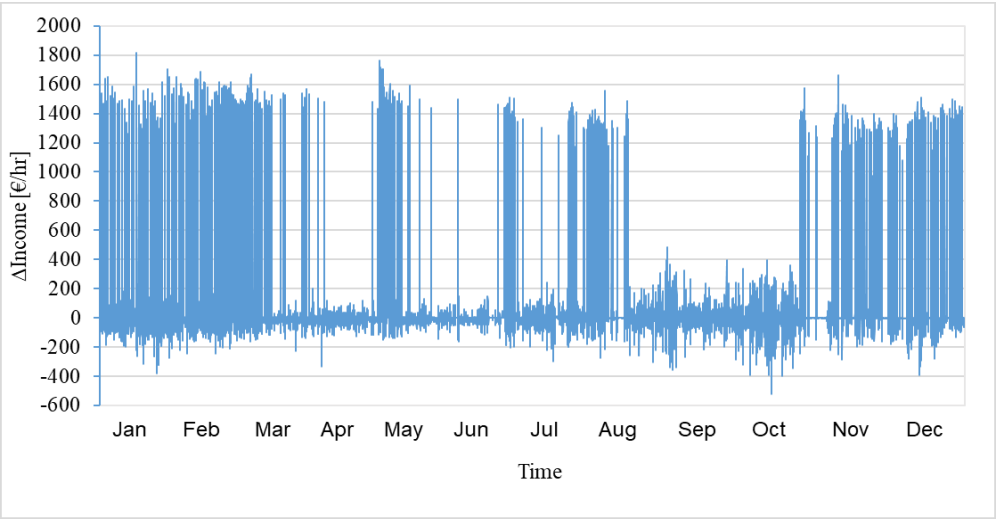

Figure 64 Annual income difference between Mode 4 and CHP Reference plant model.

6.6 Sensitivity analysis

In this chapter the sensitivity analyses carried out for this study are described. Afterward, the results are shown and commented.

6.6.1 Unit cost variation

To figure out the influence of the PHCC units costs on the economic performance of the new combined cycle layout a second sensitivity on the TES and HP unit's costs has been carried out. In particular, a multiplication factor of 0.5 was used to vary the units' costs, thus calculating the same economics considering half of the expenses for the PHCC layout (i.e. 3.4 M€ for the HP and 0.4 M€ for the TES).

Table 27 KPIs CHP plant for Mode 4 (unit cost variation).

KPI	**Mode 4**		
	Series	**Parallel**	**Unit**
Total Investment Cost	635.4	635.4	M€
NPV	1206	1206.4	M€
PBT	8	8	yr
LCoE	66.3	66.3	€/MWh$_{el}$
IRR	11.69	11.70	%

Table 27 shows a IRR of about 11.70% which is approximately the same IRR of the Reference CHP plant. Therefore, this means that the PHCC configuration becomes more cost-effective as the price is reduced to at least to half of the current price.

6.6.2 Power plant load variation

In addition to the units' cost variation, a sensitivity has been carried out in order to test the influence of the load on the combined cycle performance and in particular the boundary points in Step 1 (Load control 6.3.3) have been modified. In turn, if the ratio is above 1.4, then the load is 100 %. Below 0.6 the load is at the minimum. In the range between 0.6 and 1.4 the load varies accordingly so that at ratio equal to 1, the power plant is operating at half load. Table 28 shows the number of hours per each of the load condition over one year.

Table 28 Load operating hours (load variation).

Load	**Full**	**Half**	**Minimum**
Operating hours (hr/yr)	2325	1906	471

For the best case (Mode 4), the KPIs with respect to the change in power plant load are presented in Table 29.

Table 29 KPIs CHP plant (load variation).

KPI	Reference	Mode 4		
		Series	Parallel	Unit
Electricity Generation	2709.1	2705.5	2706.1	GWh_{el}/yr
Thermal Production	1317.5	1333.2	1333.2	GWh_{th}/yr
Alpha value	2.0562	2.0293	2.0297	-
Electrical efficiency	50.94	50.87	50.88	%
thermal efficiency	24.8	25.1	25.1	%
Total efficiency	75.74	75.97	75.98	%
TES utilization (annual basis)	-	45	45	%
TES utilization (seasonal usage)	-	77	77	%
Specific CO2 emissions	374.4	374.9	374.8	kg/MWh_{el}
Specific water consumption	32.9	32.9	32.9	l/MWh_{el}
Total Investment Cost	630.3	640.6	640.6	M€
NPV	1230.7	1237.4	1237.9	M€
PBT	8	8	8	yr
LCoE	65.2	65.7	65.7	$€/MWh_{el}$
IRR	12.19	12.0008	12.007	%

The results show that if the load is operating at overall higher loads more frequently both the electricity generation and thermal production are enhanced. However, the economic performance of the plant is not sensitively improved when compared with the CHP Reference plant due to the same considerations previously assessed on the current Italian energy market.

7 Conclusion

For Layout 1, a techno-economic model of an innovative CCGT integrated with an inlet GT mass flow pre-cooling loop consisting of a heat pump and a cold thermal energy storage unit has been developed and used to evaluate the feasibility of such a concept. The proposed layout is shown to increase the power output of a CCGT during times of peak electricity prices and at high ambient temperatures. This comes at the expense of significantly decreasing the power during off-peak hours, limiting the economic benefit of the system (due to the required charging and HP consumption). The study shows that, for the cost assumptions undertaken and for the specific market considered, the integration of such a system with the TES is not viable as it would be less profitable than building a conventional CCGT. However, implementing the heat pump alone can bring cost-effective benefits to the cycle performance. It is also shown that depending on the difference between peak electricity price and off-peak prices then the system could be profitable, being thus highly dependent to the evolution of electricity prices in the market itself. For instance, a market with higher price volatility and more pronounced peaks would potentially justify the investment. The latter though, is highly dependent on the evolution of both demand and new type of generation technologies integrated into such a system, which is hard to predict. Specifically, for the study case considered in the study utilizing only continuous cooling and using the heat pump during off-peak hours to cool down the GT inlet air as close to the minimum temperature (5°C) as possible will lead to the largest profit that this layout can provide. Additionally, one clear benefit of integrating the pre-cooling system is that it adds more flexibility to the operation of the plant. Such flexibility benefits were not explicitly quantified in this analysis. Furthermore, as both the control logic implemented and the cost assumptions play an important role in the results, a thorough sensitivity analysis with regards to such assumptions is also recommended. Lastly, it is pertinent to the reliability of the model to see that pressure drop, condenser temperature, storage thermal losses and heat pump COP are properly implemented in the improved model.

For Layout 2 and 3, a techno-economic performance evaluation of the proposed CHP cogenerative plant with the implementation of an innovative heat addition system, consisting of a water-water heat pump coupled with a thermal energy storage has been developed to evaluate the feasibility of such layout. A flexible model was developed and used specifically for the case corresponding to market boundaries present at Turin (historic hourly electricity price and weather used).

For the cogenerative CHP plant, several layout options were analyzed, and a comparative analysis was performed with respect to the Reference CHP plant model. The most appealing in term of thermodynamic performance resulted to be the one with a water tank of 2000 m^3 and a heat pump of 4.34 MW_{el}, namely Mode 4. The proposed system leads to an enhanced thermal energy output of 15 up to 20 MW_{th} on average, even though this comes at the expense of a noticeable decrease in electricity generation. Furthermore, the parallel configuration, i.e. the heat pump in parallel with the low temperature district heating condenser, was chosen as the best district heating system design since it results in lower energy consumption due to the lower parasitic losses in the piping system, thus resulting in lower operating costs.

From an economic performance prospective, the integration of the HP+TES layout does not necessarily enhance the profitability of the plant in the current Italian market when benchmarked against the reference plant (stated from the lower IRR and higher LCoE when

compared with the results of the Reference CHP plant model). However, it does grant flexibility in the operation and allows to maximize production and revenues in times of higher heat prices and/or demand. Moreover, the seasonal behavior observed, allows to infer that in the regions with more stable and/or larger heat demand then the integration of TES and HP will probably enhance the profitability of the plants. Furthermore, a greater NPV has been estimated when the PHCC configuration is operated, meaning that this layout generates profits and may also be adding a great deal of overall value to the basic combined cycle.

Finally, the sensitivity analysis shows that the project becomes more economically viable when capital costs of the HP and TES are lower, thus leading to lower total investment costs. In this scenario, the PHCC configuration becomes more cost-effective and economically appealing. Furthermore, the load has been varied and was found affecting sensitively the thermodynamic performance of the power plant, with a greater thermal and electricity production when the load is generally higher throughout the year, however it showed no major impact on the results trends. Thus, the load control as well as the control logic implemented, and cost assumptions represent key factors in the overall resulting performance of the power plant, so a thorough sensitivity analysis with regards to such assumptions is also recommended for these layouts.

8 Future work

This master thesis has been performed as part of an on-going EU funded project on partnership with different institutions and companies, looking at different aspects of modeling, component design, operations and layout definition. This thesis simply represents the first work-package of this project.

It was noted as a conclusion that the power oriented layout brings operational flexibility and even some economic benefits due to an increased power generation during peak electricity price. It was not, however, part of this analysis to study the benefits that implementing this system could provide for the local energy grid. This type of flexibility as a service has been studied by Olivella-Rosell et al [38], who proposed a local flexibility market where distribution system operators can increase or decrease the load and generation within a local area.
For the cogenerative CHP plant layouts, it has been found that it adds another layer to the plant flexibility due to the additional thermal energy that the heat pump is able to provide to the district heating network, even if it comes at the expense of the electricity generation. Hence, a detailed analysis on the electrical consumption of the heat pump should be conducted and further discussed with the manufacturers to find the most suitable unit in term of performance and technology. Moreover, the district heating system with parallel configuration has been found to be the best layout due to the lower parasitic losses, however both the two solutions shall be analyzed in depth in all operating conditions of the power plant and off-design operation of heat exchangers shall be investigated.
However, the thesis' scope was limited to the level where a power plant is considered as a system yet changing the operational scheme of a plant will have repercussions to other power generation sites nearby. Answering the problem of increased flexibility demand on a larger system and grid level would be useful when striving to implement the studied layouts in the numerous combined cycle power plants across Europe.

When it comes to the technical aspects of the models built, it is proposed for the first layout that some pertinent details are carefully assessed for future versions of the work. For instance, the pressure drop caused by installing the gas turbine heat exchanger at the gas turbine inlet must be properly accounted for. In the current version of the model a simplification was made to assume the pressure drop to be constant due to keeping the fuel and air mass flows and thus, the gas turbine load constant on an annual basis. Here an improvement to the operational strategy could also be suggested; the scheme of operating the plant always at full load is not necessarily the most profitable one. An important parameter completely bypassed in the model was thermal losses in the storage tank. This is sure to further decrease the profitability of the layout with TES and therefore it is not recommendable to put too much effort in making the combination of TES and HP profitable. On the contrary, operating the layout with the heat pump alone should be further studied. As for the heat pump, an initial COP (4.5) was assumed to occur always in the first time step of entering a continuous cooling or charging loop. There may be more accurate methods to calculate the COP with temperature levels and mass flows estimated to take place thereafter. In general, using MATLAB as the tool to model a transient system is a limited approach in itself. Therefore, it is finally suggested to create a similar model of the power oriented layout in TRNSYS or a comparable tool able to more accurately evaluate dynamic system operation.

Concerning the second and third layouts, the inefficiencies due to the load variation in the gas turbine have not been assessed, so a proper GT component which account for those shall be implemented in TRNSYS. In the current version of the model, the isentropic efficiency is kept constant to the value estimated in the steady-state model. Moreover, some issues with the charging and discharging of the TES have been encountered due to the assumption related to the control logic and the lack of data in the power production of the reference CHP plant for long periods throughout the year, that was used to implement the operational strategy. This in turn led to a lower usage of the thermal energy storage system than the one expected, thus meaning that the operational strategy currently adopted in Moncalieri power plant reduces the TES utilization factor in the new layout. Hence, a test of the new cogenerative CHP plant under different operational strategies is also recommended.
For both the layouts, condenser temperature was considered stable throughout the year, although the Po river water has a certain behavior annually. This would certainly cause a variation in power generation as well, although it is not taken into account in the power curve equation provided by IREN and thus in these models.

Bibliography

[1] European Commission, “The EU Emissions Trading System (EU ETS),” 2013.

[2] P. Vithayasrichareon, J. Riesz, and I. MacGill, “Operational flexibility of future generation portfolios with high renewables,” *Appl. Energy*, vol. 206, no. August, pp. 32–41, 2017.

[3] R. Pavri and G. Moore, “Gas turbine emissions and control,” *Gen. Electr. Rep. No. GER-4211*, 2001.

[4] M. A. Gonzalez-Salazar, T. Kirsten, and L. Prchlik, “Review of the operational flexibility and emissions of gas- and coal-fired power plants in a future with growing renewables,” *Renew. Sustain. Energy Rev.*, vol. 82, no. July 2017, pp. 1497–1513, 2018.

[5] A. Benato, S. Bracco, A. Stoppato, and A. Mirandola, “Dynamic simulation of combined cycle power plant cycling in the electricity market,” *Energy Convers. Manag.*, vol. 107, pp. 76–85, 2016.

[6] A. Benato, A. Stoppato, and S. Bracco, “Combined cycle power plants: A comparison between two different dynamic models to evaluate transient behaviour and residual life,” *Energy Convers. Manag.*, vol. 87, pp. 1269–1280, 2014.

[7] F. Alobaid, R. Postler, J. Ströhle, B. Epple, and H.-G. Kim, “Modeling and investigation start-up procedures of a combined cycle power plant,” *Appl. Energy*, vol. 85, no. 12, pp. 1173–1189, 2008.

[8] L. Balling, “Fast cycling and rapid start-up: new generation of plants,” *Mod. Power Syst.*, no. January, pp. 35–41, 2011.

[9] G. Renaud, “Main Conventional Cycle,” *Energy Syst.*, pp. 567–576, 2012.

[10] U. Desideri, “Fundamentals of gas turbine cycles: thermodynamics, efficiency and specific power,” in *Modern Gas Turbine Systems*, P. B. T.-M. G. T. S. Jansohn, Ed. Woodhead Publishing, 2013.

[11] A. Guagliardi and V. Casamassima, “Avviamenti rapidi dei cicli combinati,” *RSE*, pp. 1–17, 2013.

[12] G. F. Hundy, A. R. Trott, and T. C. Welch, *Refrigeration, Air Conditioning and Heat Pumps*. Butterworth-Heinemann, 2016.

[13] JRC, *Background Report on EU-27 District Heating and Cooling Potentials, Barriers, Best Practice and Measures of Promotion*. 2012.

[14] JRC, *Background Report on EU-27 District Heating and Cooling Potentials, Barriers, Best Practice and Measures of Promotion*. 2012.

[15] “Key Performance Indicators.” [Online]. Available: https://www.intrafocus.com/key-performance-indicators/. [Accessed: 21-Mar-2018].

[16] M. Nadir, A. Ghenaiet, and C. Carcasci, “Thermo-economic optimization of heat recovery steam generator for a range of gas turbine exhaust temperatures,” *Appl. Therm. Eng.*, vol. 106, pp. 811–826, 2016.

[17] G. Mohan, S. Dahal, U. Kumar, A. Martin, and H. Kayal, “Development of natural gas fired combined cycle plant for tri-generation of power, cooling and clean water using waste heat recovery: Techno-economic analysis,” *Energies*, vol. 7, no. 10, pp. 6358–6381, 2014.

[18] R. Kehlhofer, F. Hannemann, B. Rukes, and F. Stirnimann, *Combined-Cycle Gas & Steam Turbine Power Plants*. 2009.

[19] M. A. Ancona, M. Bianchi, F. Melino, and A. Peretto, "Power Augmentation Technologies: Part II — Thermo-Economic Analysis," no. 56673. p. V003T20A014, 2015.

[20] C. Jones and J. A. Jacobs Iii, "GER-4200 - Economic and Technical Considerations for Combined-Cycle Perfomance-Enhancement Options."

[21] U. Desideri, "Fundamentals of gas turbine cycles: thermodynamics, efficiency and specific power," in *Modern Gas Turbine Systems*, P. B. T.-M. G. T. S. Jansohn, Ed. Woodhead Publishing, 2013.

[22] GE Power, "Combined cycle power plant." [Online]. Available: https://www.ge.com/power/resources/knowledge-base/combined-cycle-power-plant-how-it-works.

[23] S. Kalaiselvam and R. Parameshwaran, "Thermal Energy Storage Technologies for Sustainability," *Therm. Energy Storage Technol. Sustain.*, pp. 1–444, 2014.

[24] IEA-ETSAP and IRENA, "Thermal Energy Storage - Technology Brief," vol. 92, no. January, p. 24, 2013.

[25] J. N. W. Chiu and V. Martin, "Submerged finned heat exchanger latent heat storage design and its experimental verification," *Appl. Energy*, vol. 93, pp. 507–516, 2012.

[26] U.S. Energy Information Administration, "Capital Cost Estimates for Utility Scale Electricity Generating Plants," 2016.

[27] J. Song, H. Li, and F. Wallin, "Cost Comparison between District Heating and Alternatives during the Price Model Restructuring Process," *Energy Procedia*, vol. 105, pp. 3922–3927, 2017.

[28] ENEA, "Energy: In the first semester price of kilowatt-hour for Italian companies dropped by 6%, Italy/UE gap shrunk — Enea." [Online]. Available: http://www.enea.it/en/news-enea/news/energy-in-the-first-semester-price-of-kilowatt-hour-for-italian-companies-dropped-by-6-italy-ue-gap-shrunk. [Accessed: 18-Mar-2018].

[29] D. V. Punwani, "Turbine Inlet Air Chilling," 2013.

[30] A. Huicochea, W. Rivera, G. Gutiérrez-Urueta, J. C. Bruno, and A. Coronas, "Thermodynamic analysis of a trigeneration system consisting of a micro gas turbine and a double effect absorption chiller," *Appl. Therm. Eng.*, vol. 31, no. 16, pp. 3347–3353, 2011.

[31] J. Spelling, "Hybrid Solar Gas-Turbine Power Plants - A Thermoeconomic Analysis," 2013.

[32] TESS, "Trnsys 17 Component Library Overview."

[33] "TYPE 668: WATER – WATER HEAT PUMP General," 2013.

[34] V. Bianco, M. De Rosa, F. Scarpa, and L. A. Tagliafico, "Implementation of a cogeneration plant for a food processing facility. A case study," *Appl. Therm. Eng.*, vol. 102, pp. 500–512, 2016.

[35] "OECD Data - inflation forecast." [Online]. Available: https://data.oecd.org/price/inflation-forecast.htm.

[36] J. de Wit, “Heat Storages for CHP Optimisation,” *PowerGen Eur. 2007*, pp. 1–18, 2007.

[37] P. Valbonesi, “Water Sector Regulation in Europe: the Italian case.”

[38] P. Olivella-Rosell *et al.*, “Optimization problem for meeting distribution system operator requests in local flexibility markets with distributed energy resources,” *Appl. Energy*, vol. 210, no. April 2017, pp. 881–895, 2018.

Appendix

A.1. Layout 1

Heat Exchanger design function

The function, with which the design UA value and efficiency of the heat exchanger are evaluated is as follows:

```
    function                    [EFF,                    UA]                    =
economizer(TinAir,MFAir,CpAir,TinWater,ToutWater,MFWater,CpWater)
        CH      = MFAir   * CpAir;
        CC      = MFWater * CpWater;
        CMAX2    = max(CH,CC); CMIN2 = min(CH,CC);
        RAT2     = CMIN2/CMAX2;
        EFF     = (ToutWater - TinWater)/(TinAir - TinWater);
        UA      = (log((EFF - 1.0)/(EFF*RAT2 - 1.0))/(RAT2 - 1.0))*CMIN2;
    End
```

Heat Exchanger transient function

```
function           [ToutAir,           ToutWater,           QHx]           =
HxPerformance(TinAir,TinWater,MFAir,MFWater,MFWaterREF,CpAir,CpWater,UAREF)

EXP_UA   = 0.8;     %UA exponent

%Calculate maximum and minimum capacity rates
CAir     = CpAir   *MFAir;
CWater   = CpWater *MFWater;
CMAX     = max(CWater,CAir);
CMIN     = min(CWater,CAir);

if EXP_UA == 0 || MFWater <= 0  || MFWaterREF <= 0
    UA = UAREF;
else
    UA  =  min(max(0.1*UAREF  ,  UAREF  *  (MFWater  /  MFWaterREF)^EXP_UA),
2*UAREF);
end

RAT  = CMIN/CMAX;
UC   = UA/CMIN;

if (RAT) <= 0.01
    EFF  = 1-exp(-UC);

elseif abs(1-RAT) < 0.01
    EFF  = UC/(UC+1);

else
    EFF  = (1-exp(-UC*(1-RAT)))/(1-RAT*exp(-UC*(1-RAT)));

end

ToutAir  = TinAir-EFF*(CMIN/CAir)*(TinAir-TinWater);
ToutWater  = EFF*(CMIN/CWater)*(TinAir-TinWater)+TinWater;
QHx   = abs(EFF*CMIN*(TinAir-TinWater));

End
```

Pumping power

```
function [ReqPower] = pumpPerformance(MFWater,Rho,PumpEff,Pout,Pin)

ReqPower  = MFWater*(Pout-Pin)*1e-1/(Rho*PumpEff);
End
```

TES transient function

```
function [a,Tout,SoCout] = TESperformance(a,Tin,SoCin,MF,Timestep,OM)

MF = MF/a.TES.NoU;
SoCin = SoCin*100;
```

Scale down the mass flow

```
if OM == 1 %Discharging
```

Polynomial evaluation

```
    SimT281MF1_Tout = polyval(a.TES.SimT281.polyMF1,SoCin);
    SimT281MF2_Tout = polyval(a.TES.SimT281.polyMF2,SoCin);
    SimT281MF3_Tout = polyval(a.TES.SimT281.polyMF3,SoCin);

    SimT293MF1_Tout = polyval(a.TES.SimT293.polyMF1,SoCin);
    SimT293MF2_Tout = polyval(a.TES.SimT293.polyMF2,SoCin);
    SimT293MF3_Tout = polyval(a.TES.SimT293.polyMF3,SoCin);
```

Interpolation

```
    Tout281     =     interp1([a.TES.SimT281.MF1(1);     a.TES.SimT281.MF2(1);
a.TES.SimT281.MF3(1)],[SimT281MF1_Tout;                      SimT281MF2_Tout;
SimT281MF3_Tout],MF,'pchip'); %[K]
    Tout293     =     interp1([a.TES.SimT293.MF1(1);     a.TES.SimT293.MF2(1);
a.TES.SimT293.MF3(1)],[SimT293MF1_Tout;                      SimT293MF2_Tout;
SimT293MF3_Tout],MF,'pchip'); %[K]

    Tout                                =       interp1([a.TES.SimT281.Tin(1);
a.TES.SimT293.Tin(1)],[Tout281;Tout293],Tin,'pchip');
```

```
    Etot281     =     interp1([a.TES.SimT281.MF1(1);     a.TES.SimT281.MF2(1);
a.TES.SimT281.MF3(1)],[a.TES.SimT281.EtotTESMF1;   a.TES.SimT281.EtotTESMF2;
a.TES.SimT281.EtotTESMF3],MF,'pchip'); %[K]
    Etot293     =     interp1([a.TES.SimT293.MF1(1);     a.TES.SimT293.MF2(1);
a.TES.SimT293.MF3(1)],[a.TES.SimT293.EtotTESMF1;   a.TES.SimT293.EtotTESMF2;
a.TES.SimT293.EtotTESMF3],MF,'pchip'); %[K]

    Etot                    =                   interp1([a.TES.SimT281.Tin(1);
a.TES.SimT293.Tin(1)],[Etot281;Etot293],Tin,'pchip');

    %Change in TES energy content
    dt      = Timestep;          %[sec]
    dT      = Tin-Tout;          %[K]
    Cp      = a.TES.Sim.cp;      %[Kj/Kg.K]
    dE      = MF*Cp*dT*dt;       %[kJ]
```

```
    SoCout  = SoCin - dE/(Etot*3600)*100;

elseif OM == 2 %Charging

    SimT265MF1_Tout = polyval(a.TES.SimT265.polyMF1,SoCin);
    SimT265MF2_Tout = polyval(a.TES.SimT265.polyMF2,SoCin);
    SimT265MF3_Tout = polyval(a.TES.SimT265.polyMF3,SoCin);

    SimT266MF1_Tout = polyval(a.TES.SimT266.polyMF1,SoCin);
    SimT266MF2_Tout = polyval(a.TES.SimT266.polyMF2,SoCin);
    SimT266MF3_Tout = polyval(a.TES.SimT266.polyMF3,SoCin);


    Tout265     =     interp1([a.TES.SimT265.MF1(1);     a.TES.SimT265.MF2(1);
a.TES.SimT265.MF3(1)],[SimT265MF1_Tout;                     SimT265MF2_Tout;
SimT265MF3_Tout],MF,'pchip'); %[K]
    Tout266     =     interp1([a.TES.SimT266.MF1(1);     a.TES.SimT266.MF2(1);
a.TES.SimT266.MF3(1)],[SimT266MF1_Tout;                     SimT266MF2_Tout;
SimT266MF3_Tout],MF,'pchip'); %[K]

    Tout                                =       interp1([a.TES.SimT265.Tin(1);
a.TES.SimT266.Tin(1)],[Tout265;Tout266],Tin,'pchip');


    Etot265     =     interp1([a.TES.SimT265.MF1(1);     a.TES.SimT265.MF2(1);
a.TES.SimT265.MF3(1)],[a.TES.SimT265.EtotTESMF1;   a.TES.SimT265.EtotTESMF2;
a.TES.SimT265.EtotTESMF3],MF,'pchip'); %[K]
    Etot266     =     interp1([a.TES.SimT266.MF1(1);     a.TES.SimT266.MF2(1);
a.TES.SimT266.MF3(1)],[a.TES.SimT266.EtotTESMF1;   a.TES.SimT266.EtotTESMF2;
a.TES.SimT266.EtotTESMF3],MF,'pchip'); %[K]

    Etot                    =                   interp1([a.TES.SimT265.Tin(1);
a.TES.SimT266.Tin(1)],[Etot265;Etot266],Tin,'pchip');

    %Change in TES energy content
    dt      = Timestep;          %[sec]
    dT      = Tin-Tout;          %[K]
    Cp      = a.TES.Sim.cp;      %[Kj/Kg.K]
    dE      = MF*Cp*dT*dt;       %[kJ]

    SoCout  = SoCin + dE/(Etot*3600)*100;

end

SoCout  = SoCout / 100;

end
```

TES utilization factor

```
for i = 1:length(a.test)-1
    if a.x(i+1) - a.x(i) > 0
       a.TES.teslevel(i) = (a.x(i+1) - a.x(i));
    end
end
a.techKPIs(1,17) = sum(a. TES.teslevel) / ((1-a.TESmin)*365);
a.techKPIs(2,17) = sum(a.TES.teslevel) / 365;
```

Differential in state of charge, i.e. charge increase

Method 1

Method 2

A.2. Layout 2 and 3

Electricity price Turin 2017

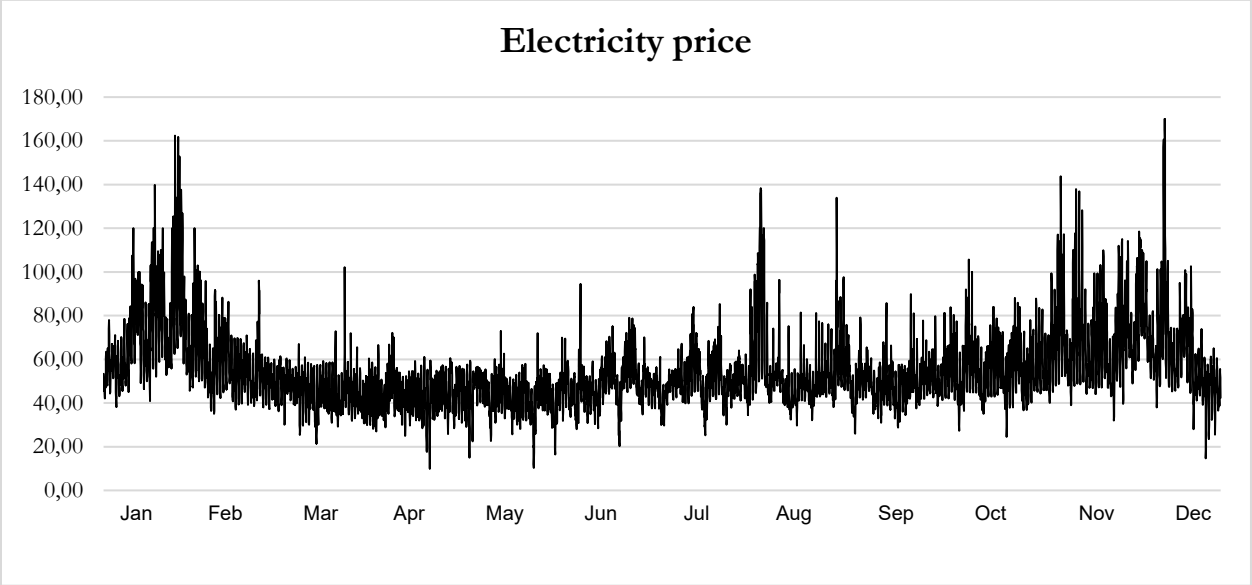

Trnsys model of GT cycle

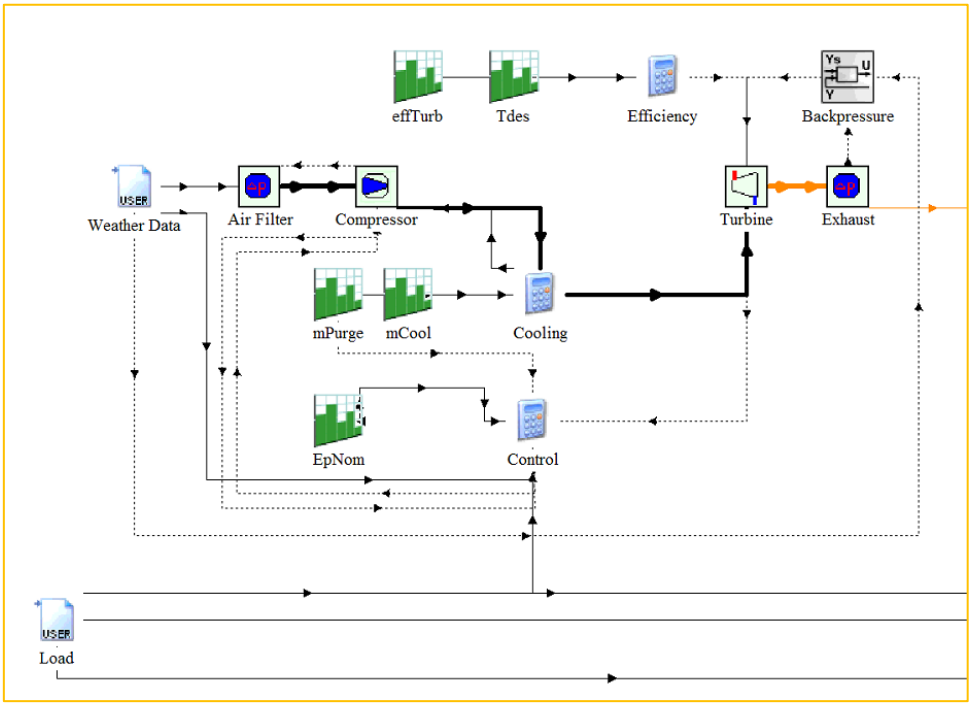

Trnsys model of TES+HP layout

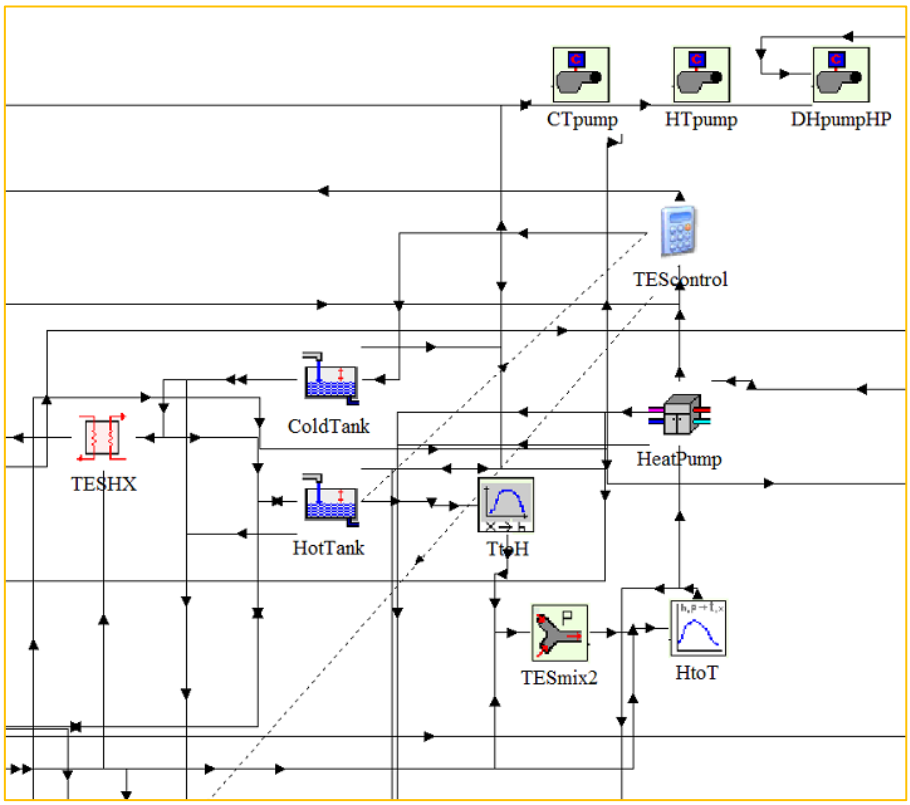

Cost functions

Gas turbine

$$C_{GT} = C_{comp} + C_{turb} + C_{comb} + C_{aux}$$

- $C_{comp} = c_1 \cdot \dot{m}_{inlt}^{ref} \left(\frac{\dot{m}_{inlt}}{\dot{m}_{inlt}^{ref}}\right)^{0.7} \prod_c^{ref} \ln(\prod_c) \cdot f_\eta$

$$f_n = \frac{1}{c_2 - \eta_p}$$

$\dot{m}_{inlt}$: inlet air mass flow at ISO conditions

$\prod_c$: nominal compressor pressure ratio

f_η: correction factor for compressor efficiency

- $C_{turb} = c_3 \cdot \dot{m}_{exh}^{ref} \left(\frac{\dot{m}_{exh}}{\dot{m}_{exh}^{ref}}\right)^{0.7} \prod_t^{ref} \ln(\prod_t) \cdot f_T \cdot f_\eta$

$\dot{m}_{exh}$: exhaust mass flow rate at standard conditions

$\prod_t$: nominal turbine pressure ratio

To note that temperature correction factor f_T considers the effect of the inlet hot gas temperature on the cost of the unit [31].

$$f_T = 1 + \exp(0.025 \cdot (T_6 - 1600))$$

T_6: combustor outlet temperature

1600 K: combustor temperature

- $C_{comb} = c_4 \cdot \dot{m}_{comb}^{ref} \left(\frac{\dot{m}_{comb}}{\dot{m}_{comb}^{ref}}\right)^{0.7} f_T \cdot f_P$

$$f_P = \frac{1}{f_{dP} - 0.005}$$

$\dot{M}_{comb}$: nominal exhaust gas mass flow at the exit of the combustor

f_{dP}: relative pressure drop in the combustor at nominal conditions

f_P considers the effect of the design pressure loss on the cost of the unit.

- $C_{aux} = C_{ref}^{aux} \left(\frac{\dot{E}_{GT}}{\dot{E}_{GT,ref}}\right)^{0.7}$

$\dot{E}_{GT}$: nominal power output of the gas turbine

- $C_{pump} = n_{pump} \cdot 940\ USD \cdot P_{pump}^{0.71} \cdot \left(1 + \frac{0.2}{1-\eta_{pump}}\right)$

According to J. Spelling and Gas Turbine World Data [31]:

- The reference $\dot{m}_{inlt}^{ref}$, $\dot{m}_{exh}^{ref}$ and $\dot{m}_{comb}^{ref}$ are 515 kg/s, 460 kg/s and 460 kg/s, respectively.
- $\prod_c^{ref}$ is 15.
- c_1, c_2, c_3 and c_4 are 27.7 $USD/(\frac{kg}{s})$ 0.96, 12.4 $USD/(\frac{kg}{s})$ and 17.9 $USD/(\frac{kg}{s})$, respectively.
- C_{ref}^{aux} is 4 million USD for a reference turbine output of 160 MW.